(12) INTERNATIONAL APPLICATION PUBLISHED UNDER THE PATENT COOPERATION TREATY (PCT)

(19) World Intellectual Property Organization
International Bureau

(43) International Publication Date
07 October 2021 (07.10.2021)

WIPO | PCT

(10) International Publication Number
WO 2021/198726 A1

(51) International Patent Classification:
C12Q 1/6827 (2018.01) *C12Q 1/6883* (2018.01)
C12Q 1/6853 (2018.01)

(21) International Application Number:
PCT/IB2020/053011

(22) International Filing Date:
30 March 2020 (30.03.2020)

(25) Filing Language: English

(26) Publication Language: English

(71) Applicant: **VILNIUS UNIVERSITY** [LT/LT]; Universiteto st. 3, 01513 Vilnius (LT).

(72) Inventors: **KRIUKIENE, Edita**; Sauletekio av. 7, LT-10257 Vilnius (LT). **GORDEVICIUS, Juozas**; Sauletekio av. 7, LT-10257 Vilnius (LT). **NARMONTE, Milda**; Sauletekio av. 7, LT-10257 Vilnius (LT). **GIBAS, Povilas**; Sauletekio av. 7, LT-10257 Vilnius (LT).

(74) Agent: **PETNIUNAITE, Jurga**; A. Gostauto 40B, 03163 Vilnius (LT).

(81) Designated States *(unless otherwise indicated, for every kind of national protection available)*: AE, AG, AL, AM, AO, AT, AU, AZ, BA, BB, BG, BH, BN, BR, BW, BY, BZ, CA, CH, CL, CN, CO, CR, CU, CZ, DE, DJ, DK, DM, DO, DZ, EC, EE, EG, ES, FI, GB, GD, GE, GH, GM, GT, HN, HR, HU, ID, IL, IN, IR, IS, JO, JP, KE, KG, KH, KN, KP, KR, KW, KZ, LA, LC, LK, LR, LS, LU, LY, MA, MD, ME, MG, MK, MN, MW, MX, MY, MZ, NA, NG, NI, NO, NZ, OM, PA, PE, PG, PH, PL, PT, QA, RO, RS, RU, RW, SA, SC, SD, SE, SG, SK, SL, ST, SV, SY, TH, TJ, TM, TN, TR, TT, TZ, UA, UG, US, UZ, VC, VN, WS, ZA, ZM, ZW.

(84) Designated States *(unless otherwise indicated, for every kind of regional protection available)*: ARIPO (BW, GH, GM, KE, LR, LS, MW, MZ, NA, RW, SD, SL, ST, SZ, TZ, UG, ZM, ZW), Eurasian (AM, AZ, BY, KG, KZ, RU, TJ, TM), European (AL, AT, BE, BG, CH, CY, CZ, DE, DK, EE, ES, FI, FR, GB, GR, HR, HU, IE, IS, IT, LT, LU, LV, MC, MK, MT, NL, NO, PL, PT, RO, RS, SE, SI, SK, SM, TR), OAPI (BF, BJ, CF, CG, CI, CM, GA, GN, GQ, GW, KM, ML, MR, NE, SN, TD, TG).

(54) **Title:** METHODS AND COMPOSITIONS FOR NONINVASIVE PRENATAL DIAGNOSIS THROUGH TARGETED COVALENT LABELING OF GENOMIC SITES

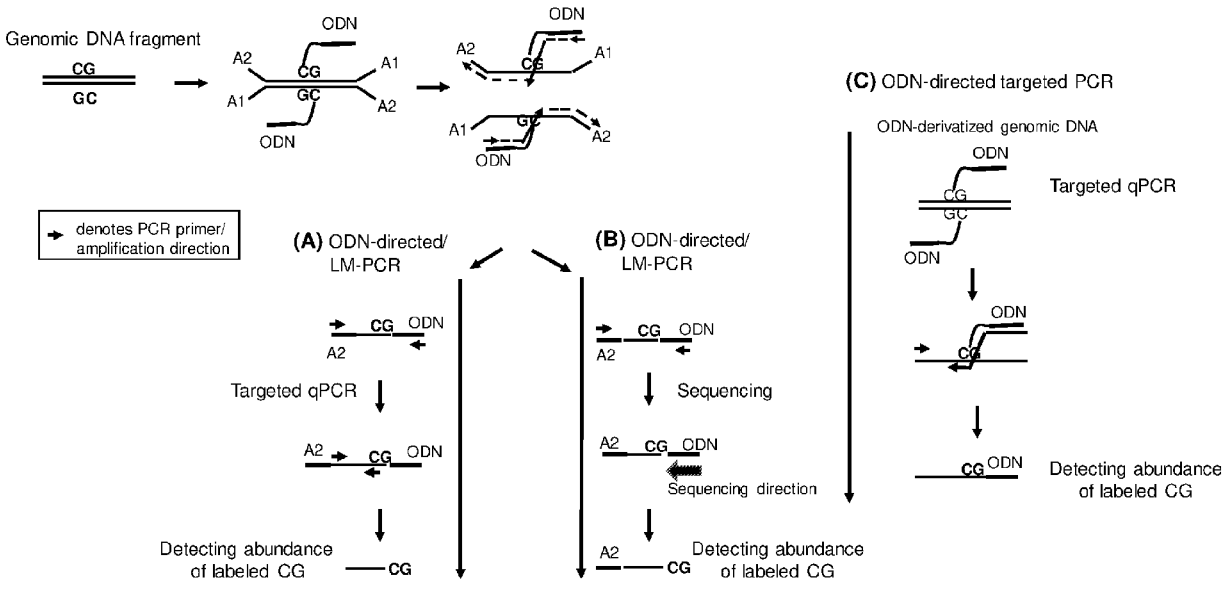

[Fig. 8]

(57) **Abstract:** This invention relates to a method that covalently modifies unmodified and hydroxymethylated genomic sites in fetal specific genetic material present in maternal blood DNA samples and produce the adjacent genomic regions for detecting fetal aneuploidies and fetal gender using quantitative real time PCR or sequencing. A large panel of differently labeled sites and regions between maternal and fetal genetic material has been identified and they validity for diagnostic purposes of fetal trisomy of chromosome 21 has been demonstrated.

[Continued on next page]

WO 2021/198726 A1

Declarations under Rule 4.17:

— *of inventorship (Rule 4.17(iv))*

Published:

— *with international search report (Art. 21(3))*

— *with sequence listing part of description (Rule 5.2(a))*

— *in black and white; the international application as filed contained color or greyscale and is available for download from PATENTSCOPE*

METHODS AND COMPOSITIONS FOR NONINVASIVE PRENATAL DIAGNOSIS THROUGH TARGETED COVALENT LABELING OF GENOMIC SITES

Technical Field

[0001] This invention relates to the field of genetic testing for pregnant females in order to diagnose chromosomal aneuploidy and fetal gender from maternal peripheral blood samples.

Background Art

[0002] Fetal chromosomal aneuploidy results from the presence of abnormal dose(s) of a chromosome or chromosomal region. The Down syndrome or Trisomy 21 (T21) is the most common incurable chromosomal aneuploidy in live born infants, which is typically associated with physical and mental disability (Parker et al. 2010). The overall incidence of T21 is approximately 1 in 700 births in the general obstetrical population, but this risk increases to 1 in 35 term births for women 45 years of age. An invasive diagnostic procedure is currently the only way to confirm the diagnosis of T21, commonly by a fetal cytogenetic analysis (such as karyotyping), which requires fetal genetic material to be invasively obtained by amniocentesis, chorionic villus sampling or cordocentesis. Due to the current risk of prenatal testing it is currently offered only for women in the high-risk group. Although the safety of invasive procedures has improved since their introduction, a well-recognized risk of fetal loss (0.5 to 1% for chorionic villus sampling and amniocentesis) and follow-up infections still remain (Akolekar et al. 2015). Hence, non-invasive and highly confident prenatal screening tests to reduce the number of invasive diagnostic procedures are still required.

[0003] Since the discovery of fetal genomic material in the form of circulating cell-free fetal DNA (cffDNA) in the blood plasma of pregnant women (Lo, et al., 1997) many attempts have been made aiming at using cffDNA for non-invasive risk-free prenatal testing (NIPT). Early applications of NIPT included the determination of Rhesus D blood-group status and fetal sex as well as the diagnosis of autosomal dominant disorders of paternal inheritance by quantitative real time PCR (qPCR) (Lo et al., 1998; Daniels et al, 2006). However, the application of cffDNA to the prenatal detection of fetal chromosomal aneuploidies has represented a considerable challenge. First of all, the cffDNA represents only a subfraction of 6–10% of the total cfDNA (cell-free DNA) of

maternal origin in first and second trimester pregnancies and rises up to 10–20% in third trimester pregnancies (Lun et al., 2008; Lo et al., 2010), and this can often interfere with the analysis of fetal nucleic acids. One way to deal with the low abundance of the fetal DNA was the evaluation of the dosage of chromosome 21 calculating the ratios of polymorphic alleles in the placenta-derived DNA/RNA molecules (Lo, and Chiu, 2007). However, this method can only be applied to fetuses that are heterozygous for the targeted polymorphisms.

[0004] A study of Zimmermann et al (2002) was able to distinguish between trisomic 21 and euploid fetuses using qPCR based on the 1.5-fold increase in chromosome 21 dosage in the trisomic cases. Since a 2-fold difference in DNA template concentration constitutes a difference of only one threshold cycle (C_T), the discrimination of a 1.5-fold difference is at the limit of conventional qPCR.

[0005] With the development of massive parallel sequencing (MPS) the detection of fetal aneuploidy is carried out through counting cfDNA molecules and measuring the over- or underrepresentation of any chromosome in maternal plasma. As previous reports have indicated that fetal cffDNA is shorter than its maternal counterpart (Chan et al, 2004; Li et al, 2004; Fan et al, 2010), MPS has been combined with size fractionation prior to sequencing or *in silico* of plasma DNA fragments to enrich for fetal DNA. However, even though MPS has been widely used in commercial prenatal testing, such an approach which requires deep coverage or paired-end sequencing, increases the cost of service.

[0006] An alternative approach to improve the sensitivity and cost-effectiveness of NIPT is preferential targeting of fetal DNA sequences by utilizing epigenetic differences between maternal blood DNA and cffDNA.

[0007] Bisulfite conversion that enables analysis of the methylation status of each CG site, followed by either methylation-specific PCR or sequencing has been applied to detect methylation differences between maternal and fetal DNA (Chim, et al. 2005; Chiu, et al. 2007; Chim, et al. 2008; Lun et al, 2013; Jensen et al, 2015). However, although providing high resolution, bisulfite treatment reinforces the degradation of low amounts of fetal DNA, complicating fetal specific methylome analysis. Furthermore, screening genomes for diagnostic of DMRs by whole-genome bisulfite-sequencing is technologically demanding and extremely expensive leading to an unnecessary increase in cost of NIPT.

[0008] The application of methylation sensitive restriction digestion involves the use of methylation-sensitive restriction enzymes to remove hypomethylated maternal DNA thus allowing direct polymerase chain reaction (PCR) analysis of cffDNA (Old, et al. 2007; Tong et al, 2010). However, methylation sensitive restriction digestion is inherently limited by the sequence-specificity of available enzymes what restricts the number of DMR regions suitable for testing.

[0009] The methylcytosine-immunoprecipitation based approach (MeDIP) was used in combination with oligonucleotide array analysis, sequencing and MeDIP-qPCR for the quantification of selected hypermethylated fetal DMRs on chromosome 21 (Papageorgiou et al., 2009, Tsaliki et al, 2012, Keravnou et al, 2016). However, MeDIP enrichment is biased to highly methylated sequences (Weber et al. 2005) and thus, the potential diagnostic informativeness of the less CG dense or less methylated sequences might be lost. Therefore, further developments and advances are necessary for the identification and detection of highly specific and stable fetal-specific markers.

[0010] Placental DNA was reported to be generally hypomethylated as compared to maternal blood DNA. Examination of the differential methylation between placenta and maternal blood uncovered large contiguous genomic regions with significant placental hypomethylation relative to non-pregnant female cfDNA (Jensen et al, 2015). Moreover, these regions are of low CpG and gene density and thus could be poorly covered by affinity enrichment methods, such as MeDIP. Since unmodified CG fraction represents smaller portion of the human genome (20-30% of CGs are unmethylated), its targeted analysis is more relevant for cost-effective and sensitive detection of fetal specific DNA fragments in maternal circulation.

[0011] In recent years, we and others have been adapted covalent derivatization for epigenome-wide studies of various cytosine modifications (Song et al. 2011; Kriukienė et al. 2013; Staševskij et al. 2017; Gibas et al, 2020, accepted). Generally, robust and highly specific enrichment of a covalently modified minor fraction of cytosines in the fetal cffDNA, for example of unmodified CGs or hydroxymethylated cytosines, could potentially help achieve superior sensitivity and specificity in prenatal diagnostics. More importantly, a method for highly specific targeted analysis of a particular fraction of fetal regions combined with lower cost next generation sequencing devices or real time quantitative PCR (qPCR) can significantly alter the cost and turnaround time of

NIPT, increasing the availability of NIPT screening for all pregnancies without the restriction to a high risk group.

Summary of Invention

[0012] In the first aspect, the present invention provides a new method for noninvasive prenatal diagnosis based on analysis of unmodified CG sites (uCG) or hydroxymethylated CGs (hmCGs) in nucleic acid molecules extracted from a biological sample obtained from a pregnant female typically during the first trimester of gestational age through use covalent modification of uCGs or hmCs and subsequent estimation of the labeled fraction of CG sites, enabling genome-wide identification of the fetal-specific regions.

[0013] According to one exemplary embodiment, a biological sample received from a pregnant female is analyzed to perform a prenatal diagnosis of a fetal chromosomal aneuploidy, such as trisomy T21, and fetal gender.

[0014] A maternal biological sample includes nucleic acid molecules found in various maternal body fluids, such as peripheral blood or a fractionated portion of peripheral blood, urine, plasma, serum, and other suitable biological samples. In a preferred embodiment, the maternal biological sample is a fractionated portion of maternal peripheral blood.

[0015] A large number of differentially labeled regions (DLRs) on chromosome 21, 13 and 18 which are differentially modified between non-pregnant female peripheral blood DNA sample and DNA of placental origin (chorionic villi (CV) of the fetal part of placenta which are enriched in fetal trophoblasts) or between non-pregnant female peripheral blood DNA sample and peripheral blood DNA sample of pregnant women have been identified using covalent chemical modification of the cytosine base of naturally unmodified CG sites or hydroxymethylated CG sites in maternal nucleic acid molecules. Subsequent PCR amplification with or without enrichment of the labeled fraction of CG sites coupled with sequence determination of the labeled and amplified nucleic acid molecules enabled genome-wide identification of the fetal-specific labeled regions. As used herein, the term DLR refers to a "differently labeled genomic region" that is more or less intensively labeled through enzymatic transfer of a reactive group onto the cytosine base in the nucleic acid molecule. For the purposes of the invention, the preferred DLRs (selected u-DLRs; see Table 4) are those that are hypomethylated and thus, more intensively labeled, in fetal DNA and hypermethylated in maternal DNA.

In another aspect, the preferred DLRs (selected hm-DLRs; see Table 5) are those that are hyper-hydroxymethylated and thus, more intensively labeled, in fetal DNA and hypo-hydroxymethylated in maternal DNA.

[0016] In one embodiment, a DLR can be confined to a single cytosine or a dinucleotide, preferentially a CG dinucleotide (CG-DLRs).

[0017] Representative examples of a subset of these u-DLRs, hm-DLRs and CG-DLRs have been used to accurately predict trisomy 21, in a method based on analysis of fetal-specific hypomethylated or hydroxymethylated DNA in a sample of maternal blood, typically during the first trimester of gestational age. Thus, the effectiveness of the disclosed DLRs and methodologies for diagnosing fetal aneuploidies have been demonstrated.

[0018] In addition, representative examples of a subset of these u-DLRs and hm-DLRs have been used to accurately predict fetal gender from X and Y chromosomes, in a method based on analysis of fetal-specific hypomethylated DNA in a sample of maternal blood, typically during the first trimester of gestational age. Thus, the effectiveness of the disclosed DLRs and methodologies for diagnosing fetal gender have been demonstrated.

[0019] Accordingly, the invention pertains to a method for prenatal diagnosis of a trisomy 21, and fetal gender using a sample of maternal blood, the method comprising:

(a) enzymatic labeling of uCG and hmC sites of nucleic acid molecules in a sample of maternal blood with a first reactive group, preferably an azide group;

(b) chemically tethering of an oligodeoxyribonucleotide (ODN) having the second reactive group, preferably an alkyne group, to the first group in a template nucleic acid;

(c) producing nucleic acid molecules from a template nucleic acid sequence using a nucleic acid polymerase which contacts a template nucleic acid sequence at or around the site of the labeled uCG/hmC and starts polymerization from the 3'-end of a primer non-covalently attached to the ODN;

(d) determining the presence or availability of the CG target sites and hence the level of the unmodified or hydroxymethylated template genomic nucleic acid molecules across the regions of chromosomal DNA shown in Tables 4 or 5, or 6;

(e) comparing the acquired value of the regions of step (d) to a standard reference value for the combination of at least one region from the list shown in Tables 4-6,

wherein the standard reference value is (i) a value for a DNA sample from a woman bearing a fetus without trisomy 21; or (ii) a value for a DNA sample from a woman bearing a fetus with trisomy 21.

(f) diagnosing a trisomy based on said comparison, wherein trisomy 21 is diagnosed if the acquired value of the regions of step (d) is (i) higher than the standard reference value from a woman bearing a fetus without trisomy 21; or (ii) lower than the standard reference value from a woman bearing a fetus without trisomy 21; or (iii) comparable to the standard reference value from a woman bearing a fetus with trisomy 21.

(g) detecting fetal gender based on said comparison wherein female gender of a fetus is detected if the acquired value of the regions of step (d) is comparable to the standard reference value from a woman bearing a female fetus, and male gender of a fetus is detected if the acquired value of the regions of step (d) is comparable to the standard reference value from a woman bearing a male fetus.

Brief Description of Drawings

Fig.1

[0020] [Fig.1] is a diagram of the methodology for identification of Differentially Labeled Regions (DLRs) across chromosome 21 (or chromosomes 13 and 18) comparing the two tissue pairs: chorionic villi tissue DNA of the 1st trimester fetuses and fractionated peripheral blood DNA samples of non-pregnant controls and fractionated peripheral blood DNA samples of non-pregnant female and pregnant female carrying a healthy fetus from the 1st trimester pregnancies. Further strategy for area under curve (AUC) determination for diagnosing T21-affected fetuses is also shown.

Fig.2

[0021] [Fig.2] shows the difference in (a) uCG and (b) hmCG signal for the exemplary DLRs (tissue-specific u-DLR chr21:33840400-33840500; pregnancy-specific u-DLR chr21:33591700-33591800; tissue-specific hm-DLR chr21:35203200-35203300; pregnancy-specific hm-DLR chr21:43790900-43791000, selected from Tables 4 or 5) identified in chromosome 21 between chorionic villi tissue DNA of the 1st trimester fetuses and fractionated peripheral blood DNA samples of non-pregnant controls; and between fractionated peripheral blood DNA samples of non-pregnant female and pregnant female carrying a healthy fetus from the 1st trimester pregnancies (left panel). For diagnosing purposes of trisomy 21, the signal intensity across the exemplary

DLRs is also shown for the samples of pregnant female carrying T21-diagnosed fetuses from the 1st trimester pregnancies (right panel).

Fig.3

[0022] [Fig.3] shows the difference in (a) uCG and (b) hmCG signal for the exemplary DLRs (u-DLR chr21:43933400-43933500; hm-DLR chr21:36053400-36053500; selected from the Tables 4 or 5) identified in chromosome 21 between fractionated peripheral blood DNA samples of pregnant female carrying a healthy fetus or a T21 diagnosed fetus from the 1st trimester pregnancies.

Fig.4

[0023] [Fig.4] shows the difference in mean signal of labeled individual CG-DLRs, namely, (a) u-CG-DLRs and (b) hm-CG-DLRs (selected from Table 6) in chromosome 21 for detection of fetal T21 aneuploidy.

Fig.5

[0024] [Fig.5] shows the difference in mean signal of labeled individual CG-DLRs, namely u-CG-DLRs (selected from Table 6) in chromosome X for fetal gender determination. Samples from pregnant women and fetal CV tissue were labeled either XX or XY according to the gender of a fetus, Female and Male, respectively. Samples from non-pregnant women, NPC, were labeled as None, 00.

Fig.6

[0025] [Fig.6] shows the relative quantification of individual or a combination of (a) u-CG-DLRs and (b) hm-CG-DLRs of fetal specific DNA regions located on chromosome 21 using real time quantitative PCR for replicated DNA samples of peripheral blood plasma DNA of women pregnant with healthy or T21-diagnosed fetuses. Y-axis indicates the threshold cycle values (C_T) calculated in qPCR for the regions selected from Table 6 whose genome coordinates are shown above the graphs. Notably, numerical values of C_T inversely correlate to the abundance of the DLR region, indicating higher abundance of the region in the blood samples of pregnant female carrying a T21-diagnosed fetus.

Fig.7a, b, c

[0026] [Fig.7a and b] show simulation of a PCR-based test for fetal gender determination by measuring DNA methylation differences in (a) chromosome X or (b) chromosome Y, according to the scheme shown in Fig. 8c. DNA of the 1st trimester CV tissue of

both genders was mixed with nonpregnant female peripheral blood plasma DNA to the ratio 20/80 or 0/100, respectively, and the difference in the threshold cycle was evaluated by qPCR. ΔC_T indicates the difference in the threshold cycle values between the mixtures using the CV samples of both genders (indicated as XX and XY for female and male genders, respectively). Fig.7c shows relative quantification of fetal specific DNA regions located on chromosome X for fetal gender determination using qPCR for the replicated DNA samples of untreated, i.e. non-preamplified, pregnant female peripheral blood plasma, according to the scheme shown in Fig.8c.

Fig.8

[0027] [Fig.8] is a schematic illustration of the analytical approach for calculation of DLRs using labeling and enrichment of unmodified CG or hydroxymethylated CG sites coupled with analysis by (a) real time quantitative PCR of pre-amplified samples; (b) sequencing of labeled CGs; (c) real time quantitative PCR of non-preamplified DNA samples, of fractionated peripheral blood DNA of pregnant female. ODN – the attached deoxyribonucleotide, A1/A2 – the two strands of the ligated to DNA fragments partially complementary adaptors.

Fig.9

[0028] [Fig.9] shows the difference in (a) uCG and (b) hmCG signal for the exemplary DLRs (selected from Table 7; the genomic coordinates are shown above the graphs) identified for chromosome 13 and chromosome 18 between CV tissue DNA of the 1st trimester fetuses and fractionated peripheral blood DNA samples of non-pregnant controls; and between fractionated peripheral blood DNA samples of non-pregnant female and pregnant female carrying a healthy fetus from the 1st trimester pregnancies.

Fig.10

[0029] [Fig.10] shows the relative quantification of (a) u-CG-DLRs and (b) hm-CG-DLRs of T21 fetal-specific DNA regions located on chromosome 21 using real time quantitative PCR for an independent group of peripheral blood plasma DNA samples of women pregnant with healthy or T21-diagnosed fetuses. Y-axis indicates the threshold cycle values (C_T) calculated in qPCR for the regions selected from Table 6.

Description of Embodiments

[0030] In the present embodiment, the method comprises the measurement of the presence or availability of the target CG sites in the template nucleic acid molecules by sequencing of the amplified nucleic acid molecules of the biological sample, such that only the sequence of the targeted CGs and hence the unmodified/hydroxymethylated fraction of CGs is determined. In this embodiment, amplification prior to sequencing is performed through the ODN-directed and ligation-mediated PCR using one primer bound complementary to the ODN or a part of it in the absence of complementarity to the genomic template region, and the second primer bound through non-covalent complementary base pairing to oligonucleotide linkers ligated to both ends of the template nucleic acid molecule. In another aspect of this embodiment, amplification prior to sequencing can be performed by targeted PCR amplification utilizing one primer bound complementary to the ODN or a part of it in the presence (5-7 nucleotides complementarity to the genomic template DNA in the proximity of a CG site) or absence of complementarity to the genomic template DNA, and the second primer bound through non-covalent complementary base pairing to the template DNA in the chromosomal regions shown in Tables 4 or 5 or 6 or 7.

[0031] In further embodiments, the method comprises the measurement of the presence or availability of the labeled target sites and hence the level of the unmodified or hydroxymethylated template nucleic acid molecules by real time quantitative polymerase chain reaction (qPCR) of the enriched fetal CGs and DNA regions, which have been previously covalently targeted and pre-amplified using attached ODN as described above, utilizing one primer with its 5' end bound complementary to the chromosomal regions shown in Tables 4-7 in the very close vicinity (its 5' end binds at or more than 5 nucleotides to a labeled CG site) to the labeled cytosine, and the second primer bound complementary to the template DNA in the selected chromosomal regions shown in Tables 4 or 5 or 6 or 7.

[0032] In yet another aspect, the method comprises the measurement of the presence or availability of the labeled target sites and hence the level of the unmodified or hydroxymethylated template nucleic acid molecules in a non-preamplified DNA sample by real time quantitative polymerase chain reaction, utilizing one primer that recognizes and binds to the ODN and 5-7 nucleotides adjacent to the target CG site in a template genomic DNA through non-covalent complementary base pairing, and a

second primer binds complementary to the template DNA in the selected chromosomal regions shown in Tables 4 or 5 or 6 or 7.

[0033] In the preferred embodiment of the invention, the plurality of differentially labeled regions (DLRs) preferably is chosen from the lists shown in Tables 4-7. In various embodiments, the levels of the plurality of DLRs are determined for at least one DLR, for example chosen from the lists shown in Tables 4-7. Preferably, the levels of the plurality of DLRs in the labeled DNA sample are determined by real time quantitative polymerase chain reaction (qPCR). As used herein, the term "a plurality of DLRs" is intended to mean one or more DLRs (or CG dinucleotides).

[0034] In a further aspect, the present invention pertains to a kit, comprising the composition of the invention. In other embodiments, the kit further comprises:

(a) an enzyme capable of covalent derivatization of the cytosine base with an active group, preferentially an azide group;

(b) a compound comprising the active group (an azide group);

(c) an ODN attached to the second reactive group, preferably an alkyne group; and

(d), oligonucleotide primers (e.g., two or more) for assessment of DLR regions through PCR amplification, wherein one primer binds to the ODN or in the close vicinity to the ODN attachment site through non-covalent complementary base pairing and is able to prime a nucleic acid polymerization reaction from the labeled CG and the second primer binds to the genomic regions described in Tables 4-7;

(e) in another embodiment, the kit can further comprise oligonucleotide linkers for ligation and/or oligonucleotide primers for PCR amplification of the nucleic acid molecules to be analyzed by qPCR or sequencing.

Detailed Description of the Invention

[0035] The present invention is based, at least in part, on the inventors' identification of a large panel of differentially labeled regions (DLRs) and CGs (CG-DLRs) that exhibit strong labeling in fetal DNA and weak or absence of labeling in maternal DNA. Still further, the invention is based, at least in part, on the inventors' demonstration that hypomethylated/hydroxymethylated fetal DNA can be specifically targeted and enriched through covalent modification of CGs, thereby resulting in a sample enriched for fetal DNA. Still further, the inventors have accurately diagnosed trisomy 21 and fetal gender in a panel of maternal peripheral blood samples using representative

examples of the DLRs disclosed herein, thereby demonstrating the effectiveness of the identified DLRs and disclosed methodologies in diagnosing fetal aneuploidy T21 and fetal gender.

[0036] Various aspects of this disclosure are described in further detail in the following subsections.

[0037] I. A METHOD FOR NON-INVASIVE DETECTION OF FETAL ANEUPLOIDY T21 AND FETAL GENDER

[0038] Accordingly, the invention pertains to a method for prenatal diagnosis of a trisomy 21, and fetal gender using a sample of maternal blood, the method comprising:

(a) enzymatic labeling of uCG or hmC sites of nucleic acid molecules in a sample of maternal blood with a reactive azide group;

(b) chemically tethering of an oligodeoxyribonucleotide (ODN) having an alkyne group to the introduced azide groups in a template nucleic acid;

(c) producing nucleic acid molecules from a template nucleic acid sequence starting at the azide-labeled CG sites through PCR amplification;

(d) determining the labeling intensity level of unmodified or hydroxymethylated template genomic nucleic acid molecules across the regions or CG sites of chromosomal DNA shown in Tables 4 or 5, or 6 using, preferably qPCR, or sequencing of labeled genomic fraction;

(e) comparing the experimentally acquired value of the regions of step (d) to a standard reference value for the combination of at least one region, or at least two regions from the list shown in Tables 4-6, wherein the standard reference value is (i) a value for a DNA sample from a woman bearing a fetus without trisomy 21; or (ii) a value for a DNA sample from a woman bearing a fetus with trisomy 21.

(f) diagnosing a trisomy 21 based on said comparison, wherein trisomy 21 is diagnosed if the experimentally acquired value of the sample is (i) higher than the standard reference value from a woman bearing a fetus without trisomy 21; or (ii) lower than the standard reference value from a woman bearing a fetus without trisomy 21; or (iii) comparable to the standard reference value from a woman bearing a fetus with trisomy 21.

[0039] A schematic illustration of the analytical approach for evaluation of labeling intensity in DLRs using labeling and enrichment of unmodified or hydroxymethylated CGs is demonstrated in Fig.8.

[0040] II. LABELING OF UNMODIFIED OR HYDROXYMETHYLATED CG SITES

[0041] Methods for the first step of covalent derivatization of genomic DNA sites are known in the art. Covalent labeling of genomic uCG or hmC sites can be performed using an enzyme capable of transfer of a covalent group onto genomic DNA. The enzyme may comprise a methyltransferase or a glucosyltransferase.

[0042] An enzyme for covalent labeling of uCG sites is preferably the C5 DNA methyltransferase M.SssI or a modified variant of it, such as M.SssI variant Q142A/N370A (Kriukiene et al., 2013; Stasevskij et al, 2017) which is adapted to work with synthetic cofactors, such as Ado-6-azide cofactor (Kriukiene et al., 2013; Masevicius et al., 2016).

[0043] An enzyme for covalent labeling of hmC/hmCG sites is preferably the phage T4 beta-glucosyltransferase (BGT) which is adapted to work with synthetic cofactors, such as UDP-6-azidoglucose (Song et al, 2011).

[0044] The ODN is preferably from 20 to 90 nucleotides in length, as shown in the exemplary embodiment preferably 39 nt. The ODN contains the reactive group at the second base position from its 5'-end, preferably the alkyne group, which reacts with the azide group which was enzymatically introduced in a template nucleic acid molecule.

[0045] It should be noted that DNA after covalent labeling becomes enzymatically and chemically altered but preserves base specificity. As used herein, the term "enzymatically altered" is intended to mean reacting the DNA with an enzymatically transferred chemical group that enables the conversion of respective CG sites into the azide-CG sites, giving discrimination of the labeled sites from template CGs. As used herein, the term "chemically altered" is intended to mean enzymatic transformation of template cytosine into the azide-modified cytosine in CG sites. Thus, in the instant method the fetal specific regions are calculated between more intensively and less intensively labeled CG sites in DNA without the need to directly determine methylation or hydroxymethylation levels of template DNA. Furthermore, in the instant method, the DNA of the maternal blood sample is not subjected to sodium bisulfite conversion or any other similar chemical reactions that alter base specificity, such as sodium

bisulfite conversion, nor the maternal blood sample is treated with a methylation-sensitive restriction enzyme(s) or through direct or indirect immunoprecipitation to enrich for a portion of maternal blood sample DNA.

[0046] Alternatively, the ODN-derivatized template DNA can be enriched on solid surfaces using an affinity tag that is introduced in the composition of the ODN. A useful affinity tag preferably is but not restricted to the biotin and can be used in the methods of the present invention. In this aspect, the invention includes an additional step of separating maternal nucleic acid sequences on a solid surface, for example on streptavidin/avidin beads, thereby further enriching for nucleic acid molecules containing labeled CG sites. Other approaches known in the art for physical separation of components can be also used. The captured DNA is to be used for further analysis without detachment or can be detached from beads in mild conditions, such as, for example pure water and heating to 95°C for 5 min.

[0047] III. PRODUCING OF TEMPLATE NUCLEIC ACID MOLECULES FROM THE SITE OF COVALENT LABELING

[0048] In the diagnostic method, a nucleic acid polymerase primes polymerization of the template nucleic acid at or around the site of labeling using the 3'-end of an externally added primer which is non-covalently attached to the ODN. Non-covalent bonding preferably involves base pairing interaction between the ODN and the externally added primer. In the preferred embodiments shown in Fig.8a and b, the structure of the ODN permits correct positioning of the externally added primer to the template at the site of the ODN attachment; the primer should be complementary to the sequence of the ODN while should not make any complimentary base pairing with the template nucleic acid at its 3'-end. In yet another aspect, shown in Fig.8c the primer at its 5'-end should be complementary to the sequence of the ODN while its 3'-end should make complementary base pairing with preferably at least 5 nucleotides and not more than 7 nucleotides of the template nucleic acid that are adjacent to the site of the attached ODN.

[0049] In the diagnostic method, typically after tagging of CGs in the maternal blood sample with the ODN, the tagged CGs and adjacent template nucleic acid are pre-amplified starting from the site of the attachment of the ODN. As used herein, the term "pre-amplified" is intended to mean that additional copies of the DNA are made to thereby increase the number of copies of the DNA, which is typically accomplished using the polymerase chain reaction (PCR).

[0050] In the preferred embodiment, the experimentally acquired value for the presence or availability of labeled CG that were tagged with the ODN in the maternal blood sample can be acquired by amplification of the DNA molecules starting from the tagged CG sites using the ODN-directed and partially ligation mediated (LM-PCR) polymerase chain reaction. The skilled person will be well aware of suitable methods for ligating adaptor sequences to the DNA fragments. In LM-PCR of the present invention, an adaptor nucleic acid sequences are added onto both ends of each DNA fragments through preferably sticky end or blunt-end ligation, wherein each strand of an adaptor sequences is capable of hybridizing with a primer for PCR, thereby amplifying the DNA fragments to which the linkers have been ligated. In this aspect of the present invention, only one strand of the ligated partially complementary double-stranded adaptor sequence is used to anchor a primer for amplification of the labeled template DNA strand as shown in Fig.8b. The second primer binds to the ODN sequence through complementary base pairing without contacts to the template DNA. The externally added primer should be at least 10 nucleotides and preferably at least 15 nucleotides in order to allow for a section of a primer to be involved in base pairing with the ODN without the complementary base pairing with the template DNA. This results in amplification of the labeled strands of nucleic acid samples, but not the original DNA fragment to which the adaptor sequences were ligated. In a preferred embodiment, the values of the amplified sequences are determined through real time quantitative polymerase chain reaction using oligonucleotide primers annealing within the regions shown in Tables 4, 5, 6 or 7 in the close vicinity to the labeled CGs as shown in Fig.8a. Methods of qPCR are well known in the art. Representative, non-limiting conditions for qPCR are given in the Examples.

[0051] Yet, alternatively, the values of the amplified sequences, or DLRs, are determined through massive parallel sequencing. In this aspect of the embodiments, one strand of the ligated double-stranded adaptor sequence is used to anchor a primer for amplification of the labeled template DNA strand as shown in Fig.8b. The second primer binds to the ODN sequence through complementary base pairing without contacts to the template DNA. Following PCR amplification, the values of the amplified sequences are determined through sequencing. This is only one exemplification of the presently described strategy for estimation of labeled nucleic acid through sequencing. In yet another aspect, the sub-fraction of the derivatized maternal sample DNA is selectively enriched through targeted PCR amplification prior to sequencing. Such PCR amplification makes use one primer bound complementary to the ODN or

a part of it in the presence (5-7 nucleotide complementarity right at the target sites) or absence of complementarity to the template DNA, and the second primer bound through non-covalent complementary base pairing to the template DNA in the chromosomal regions shown in Tables 4-7.

[0052] In another embodiment of the invention, the experimentally acquired value for the presence or availability of labeled CG is estimated through qPCR, in a maternal blood sample that has not been subjected to adaptor ligation or pre-amplification, as shown in Fig.8c. In this aspect, one primer to be used in qPCR hybridizes complementarily to the ODN altogether with 5-7 nucleotides of genomic template DNA near the derivatized CG site as described above and the second primer binds within the genomic DNA positions listed in Tables 4-7.

[0053] IV. DIFFERENTIALLY LABELED REGIONS (DLRs).

[0054] The diagnostic method of the invention employs a plurality of regions of chromosomal DNA wherein the regions are more intensively labeled in fetal DNA as compared to female peripheral blood samples. In theory, any chromosomic region with the above characteristics can be used in the instant diagnostic method. In particular, methods for identifying such DLRs are described in detail below and in the Examples (see Examples 1 and 2). Moreover, a large panel of DLRs for chromosomes 21, 13 and 18 suitable for use in the diagnostic methods, has now been identified (the strategy for identification of DLRs is shown in Fig.1).

[0055] Furthermore, representative examples of a subset of these DLRs (4175 tissue-specific u-DLRs; 163 pregnancy-specific u-DLRs; 8815 tissue-specific hm-DLRs, 679 pregnancy-specific hm-DLRs) have been used to accurately predict trisomy 21, in a method based on analysis of fetal-specific DLRs in chromosome 21 by sequencing of labeled CG sites in a maternal blood sample. We also evaluated labeling differences between maternal blood samples of healthy and T21 positive pregnancies and identified 3,490 u-DLRs and 2,002 hm-DLRs which are shown in Tables 4 and 5, respectively. The effectiveness of the disclosed regions and methodologies for diagnosing fetal aneuploidy T21 has been demonstrated in Fig.2 and 3. Such DLRs are shown in the lists of Tables 4 and 5, which provide the selected DLRs for chromosome 21.

[0056] According to the second exemplary embodiment, DLRs restricted to individual CGs (CG-DLRs) have been identified in chromosomes 21 and X. Representative

examples of a subset of these DLRs have been used to accurately predict trisomy 21, in a method based on analysis of fetal-specific hypomethylated or hyper-hydroxymethylated CG-DLRs in chromosome 21 by sequencing of labeled CG sites in a sample of maternal blood. Also, representative examples of a subset of these CG-DLRs have been used to accurately predict fetal gender, in a method based on analysis of fetal-specific CG-DLRs in chromosome X by sequencing of labeled CG sites in a sample of maternal blood. The effectiveness of the disclosed DLRs and methodologies for determination T21 aneuploidy and fetal gender has been demonstrated in Fig.4 and Fig.5. The list of DLRs is shown in Table 6.

[0057] In the third exemplary embodiment, representative examples of a subset of the CG-DLRs have been used to accurately predict trisomy 21 and fetal gender, in a method based on analysis of fetal-specific DLRs in chromosome 21 and chromosome X and/or Y in a sample of maternal blood by qPCR. Thus, the effectiveness of the disclosed regions and methodologies for diagnosing trisomy 21 and fetal gender has been demonstrated in Fig.6 and Fig.7.

[0058] In other methods for detecting a fetal aneuploidy, the plurality of DLRs may be on chromosome 13, chromosome 18, to allow for diagnosis of aneuploidies of any of these chromosomes. In theory, any DMR with the above characteristics in a chromosome of interest can be used in the instant diagnostic method. Methods for identifying such DLRs in chromosome 13 and chromosome 18 are described in Example 1 and the effectiveness of the disclosed regions has been demonstrated in Fig.9. The lists of selected DLRs for chromosomes 13 and 18 are provided in Table 7.

[0059] As used herein, the term "a plurality of DLRs" is intended to mean one or more regions or DLRs, selected from the list shown in Table 4-7. In various embodiments, the levels of the plurality of DLRs are determined for at least one region. Control regions or control DLRs also can be used in the diagnostic methods of the invention as a reference for evaluation of the labeled signal in the DLR region(s) of interest.

[0060] In a particularly preferred embodiment, the plurality of DLRs on chromosome 21 comprise one region or a combination of at least two regions, selected from the group shown in Table 6.

[0061] The invention also pertains to a composition comprising nucleic acid probes that selectively detect DLRs shown in Table 6.

[0062] The actual nucleotide sequence of any of the DLRs shown in Tables 4-7 is obtainable from the information provided herein together with other information known in the art. More specifically, each of the DLRs shown in Tables 4-7 is defined by a start base position on a particular chromosome, such as, for example "position 10774500" of chromosome 21. Furthermore, primers for targeted detection and/or amplification of a DLR can then be designed, using standard molecular biology methods, based on the nucleotide sequence of the DLR.

[0063] In another aspect, the invention provides nucleic acid compositions that can be used in the methods and kits of the invention. These nucleic acid compositions are informative for detecting DLRs. As described in detail in Example 3, at least one CG-DLR shown in Table 6 has been selected and identified as being sufficient to accurately diagnose trisomy 21 in a maternal blood sample during pregnancy of a woman bearing a trisomy 21 fetus.

[0064] V. DETERMINING LEVELS OF DLRS.

[0065] Labeling levels of the identified DLRs can be measured by sequencing or by qPCR. Labeling levels of a plurality of regions as described above are determined in the unmethylated or hydroxymethylated DNA sample, to thereby obtain a labeling value for the DNA sample. As used herein, the term "the levels of the plurality of DLRs are determined" is intended to mean that the prevalence of the DLRs is determined. The basis for this is that in a fetus with a fetal trisomy 21 there will be a larger amount of the DLRs as a result of the trisomy 21, as compared to a normal fetus. In another aspect, when the T21-specific DLR are being used, the amount of such DLRs can be larger or lesser then the amount in a fetus without a fetal trisomy 21.

[0066] In a preferred embodiment, the levels of the plurality of DLRs are determined by real time quantitative polymerase chain reaction (qPCR), a technique well-established in the art. The term “the labeling value” is intended to encompass any quantitative representation of the level of DLRs in the sample. For example, the data obtained from qPCR can be used as “the labeling value” or it can be normalized based on various controls and statistical analyses to obtain one or more numerical values that represent the level of each of the plurality of DLRs in the testing DNA sample. The procedure for detection of DLRs by qPCR including primers’ sequences, and the cycle conditions used were as described in Example 3.

[0067] In analysis of labeling intensity of DLRs by sequencing, the level of differential labeling was calculated for non-overlapping 100 bp regions. In more detail, for each window we computed the total log-transformed coverage and the fraction of identified CGs which we then normalized by the total log-transformed coverage and the fraction of identified CGs in reference chromosomes 16 (for uCG signal) and 20 (for hmC signal). For each window a full and null logistic regression models were fitted. Full model included coverage, identified fraction, and, for T21-specific DMRs, fetal sex and fetal fraction, as independent variables. Coverage and identified fraction were excluded from the null model. ANOVA Chi-squared test was used to compare full and null models to obtain p value. In cases where models did not converge fetal sex was removed and p value evaluated again. Model statistics were moderated using empirical Bayes. FDR was used to adjust p values for multiple testing and $q<0.05$ was used as significance threshold.

[0068] For each pregnancy-specific or tissue-specific DLR a leave-one-out cross-validation procedure was performed in order to determine its ability to diagnose T21. For each cross-validation cycle Bayesian generalized linear model (Gelman et al. 2008) with normalized coverage and identified CG as independent variables was constructed on the training samples. The model was then applied on the testing sample returning the predicted probability of the sample belonging to the T21 category. After all the cross-validation cycles the prediction probabilities for all samples were taken together. Various thresholds that would determine the discrete sample class from continuous probability measurement may have different effects on predictor's specificity and sensitivity. Therefore, a receiver-operating characteristic curve analysis was performed to estimate the effect of any threshold. The area under receiver-operating characteristic curve (AUC) indicates the overall accuracy of the model. Those DLRs for which the area under the curve was equal to 100% and, therefore, could achieve 100% prediction accuracy, were deemed to be the T21-predictive DLRs.

[0069] An approach that would combine individual DLRs into a single predictive model is also possible. Such model could be one of but not limited to elastic net, random forest or support vector machine. Model would be evaluated in the same way by assessing receiver-operating characteristic and using cross-validation for parameter tuning. Also, bootstrap could be used instead of cross-validation. Other model accuracy measures could be employed, and data could be transformed in different ways. Interactions of

DLRs could be taken into account to build new composite features that would be used for subsequent model training and evaluation.

[0070] VI. COMPARISON TO A STANDARDIZED REFERENCE VALUE.

[0071] The labeling value of the fetal DNA (also referred to herein as the "test value") present in the maternal peripheral blood is compared to a standardized reference value, and the diagnosis of trisomy 21 (or lack of such fetal trisomy 21) is made based on this comparison. Typically, the test value for the fetal DNA sample is compared to a standardized normal reference value for a normal fetus, and diagnosis of fetal trisomy 21 is made when the test value is higher than the standardized normal reference labeling value for a normal fetus. In another aspect, the test value can be lower than the standardized normal reference labeling value for a normal fetus.

[0072] Alternatively, the test value for the labeled DNA sample can be compared to a standardized reference labeling value for a fetal trisomy 21 fetus, and diagnosis of fetal trisomy 21 can be made when the test value is comparable to the standardized reference labeling value for a fetal trisomy 21 fetus.

[0073] To establish the standardized normal reference labeling values for a normal fetus, maternal blood samples from the pregnant women carrying a normal fetus are subjected to the same steps of the diagnostic method, namely amplification of the ODN-derivatized CGs and their neighboring genomic sequences to obtain a reference DNA sample, and then determining the labeling value and the levels of at least one region of chromosomal DNA by sequencing or qPCR wherein selected from Tables 4-7.

[0074] In order to establish the standardized normal reference methylation values for a normal fetus, healthy pregnant women carrying healthy fetuses or healthy non-pregnant women are selected. Pregnant women are of similar gestational age, which is within the appropriate time period of pregnancy for screening fetal chromosomal aneuploidy, typically within the first trimester of pregnancy. Standardized reference labeling values for a T21 fetus can be established using the same approach as described above for establishing the standardized reference values for a healthy fetus, except that the maternal blood samples used to establish the T21-specific reference values are from pregnant women who have been determined to be carrying a fetus with fetal trisomy 21.

Examples

[0075] Example 1. IDENTIFICATION OF DLRs

[0076] This example provides the methodology for the preparation of the labeled genomic libraries of the mentioned-above biological samples for genomic mapping of unmodified or hydroxymethylated CGs. Also, this example provides the strategy for DLRs determination and how DLRs for detection of trisomy T21 were preferentially chosen. Fig. 8b shows the application of the sequencing methodology for the identification of DLRs. In this example, DLRs in chromosomes 13 and 18 were also identified.

[0077] **Biological samples.**

[0078] We performed analysis of three distinct sample types, enabling a characterization of the unmethylated and hydroxymethylated CGs in DNA obtained from plasma of pregnant women; we created single CG resolution uCG and 5hmCG maps of placental chorionic villi (CV) tissue samples from the 1st trimester abortions (CVS; n=6 of uCG and n=3 of 5hmCG); cfDNA samples of female non-pregnant controls (NPC; uCG n=6 and 5hmCG n=7) and cfDNA samples of pregnant women carrying healthy fetuses (uCG n=7 and 5hmCG n=6) or fetuses with the trisomy 21 (uCG n=5 and 5hmCG n=4).

[0079] Circulating DNA from maternal blood samples was extracted using the MagMax Nucleic Acid Extraction kit (Thermo Fisher Scientific (TS)) or the QIAamp DNA blood Midi Kit (QIAGEN), and DNA from chorionic villi tissue was prepared by phenol extraction.

[0080] All the maternal peripheral blood DNA samples (1st trimester pregnancies) and chorionic villi samples (1st trimester abortions) were obtained at Tartu University Hospital (Tartu, Estonia) through collaboration with Tartu University (Estonia). Consent forms approved by the Research Ethics Committee of the University of Tartu (ethical permission No. 246/T-21 and 213/T-21) were collected for each of the mother participated.

[0081] **Mapping of unmodified/hydroxymethylated CGs in DNA extracted from biological samples.**

[0082] In uTOP-seq, 4-10 ng of cfDNA (or 100 ng of CV tissue DNA, sheared to 200 bp by Covaris sonicator) were labeled with 0.11 μM eM.SssI (Kriukienė et al. 2013) in 10 mM Tris-HCl (pH 7.4), 50 mM NaCl, 0.5 mM EDTA buffer supplemented with 200 μM Ado-6-azide cofactor (Masevicius et al, 2016) for 1 h at 30°C followed by thermal inactivation at 65°C for 20 min and Proteinase K treatment (0.2 mg/ml) for 30 min at

55°C and finally column purified (GeneJET PCR purification kit, (TS)). In hmTOP-seq, 5hmC glycosylation was carried with 5-10 ng of cfDNA supplemented with 50 µM UDP-6-azide-glucose (Jena Bioscience) and 2.5-5 U T4 β-glucosyltransferase (TS) for 1 h 37°C followed by enzyme inactivation at 65°C for 20 min and column purification (GeneJET PCR Purification kit (TS)). After ligation of the partially complementary adapters as described previously (Staševskij et al. 2017), covalently labeled DNA was supplemented with 20 µM alkyne-containing DNA oligonucleotide (which was biotinylated for construction of 5hmC maps) (ODN; 5'-T(alkyneT)TTTTGTGTGGTTTGGAGACTGACTACCAGATGTAACA-3' (or -(biotin)-3'), Base-click) and 8 mM CuBr: 24 mM THPTA mixture (Sigma) in 50% of DMSO, incubated for 20 min at 45°C and subsequently diluted to <1.5% DMSO before a column purification (GeneJET NGS Cleanup Kit, Protocol A (TS)). DNA recovered after biotinylation step was incubated with 0.1 mg Dynabeads MyOne C1 Streptavidin (TS) in a buffer A (10 mM Tris-HCl (pH 8.5), 1 M NaCl) at room temperature for 3h on a roller. DNA-bound beads were washed 2x with buffer B (10 mM Tris-HCl (pH 8.5), 3 M NaCl, 0.05% Tween 20); 2x with buffer A (supplemented with 0.05% Tween 20); 1x with 100 mM NaCl and finally resuspended in water and heated for 5 min at 95°C to recover enriched DNA fraction. Purified DNA after oligonucleotide conjugation (uCG) or biotin-enrichment (5hmC) was subsequently used in a priming reaction with 1 U Pfu DNA polymerase (TS), 0.2 mM dNTP, 0.5 µM complementary priming oligonucleotide (EP; 5'-TGTTACATCTGGTAGTCAGTCTCCAAACCACACAA-3). The reaction mixture was incubated at the following cycling conditions: 95°C 2 min; 5 cycles at 95°C 1 min, 65°C 10 min, 72°C 10 min. Amplification of a primed DNA library was carried out by adding the above reaction mixture to 100 µl of amplification reaction containing 50 µl of 2x Platinum SuperFi PCR Master Mix (TS) and barcoded fusion PCR primers A(Ad)-EP-barcode-primer (63 nt) and trP1(Ad)-A2-primer (45 nt) at 0.5 µM each. Thermocycler conditions: 94°C 4 min; 15 cycles (uCG) or 17 cycles (5hmC) at 95°C 1 min, 60°C 1 min, 72°C 1 min. The final libraries were size-selected for ~270 bp fragments (MagJET NGS Cleanup and Size Selection Kit, (TS)), and their quality and quantity were tested on 2100 Bioanalyzer (Agilent). Libraries were subjected to Ion Proton (TS) sequencing.

[0083] **Data analysis.**

[0084] Raw TOP-seq and hmTOP-seq sequencing reads were processed as described in Staševskij et al. (2017) and Gibas et al. (2020, accepted) except for the 3' sequence ends where adapter sequences were trimmed only if they were identified using cutadapt with maximum allowed error rate 0.1 (Martin 2011). Processed reads were mapped to reference human genome version hg19 and coverage for each CG dinucleotide was computed as the total number of reads starting at or around the CG dinucleotide on either of its strands. We define CG coverage as the total number of reads, c, on any strand starting within absolute distance, d. We retained only reads with $d \leq 3$. Only reads aligned to chromosomes 1 to 22, X and Y were used for further analysis. On average, 40% of the raw reads were retained for downstream analysis per sample.

[0085] Outlier identification was performed separately for uCG and 5hmC samples. CG coverage matrices were transformed using Hellinger transformation (Legendre and Gallagher, 2001) and then represented in two-dimensional space using non-metric multidimensional scaling (nMDS) with Bray-Curtis similarity index (Bray and Curtis, 1957). Samples that were further than two standard deviations away from the mean of their own sample group (cfDNA of non-pregnant controls, other cfDNA, CV tissue) in either nMDS1 or nMDS2 dimension were deemed outliers and removed from further analysis. There were three outlying samples in uCG and one in 5hmCG dataset.

[0086] **Identification of DLRs in chromosomes 21, 13 and 18.**

[0087] The strategy for DLR identification is show in Fig.1. We partitioned the chromosome 21 or 13 or 18 into 100 bp-wide non-overlapping windows. For each window we computed the total log-transformed coverage and the fraction of CGs covered which we then normalized by the total log-transformed coverage and the fraction of identified CGs in reference chromosomes 16 (for uCG) and 20 (for hmC).

[0088] First, we obtained the pregnancy-specific u-DLRs by comparing NPC samples with cfDNA samples of healthy pregnancies. For each window a full and null logistic regression models were fitted. Full model included coverage, identified fraction, and, for T21-specific DLRs, fetal sex and fetal fraction, as independent variables. Coverage and identified fraction were excluded from the null model. ANOVA Chi-squared test was used to compare full and null models to obtain p value. In cases where models did not converge fetal sex was removed and p value evaluated again. Model statistics were moderated using empirical Bayes adjustment. FDR was used to adjust p values for multiple testing and $q<0.05$ was used as significance threshold.

[0089] Next, we used the same strategy to obtain tissue-specific u-DLRs (FDR $q<0.05$; logistic regression) by comparing NPC and CV tissue samples. The same analytic approach was used separately for uCG and hmCG data. In case of hm-DLRs, nominal p value threshold was used when analysis did not yield any FDR significant DLRs.

[0090] Further, for each hypomodified pregnancy-specific and tissue-specific u-DLR or hyper-hydroxymethylated pregnancy-specific and tissue-specific hm-DLR in chromosome 21 a leave-one-out cross-validation procedure was performed in order to determine its ability to diagnose T21. For each cross-validation cycle Bayesian generalized linear model (Gelman et al. 2008) with normalized coverage and identified CG as independent variables was constructed on the training samples. The model was then applied on the testing sample returning the predicted probability of the sample belonging to the T21 category. After all the cross-validation cycles the prediction probabilities for all samples were taken together. Various thresholds that would determine the discrete sample class from continuous probability measurement may have different effects on predictor's specificity and sensitivity. Therefore, a receiver-operating characteristic curve analysis was performed to estimate the effect of any threshold. The area under receiver-operating characteristic curve indicates the overall accuracy of the model. Those DLRs for which area under the curve was equal to 100% and, therefore, could achieve 100% prediction accuracy, were deemed to be T21-predictive DLRs (Fig.1).

[0091] Using the strategy for DLR determination in chromosome 21, we obtained 2,761 pregnancy-specific u-DLRs (FDR $q<0.05$) and 16,555 fetal tissue-specific u-DLRs (FDR $q<0.05$; logistic regression). For hm-DLR identification, we used nominal $p<0.05$ threshold and identified 4,930 pregnancy-specific hm-DLRs and 15,986 tissue-specific hm-DLRs.

[0092] An in-depth investigation of the identified DLRs between non-pregnant female peripheral blood and placental DNA samples or non-pregnant and pregnant female cfDNA samples, has led to the selection of a list of DLRs located on chromosome 21 for diagnosing trisomy 21. The selection criteria of the regions were based firstly on the labeling intensity status of the regions in maternal blood samples and CV DNA samples, or on the labeling intensity status of the regions in the non-pregnant and pregnant female maternal blood samples. More specifically, the selected regions should demonstrate a high labeling intensity status in CV tissue DNA and a low labeling intensity or absence of labeling in peripheral blood samples of NPCs, or

should show a high labeling intensity status in pregnant female blood samples and a low labeling intensity or absence of labeling in NPCs. Using leave-one-out cross-validation as described above we discovered 4175 tissue-specific u-DLRs; 163 pregnancy-specific u-DLRs; 8815 tissue-specific hm-DLRs, 679 pregnancy-specific hm-DLRs in chromosome 21 that classified the samples according to fetal karyotype with 100% accuracy (the selected DLRs are shown in Tables 4 and 5, for the uCG and hmCG signal, respectively) (Fig.2).

[0093] Furthermore, considering global epigenetic changes in Down syndrome affected fetuses (Jin et al. 2013), we also employed an alternative approach to identify the trisomy 21-specific DLRs. We evaluated modification differences between cfDNA samples of healthy and T21-diagnosed pregnancies and identified differentially modified DLRs. A logistic regression model was fitted to each 100 bp window with the CG-coverage and CG-fraction as independent variables and karyotype as the response variable, as above. In addition, we adjusted for possible confounding effects of fetal fraction and fetal gender which could not be accounted for in the previous analyses. With such approach, we identified 3,490 u-DLRs and 2,002 hm-DLRs (FDR $q<0.05$; logistic regression). The selected T21-specific DLRs that discriminate most the sample groups of healthy and T21-diagnosed pregnancies are shown in Tables 4 and 5, for uCG and hmCG signal, respectively) (Fig.3).

[0094] Using the same strategy for DLR identification shown in Fig. 1 we also identified DLRs in chromosomes 13 and 18. For chromosome 13, we obtained 1,394 pregnancy-specific u-DLRs (FDR $q < 0.05$) and 25,091 fetal tissue-specific u-DLRs (FDR $q<0.05$; logistic regression) and using nominal $p<0.05$ threshold 4,255 pregnancy-specific hm-DLRs and 22,526 tissue-specific hm-DLRs. For chromosome 18, we obtained 1,321 pregnancy-specific u-DLRs (FDR $q<0.05$), 22,121 fetal tissue-specific u-DLRs (FDR $q<0.05$; logistic regression) and 3,626 pregnancy-specific hm-DLRs and 20,780 tissue-specific hm-DLRs. The lists of the selected DLRs across chromosomes 13 and 18 are shown in Table 7 (Fig.9).

[0095] The total number of fetal specific hypomethylated and hyper-hydroxymethylated tissue- and pregnancy-specific DLRs identified across chromosomes 21, 13 and 18 is summarized in Table 1.

[0096] [Table 1. Numbers of pregnancy- and tissue-specific DLRs identified across chromosomes 21, 13 and 18.]

Chromosome	No. of hypo-methylated tissue-specific u-DLRs	No. of hypo-methylated pregnancy-specific u-DLRs	No. of hyper-hydroxymethylated tissue-specific hm-DLRs	No. of hyper-hydroxymethylated pregnancy-specific hm-DLRs
Chr21	4175	163	8815	679
Chr13	25091	1394	22526	4255
Chr18	22121	1321	20780	3626

[0097] Example 2. IDENTIFICATION OF INDIVIDUAL LABELED CGs FOR DETECTION OF TRISOMY 21 AND FETAL SEX

[0098] This example provides the strategy for determination of individual labeled CGs (CG-DLRs) following analysis of the samples described in Example 1 that can be used for detection of fetal trisomy T21.

[0099] An investigation of labeling intensities of uCGs and hmCGs in peripheral blood samples of women that were confirmed to be carrying a fetus with trisomy 21 against labeling intensities of uCGs and hmCGs in the three types of control samples, i.e. placental CV tissue DNA, peripheral blood samples of non-pregnant women and peripheral blood samples of women pregnant with healthy fetuses, has led to the selection of individual CG-DLRs located on chromosome 21 for detection of fetal T21. The selection criteria of the CG-DLRs were based firstly on a labeling intensity status of CGs in blood samples of women pregnant with T21-diagnosed fetuses. More specifically, the selected CG-DLRs should demonstrate a high labeling intensity status in blood samples of women pregnant with T21-diagnosed fetuses and a low labeling intensity or absence of labeling in the three other sample types: CV tissue DNA, peripheral blood samples of NPC and pregnant female carrying a healthy fetus.

[0100] The CGs with non-zero coverage and non-zero variance were used. The read coverage was log transformed. CGs from chromosome 21 were used for detection of T21 markers. Samples from non-pregnant female and pregnant with healthy fetuses women and CV tissue samples were marked as control, whereas only the female samples with T21 positive fetuses were marked as cases. A linear regression model was fitted for every CG, and resulting model fits were moderated using empirical Bayes adjustment. The CGs with FDR q value less than 0.05 and log fold change more than 1.2 were taken as significant. The list of the selected T21 CG-DLRs is shown in Table 6 (Fig.4).

[0101] **Identification of CG-DLRs for determination of fetal sex.**

[0102] Similarly, CGs from chromosome X (and Y) were analyzed for identification of CG-DLRs for fetal gender determination. A no intercept linear regression model was fitted for each CG and a contrast fit was used to determine differences between male and female samples. Resulting model fits were moderated using empirical Bayes adjustment. The CGs with FDR q value less than 0.05 and log fold change more than 1 were taken as significant. The list of the selected gender CG-DLRs is shown in Table 6 (Fig.5).

[0103] Example 3. EVALUATION OF CG-DLRs BY QPCR

[0104] In this example, individual CGs or CG-DLRs identified according to the methodology described in Examples 1 and 2 were used for their validation by qPCR. A flowchart diagram of the methodology is shown in Fig. 8a and c. Several experiments were carried out to analyze and validate the identified DLRs or individual CGs. These experiments include an evaluation of the variability and reproducibility of the labeling intensity among different individuals and among technical replicates.

[0105] **Detection of fetal trisomy T21 by qPCR.**

[0106] The difference in labeling intensity at specific CG-DLRs, shown in Table 6, was tested in blood samples of pregnant female carrying healthy or T21-diagnosed fetuses (Fig.6). Briefly, DNA of maternal blood sample was treated as described in Example 1. Then, 0.5 ng of the final amplified DNA were used for measurement of the labeling intensity of u-CG-DLRs and hm-CG-DLRs by qPCR with a Rotor-Gene Q real-time PCR system (Qiagen) using Maxima SybrGreen/ROX qPCR Master Mix (TS). 0.3 mM of each primer pair used in each reaction, wherein one of the primers binds complementarily to a genomic region in close proximity to the CG site (its 5' end anneals more than 5 nucleotides to the CG being analyzed), and another primer binds in a vicinity of the CG to allow PCR amplification of the region (or selected DLR) to occur. The amplification conditions were set as: 95°C for 10 min, 40 cycles 95°C for 15 s, 60°C for 60 s.

[0107] In this embodiment, the plurality of CG-DLRs on chromosome 21 comprises one region or a combination of at least two regions, selected from Table 6. The invention also pertains to a composition comprising nucleic acid probes that selectively detect the regions shown in Table 6, preferably, the pair/set of oligonucleotide primers are selected from Table 2.

[0108] [TABLE 2. First position of the genomic coordinates of the selected u-CG-DLRs and hm-CG-DLR on chromosome 21 and nucleotide sequences of the primers for determination of fetal trisomy T21 by qPCR.]

u-CG-DLR coordinate	PCR product, length	Primer sequence
Chr21: 29732020	29732020-1, 109 bp	Seq ID 1: 5'CAACTCCCTACAGCCCCTTG
		Seq ID 2: 5'AAATTGCATGATTCCCCTGACA
Chr21: 29732020	29732020-2, 67 bp	Seq ID 3: 5'ATGACTGGCTTATTTCACTTAGCATC
		Seq ID 4: 5'AGTCCTGCTATATGCAACACCTT
Chr21:33462648	33462648, 97 bp	Seq ID 5: 5'GGTATTTACAAAAGTCTGCACCTTAGTC
		Seq ID 6: 5'CTGCCAACTTCACCCAGAGT
Chr21:34672959	34672959, 73 bp	Seq ID 7: 5'TAGAAATCTTTAGGAGGTGGTGAATG
		Seq ID 8: 5'CATGGTGGAAGAGATGGGC
hm-CG-DLR coordinate	PCR product, length	Primer sequence
Chr21:30341466	30341466, 101 bp	Seq ID 9: 5'GCAGAGGTTGCAGTGAGCTG
		Seq ID 10: 5'GTCTGGATGCAAAAATCCCTTT
Chr21: 46964859	46964859, 88 bp	Seq ID 11: 5'GCTGTCCCTGTGGTTAAGGTC
		Seq ID 12: 5'GCCACCACAACAGCACCA
Chr21:44084933	44084933, 89 bp	Seq ID 13: 5'CCCCATCACCAACTTCACTC
		Seq ID 14: 5'GAAACTGAGTCTCTCGCAAGG

[0109] **Detection of fetal gender by qPCR.**

[0110] In another embodiment of the invention, the experimentally acquired value for the presence or availability of labeled CGs is estimated through qPCR, in a total untreated, i.e. non-ligated to adaptors and non-preamplified, maternal blood sample as shown in Fig.8c, for fetal gender determination. Notably, analysis of the selected CG-DLRs in chromosome X is sufficient for detection of fetal gender. This is only one exemplification of the strategy; the similar strategy may be used for determination of fetal trisomy.

[0111] Firstly, the difference in the abundance of DLR regions starting at specific CGs shown in Table 6 was tested in the 1st trimester CV tissue DNA of both genders and non-pregnant female blood sample DNA. Then, we mixed CV tissue DNA and non-pregnant female peripheral blood plasma DNA to the ratios 20/80 and 0/100 of the CV and plasma DNA, respectively. 10 ng of each sample mixture were labeled and derivatized with the ODN as described above. Next, 1.5 ng of each sample was analyzed in replicates by qPCR. The coordinates of the u-CG-DLRs on chromosomes X and Y and primers for qPCR are shown in Table 3.

[0112] [TABLE 3. First position of the genomic coordinates of the selected u-CG-DLRs on chromosomes X and Y and nucleotide sequences of the primers for determination of fetal gender by qPCR.]

u-CG-DLR coordinate	PCR product length	Primer sequence
ChrX: 138802516	160 bp	Seq ID 15: 5'-CCTCTCTATGGGCAGTCGGTGATTGACCTGCTTCCTGTGTTGAGC
		Seq ID 16: 5'-TGTTACATCTGGTAGTCAGTCTCCAAACCACACAAAAAAGTGGAG
ChrY: 14774154	123 bp	Seq ID 17: 5'-GTAGAAAAGGGGAAGAAAAGTAGAAACAGC
		Seq ID 18: 5'-TGTTACATCTGGTAGTCAGTCTCCAAACCACACAAAAAAGCCCCT

[0113] In more detail, DNA of each sample were labeled with eM.SssI MTase in the presence of 200 μM Ado-6-azide cofactor for 1 hour at 30°C as described in Example 1 followed by column purification (Oligo Clean&Concentrator-5, Zymo Research). Then, DNA eluted in 8 ul of Elution Buffer was supplemented with 20 uM alkyne DNA oligonucleotide (ODN, 5'-T(alkyneU)TTTTGTGTGGTTTGGAGACTGACTACCAGATGTAACA), the mixture of 8 mM CuBr and 24 mM of THPTA (Sigma) in 50% of DMSO, incubated for 20 min at 45°C and subsequently diluted to <1.5% DMSO before purification through the GeneJET NGS Cleanup kit (TS). 1.5 ng of the purified DNA were used for measurement of the labeling intensity of uCGs by qPCR with a Rotor-GeneQ real-time PCR system (Qiagen) using Maxima SybrGreen/ROX qPCR Master Mix (TS). 0.3 mM of each primer pair was used in each reaction, wherein one of the primers binds complementarily to the ODN and to 5 nucleotides of the template genomic DNA adjacent to the derivatized CG site, and another primer binds in a vicinity of the CG to allow PCR amplification of the region (or selected DLR) to occur. The amplification program was set as: 95°C for 10 min, 40 cycles 95°C for 15 s, 65°C for 30 s, 72°C for 30 s (Fig. 7a,b,c).

[0114] Example 4. QPCR-BASED NONINVASIVE DIAGNOSTICS OF TRISOMY 21

[0115] This example describes the independent validation of non-invasive testing for fetal trisomy 21. For this purpose, we have performed qPCR-based analysis of a small group of samples which have not been used in the previous Examples for identification of validation of DLRs. The group consists of 3 maternal peripheral blood samples from

women bearing a normal fetus and 2 maternal peripheral blood samples from women bearing a trisomy 21-affected fetus.

[0116] These maternal peripheral blood samples were obtained at a gestational age of between 12-13 weeks at Tartu University Hospital (Tartu, Estonia) through collaboration with Tartu University (Estonia). Consent forms approved by the Research Ethics Committee of the University of Tartu (ethical permission No. 246/T-21 and 213/T-21) were collected for each of the mother participated.

[0117] The fetal specific approach used herein is illustrated schematically in Fig. 8a, wherein the ability to discriminate normal from trisomy 21 cases is achieved by comparing the values obtained from normal and trisomy 21 cases using T21-specific differentially modified CG dinucleotides, or CG-DLRs, located on chromosome 21. A fetus with trisomy 21 has a differentially modified genome in relation to normal genome and an extra copy of chromosome 21, and thus the increased abundance of a fetal specific region compared to a normal fetus. Therefore, the amount of T21-specific fetal region will increase more in fetuses with trisomy 21 compared to normal cases.

[0118] An in-depth investigation of our previously identified DLRs, described in Examples 1 and 2, has led to selection of DLRs located on chromosome 21. A group of selected DLRs has been used for identification of fetal trisomy 21 by qPCR (Example 3). These DLRs demonstrate a hypomethylated or hyper-hydroxymethylated, and thus more labeled, status in peripheral blood DNA of pregnant women carrying a T21-diagnosed fetus and a hypermethylated or hypo-hydroxymethylated, and thus less labeled, status in CV tissue DNA and peripheral blood DNA of pregnant women carrying a normal fetus and in peripheral blood DNA of non-pregnant women in order to achieve the enrichment of fetal T21-specific CG-labeled regions. These selected CG-DLRs shown in Table 2 were used for analysis of the samples by qPCR.

[0119] The procedure of sample processing and qPCR cycle conditions used were as described in Examples 1 and 3. Briefly, 5-10 ng of maternal cfDNA was covalently derivatized with the ODN and the adaptors were ligated to the ends of DNA fragments. The labeled CG regions were enriched through the ODN-mediated polymerization of the adjacent genomic regions and such regions were subsequently amplified using the primers complementary to the ODN and one strand of the adaptors. Then, the amounts of u-CG-DLRs and hm-CG-DLRs was calculated by qPCR as shown in Example 3 using a combination of CG-DLRs and qPCR primers listed in Table 2.

[0120] Comparing the obtained test values of the samples with known karyotype (the T21-diagnosed samples show lower test values than normal cases), all T21-diagnosed samples were confirmed as having trisomy 21, indicating 100% specificity and 100% sensitivity of the approach (Fig.10).

APPENDICES

[0121] [Table 4. The coordinate is shown for the first base pair of 100 bp u-DLRs in chromosome 21]

Pregnancy-specific u-DLRs							
10774500	26212900	35812700	38891600	43228800	45323700	46743900	47331000
11025700	26835100	35819500	38946900	43470300	45330400	46751000	47331900
15169700	28041300	35879100	38969700	43519400	45355100	46808700	47362600
15770300	28074300	36073900	39202100	43708100	45392900	46812700	47390300
16130900	28759100	36089600	39507100	43714600	45400400	46837800	47419000
16577200	28942700	36220800	39544400	43728400	45597600	46847100	47451100
17308600	29288000	36437300	39690100	43782100	45734900	46934400	47479200
17333200	31008200	36478700	39891300	43864600	45748300	46946300	47498400
18086100	32374100	36701300	41001100	43864800	45753500	46973100	47502800
18676300	32639100	36917100	41292800	43876000	45790600	46995500	47536100
18940600	32915800	37085900	42099000	44061700	45842200	46997700	47542700
20437200	33522600	37192500	42127100	44113000	46036100	46999800	47549500
20608700	33533900	37218700	42212900	44191100	46182600	47057200	47559700
21354200	33591700	37352800	42424900	44196200	46312000	47181700	48047900
21670800	33954100	37493000	42595400	44208900	46359300	47211600	48079600
22564300	34369300	37527800	42694800	44346000	46396600	47212000	9901200
24387600	34406400	37970500	42732500	44474700	46415700	47213500	
24474800	34483300	38066600	42746400	44511200	46418600	47245100	
25233800	34851100	38092400	42928900	44754300	46545400	47273200	
25693500	35365900	38104700	42936000	45065800	46720900	47287600	
26152100	35531600	38385400	43112600	45156300	46738900	47315300	
Tissue-specific u-DLRs. Only 1000 selected DLRs are shown							
10027900	15984000	17333200	18351000	19378400	20630400	21741100	22819200
10395200	15993500	17333300	18356700	19379400	20633700	21743700	22820400
10527800	16003800	17344200	18361400	19382400	20655700	21745700	22830600

10551600	16009000	17364800	18387200	19390200	20668400	21746900	22842800
10603000	16010900	17377300	18389400	19391100	20685000	21755000	22848600
10713200	16015300	17382300	18399000	19392100	20698000	21765500	22866100
10757400	16016600	17384200	18418800	19392900	20701500	21771800	22880300
10762300	16025200	17389700	18426600	19397200	20706300	21775600	22896500
10762500	16033800	17392100	18433700	19400200	20715200	21775700	22925400
10807400	16039700	17396700	18444200	19406900	20719900	21802300	22926000
10812800	16046800	17400700	18449500	19415500	20748600	21809600	22926600
10821600	16051800	17405400	18461000	19427200	20749700	21814100	22936200
10824800	16056200	17405500	18483000	19427900	20759800	21826100	22947400
10826000	16058300	17422500	18492200	19429700	20763100	21831900	22970300
10836600	16065200	17423000	18497900	19432000	20780900	21832100	22975500
10851100	16065400	17423200	18519100	19443000	20790400	21838500	22981800
10851700	16066400	17434500	18527800	19443800	20806100	21840500	22984400
10862500	16076200	17440300	18535800	19486900	20808400	21850900	23000600
10868300	16087900	17443100	18550100	19495300	20814400	21851100	23009700
10889500	16099900	17456000	18570400	19495400	20825700	21851800	23012900
10898800	16104500	17461800	18587100	19496300	20834300	21852800	23032500
10990600	16105700	17464000	18603400	19501800	20867700	21852900	23058900
11021600	16120400	17464100	18611400	19506400	20869900	21856600	23061100
11025700	16127400	17466600	18618800	19508200	20876400	21883000	23061600
11034800	16130900	17466800	18619900	19514500	20876600	21888700	23094800
11048000	16141200	17467500	18622300	19523800	20889300	21891500	23095300
11096200	16151900	17481900	18634200	19526200	20893200	21892000	23101600
11100600	16159500	17505400	18637600	19526700	20898100	21893600	23126800
11106600	16163900	17506600	18643800	19530700	20900800	21900500	23129400
11127600	16176600	17517700	18668800	19531400	20903700	21928500	23185500
11153500	16182300	17519700	18676300	19552600	20912300	21935000	23191700
11161300	16218500	17528400	18677300	19562100	20920500	21938500	23196100
11180200	16229300	17532700	18678900	19569200	20930800	21940100	23235500
14344600	16259600	17561300	18685400	19569800	20941500	21950400	23236400
14361600	16260700	17561800	18699800	19591300	20944400	21965200	23240500
14372500	16288000	17573800	18707300	19596200	20956500	21978100	23275900
14383200	16291200	17582800	18707600	19603500	20967800	21988500	23276000

14390500	16307500	17584600	18715900	19613900	21013800	22001400	23290600
14395600	16396400	17586100	18716200	19615600	21024900	22018800	23296900
14411800	16443400	17595800	18720000	19616500	21050300	22031600	23303600
14431400	16452000	17619000	18740600	19619500	21074500	22043300	23326200
14699500	16458600	17620100	18741900	19635700	21081100	22060800	23328300
14805600	16461400	17621100	18748500	19643700	21091600	22062000	23328700
14828200	16518900	17627600	18778900	19649100	21101600	22080100	23338700
14897900	16520800	17633400	18783100	19649900	21104100	22086700	23341100
14900100	16528100	17635100	18788000	19657900	21104300	22105900	23345000
14944200	16553000	17637900	18797600	19688500	21108700	22106200	23354800
14950900	16556500	17643000	18798400	19708400	21110400	22115900	23356100
15036300	16558500	17663200	18800100	19719700	21136800	22133500	23360300
15054200	16565200	17666500	18819100	19727600	21140800	22134300	23365200
15078000	16569700	17670500	18821500	19731400	21143400	22134400	23372200
15083000	16582300	17683800	18831800	19738100	21149400	22138200	23382900
15087900	16604700	17698700	18834000	19743000	21151800	22144800	23389900
15141900	16606800	17703300	18836800	19756000	21158900	22145200	23401700
15194400	16614900	17707500	18839500	19757000	21160100	22159500	23403000
15255400	16628500	17709400	18848600	19759100	21167300	22161000	23404600
15323900	16629000	17710800	18857500	19763800	21172800	22171200	23405000
15356300	16633000	17752400	18880600	19786900	21174500	22173800	23405200
15372700	16643000	17758800	18900200	19794500	21183100	22174700	23407500
15398100	16644600	17759500	18907500	19795600	21186600	22218100	23426000
15412500	16654100	17784400	18909300	19824300	21189400	22224000	23456500
15434900	16685000	17788300	18910100	19824700	21189800	22234100	23467900
15435600	16686400	17813400	18914600	19825200	21192600	22243700	23490200
15445400	16694900	17827300	18918900	19831700	21223200	22255400	23492700
15451600	16707300	17828200	18921800	19837300	21224300	22264200	23502200
15528500	16732500	17832300	18942200	19849300	21226200	22265000	23507500
15546200	16744000	17838700	18943400	19858300	21233900	22270700	23510800
15576100	16756800	17856200	18951300	19859200	21238500	22278500	23534900
15589600	16777100	17864500	18955000	19865900	21239300	22280600	23576400
15607200	16786100	17864900	18956800	19867200	21273800	22281500	23582100
15608600	16798600	17875800	18998400	19890600	21282600	22281800	23611500

15609000	16859000	17877800	18999200	19891100	21283300	22294100	23657500
15615500	16860400	17885300	19000900	19903500	21301000	22312200	23659400
15620000	16863700	17896400	19010800	19911700	21304400	22313200	23667100
15629000	16872300	17898500	19023900	19912700	21310100	22319300	23672700
15629700	16875900	17914500	19026000	19940300	21316200	22323700	23696400
15630300	16885500	17916200	19030300	19952500	21326500	22325600	23718600
15633600	16892300	17935900	19041100	19979900	21333300	22331400	23779300
15639900	16894100	17939600	19044700	19985200	21354100	22333100	23793400
15641300	16904300	17961100	19047700	20009000	21354200	22337300	23803600
15646800	16922200	17976600	19049500	20015100	21365300	22337800	23808300
15650300	16932600	17982200	19053900	20024300	21366400	22347600	23826100
15665500	16934400	17985200	19054300	20120500	21381000	22347900	23831100
15670200	16936900	17997200	19063100	20120600	21388800	22351600	23833100
15673600	16942700	18009700	19082400	20128100	21400400	22356700	23833700
15676400	16943100	18023100	19095100	20131000	21404000	22371200	23833900
15686900	16963300	18032400	19098100	20131500	21415000	22378400	23835900
15687000	16964400	18038700	19100300	20149600	21416100	22381400	23840200
15703200	16967500	18040100	19108000	20180700	21416900	22383100	23853500
15709200	16969300	18049300	19110700	20200400	21433900	22385800	23859400
15709900	16979600	18054800	19114200	20208800	21436900	22392900	23871200
15713500	16996400	18077000	19117100	20227000	21454900	22402900	23876400
15715700	16997200	18086100	19117200	20239300	21460100	22423000	23877000
15717600	17008700	18097800	19117800	20239400	21467700	22456400	23880000
15724200	17012700	18102600	19117900	20260500	21475300	22459000	23890200
15741400	17017800	18109800	19119800	20268300	21476300	22462200	23890500
15757600	17025900	18118400	19132800	20286400	21482800	22477300	23891200
15760000	17030000	18127000	19147700	20289300	21490300	22478300	23901600
15770300	17062200	18145400	19203900	20295300	21493900	22482400	23917700
15782400	17063900	18154600	19205400	20320600	21496200	22495500	23918900
15791300	17064700	18157800	19205800	20322700	21496700	22498300	23923900
15806500	17074500	18163100	19205900	20326300	21499100	22519200	23931300
15807300	17079000	18168000	19206700	20337600	21501000	22534100	23934300
15810000	17086600	18169800	19218500	20349500	21501100	22547500	23941700
15811800	17090900	18172800	19219800	20353400	21509600	22562200	23950900

15820300	17094100	18179000	19221900	20356400	21516800	22582000	23951200
15833000	17101300	18187900	19222000	20362800	21522400	22606900	23952600
15834600	17103200	18196800	19223900	20364900	21533000	22607100	23959700
15838300	17111700	18200900	19248800	20394300	21548500	22615800	23972500
15839100	17116600	18217200	19251000	20395900	21567700	22631300	23981400
15845600	17133800	18221600	19252500	20429600	21594700	22646300	23983100
15853600	17154600	18223800	19256700	20436900	21616500	22687500	23992300
15866100	17160400	18233400	19274300	20453600	21636700	22690100	23999500
15876600	17207100	18251500	19288100	20462000	21636900	22697000	24018400
15882100	17218700	18252100	19288200	20476500	21637100	22701400	24018800
15899800	17276800	18259400	19296000	20500600	21643600	22744100	24025300
15909400	17278400	18267400	19302000	20506900	21670800	22745700	24057800
15928100	17279200	18274100	19305800	20519200	21672100	22754900	24061000
15936100	17285600	18301200	19317400	20536400	21678300	22762300	24074500
15941400	17292700	18310100	19328300	20548000	21678700	22769500	24084900
15947900	17296700	18315000	19334800	20566900	21679300	22773000	24089300
15955700	17300600	18317500	19335700	20581300	21691700	22790800	24105100
15970000	17303600	18322500	19346600	20591500	21714200	22809100	24113400
15972100	17315700	18325500	19354400	20608700	21719300	22809300	24114000
15982800	17320300	18334900	19375100	20614800	21739500	22818500	24139100
The selected T21-specific u-DLRs							
15078000	20843100	24937300	31821900	34672900	42770000	47588600	38660800
15413700	21451400	25752700	32258800	34690700	43291800	9875200	41842500
15486300	21739100	25887700	32294400	34872200	43644200	18679500	45355100
15490100	21771600	26081000	32526200	35234300	43933400	22295500	45734900
15680600	22449400	28463100	32748600	36191800	44303300	22450800	45770300
16547900	22459500	29713600	32900300	36193500	44303600	26152100	45946100
17461600	22530700	29732000	33572800	37070300	45151100	31408200	46316400
18123400	22715800	29879100	33831600	38032500	45597700	32639100	48079600
18499700	22908900	31306700	33875700	39652400	45708400	33533900	
19286900	22921700	31357700	33919200	40405900	46009400	33591700	
20037100	23004300	31489300	34092400	41285400	46780500	33840400	
20042500	23380000	31568000	34460800	42378900	47329500	36220800	

[0122] [Table 5. The coordinate is shown for the first base pair of 100 bp hm-DLRs in chromosome 21]

Pregnancy-specific hm-DLRs							
15078000	30594600	35231100	38321300	42695100	44301100	45492400	46747600
15442500	30642600	35246100	38335200	42738300	44326600	45494400	46748200
15496700	30658000	35272400	38441400	42746900	44329100	45498400	46748800
15970900	30669700	35293400	38443100	42760300	44334600	45542100	46769800
16119600	30675000	35344900	38454300	42824800	44347000	45560600	46776900
16193000	30708600	35349600	38541100	42851600	44350500	45568800	46777600
16213800	30719600	35444700	38566700	42860000	44354200	45571400	46780700
16214600	30755900	35500600	38567300	42860500	44361200	45572100	46784600
16240400	31030700	35516100	38579100	42874000	44366300	45614500	46790700
16311800	31223600	35560500	38634900	43030200	44381700	45621700	46799200
16326500	32471400	35587700	38636200	43050800	44383700	45630000	46869900
16389000	32510000	35616700	38662600	43092100	44387300	45632500	46870200
16395200	32575500	35712600	38676800	43115200	44387900	45637600	46886600
16396200	32581400	35718200	38732000	43135400	44442400	45658000	46902700
16407900	32678200	35755000	38750600	43154800	44448300	45659300	46911600
16488800	32711300	35761500	38766900	43171100	44461800	45663300	46914600
16511900	32725600	35879600	38767300	43172900	44467700	45675100	46924300
16572400	32831900	35884200	38822100	43175500	44475900	45704700	46925400
16572800	32840800	35886800	38832800	43175800	44491400	45705900	46931500
16582800	32898600	35893700	38888500	43179100	44508400	45724700	46932100
16591800	32915200	35894400	38890600	43228700	44573600	45743000	46932200
16643600	32915700	35922100	38920900	43228800	44591600	45747000	46932700
16682300	32934700	35940800	38942100	43239800	44594100	45751700	46934200
16684400	32986500	35963200	38964000	43241000	44595900	45773900	46945700
16706000	32999300	36072400	39104900	43242000	44614600	45796000	46950400
16763200	33005100	36076400	39343900	43245800	44626800	45825100	46959000
16828600	33012700	36079700	39461200	43256600	44704800	45826500	46959800
16884200	33019200	36081500	39490900	43293000	44732600	45843300	46971900
16888000	33026800	36108600	39594800	43314600	44762100	45880200	46973300
17036800	33057900	36157900	39598900	43319100	44782500	45883300	46977800
17086600	33085600	36164200	39632900	43319500	44784900	45898800	46980800

17099100	33671200	36165000	39706900	43344400	44802600	45928000	47051900
17099800	33723100	36198900	39755900	43351200	44814600	45956000	47124500
17117000	33725000	36202900	39761300	43376500	44817100	46034900	47188800
17193500	33763500	36208100	39851400	43384100	44837100	46055600	47239300
17550000	33792500	36242900	39948700	43394500	44870700	46063700	47251700
17561300	33805800	36243000	39970500	43412800	44871500	46068700	47288700
17578000	33823700	36244900	39984000	43443300	44872300	46142700	47290300
17592700	33857800	36246600	40119400	43446200	44876300	46154200	47333300
17666600	33881100	36288500	40123900	43456200	44883100	46182800	47403100
17734100	33901800	36329200	40134200	43499900	44883700	46214100	47418400
18846300	33948600	36331900	40166900	43506100	44900600	46235600	47422300
18857600	33957500	36345600	40176200	43567000	44916900	46253400	47423800
18883100	33966100	36389700	40244600	43571300	44924000	46270000	47457000
19052700	34062900	36444900	40277900	43577500	44928000	46271300	47515500
19066500	34069100	36595800	40285300	43603000	44928800	46272800	47520800
19069400	34075400	36656600	40293700	43621300	44935600	46284800	47530400
19071700	34185900	36693800	40293800	43679800	45039800	46286600	47538400
19106400	34338600	36829500	40310600	43681500	45040100	46307200	47541800
19118800	34402600	36840000	40349000	43786800	45064600	46308100	47542400
19150100	34405900	36944400	40352500	43790900	45067700	46319500	47545100
19173600	34409600	37015500	40356600	43801700	45092200	46320800	47552700
19176300	34447800	37033700	40357800	43813600	45105500	46326500	47556200
19228600	34477900	37038600	40358000	43817900	45109700	46328000	47574100
21311300	34517400	37169900	40372800	43844600	45116700	46349100	47577700
21626600	34556200	37277600	40394400	43846300	45129900	46371800	47608400
22421400	34618500	37334100	40395100	43846800	45131700	46379600	47617600
23735900	34623200	37436800	40453300	43869600	45147000	46396500	47624100
25184700	34625700	37456000	40466200	43872000	45153200	46398100	47630200
25711300	34638000	37459800	40466900	43893300	45182000	46401200	47631900
27006500	34643100	37537100	40479000	43896600	45190800	46403700	47632900
27157900	34717700	37542300	40479900	43898300	45191200	46407900	47676300
27190500	34722900	37554900	40542000	43915300	45228200	46412700	47686900
27287800	34728000	37559100	40568900	43943900	45229000	46442000	47700500
27332200	34753100	37609600	40637700	43977800	45232900	46449800	47715600

27397400	34754700	37627900	40730800	43988800	45234200	46451400	47764000
27424500	34756700	37639400	40741800	44003400	45242100	46455200	47766000
27434400	34774100	37646900	40763200	44004600	45244300	46455400	47780500
27445300	34790400	37658400	40773600	44006200	45246200	46461600	47786500
27449100	34790500	37674700	40815500	44033500	45253700	46473600	47793600
27452300	34811500	37750300	40841700	44037100	45271700	46480500	47805500
27489500	34814600	37758700	40881500	44053600	45286500	46491900	47861300
27559600	34848800	37772200	41010600	44064900	45298300	46560000	47939900
27895000	34911100	37791900	41086000	44075700	45298700	46566300	47946100
27938500	34923100	37795000	41130500	44115900	45299700	46568900	47976300
28256200	35023200	37819200	41132500	44117300	45325300	46640200	47980600
28307900	35047800	37978700	41919500	44144600	45338100	46643200	47983300
28515800	35058800	38028500	42036400	44152000	45343000	46677400	47985500
29484500	35065700	38060900	42419200	44173600	45364400	46677800	47985700
30006300	35142600	38100300	42442800	44182200	45373900	46683700	48024400
30241900	35169600	38140400	42543300	44255200	45396700	46685300	48041700
30436300	35201900	38153300	42546300	44281900	45431100	46699900	48048700
30494600	35203700	38192600	42551900	44282200	45446700	46700100	48054400
30535200	35217300	38215600	42595400	44282300	45448900	46715700	48070800
30536400	35227600	38282500	42625000	44300500	45470500	46728100	
Tissue-specific hm-DLRs. Only 1000 selected DLRs are shown							
10421900	16261100	16954300	17764700	18920700	23068700	27303600	27558300
10589700	16261600	16956100	17764900	18921000	23227200	27303900	27558700
10596500	16262900	16956500	17766800	18923400	23236000	27304800	27559900
10596600	16274900	16962500	17767800	18926900	23291400	27306000	27562900
10598400	16283000	16975500	17773300	18931000	23456600	27307500	27566800
10598900	16284300	16976200	17785700	18943000	23492500	27307800	27569500
10715400	16289300	16976400	17796400	18952700	23492900	27307900	27570000
10736200	16291100	16989000	17799200	18956300	23510900	27308200	27577000
10843800	16291200	16989500	17813700	18956800	23518700	27316600	27580900
10913500	16299300	16990900	17886800	18968000	23525700	27324600	27581400
10924600	16299800	16991500	17898600	18970500	23528800	27326100	27585800
10955200	16311900	16992000	17905500	18971800	23552200	27327900	27593300
10987700	16325200	16997600	17905800	18973800	23560200	27330800	27600300

10992800	16326500	17001900	17906900	18975600	23562800	27335500	27602200
11012100	16329200	17009300	17909300	18977100	23573000	27335700	27604900
11028500	16329400	17017900	17922600	18977300	23573400	27337100	27605000
11094600	16332100	17034600	17924100	18982100	23616700	27338200	27605300
11098900	16334600	17036800	17928200	18987300	23629800	27340000	27607200
11112100	16347100	17040700	17928300	19005000	23656900	27340500	27609200
11122000	16357400	17041300	17928400	19010300	23659900	27341200	27609700
11130500	16366000	17041400	17928900	19020100	23667300	27342900	27610200
11131500	16373300	17041700	17931600	19023400	23682600	27343100	27617500
11132500	16373500	17045000	17934400	19028400	23701700	27343200	27620800
11139800	16373700	17045100	17936200	19031000	23724200	27351000	27621100
11144000	16374700	17046400	17936400	19033300	23732400	27352700	27625200
11144200	16380800	17049500	17941100	19033700	23732500	27354700	27626300
11145700	16382700	17050200	17943400	19033900	23732700	27360300	27631000
11170400	16383100	17065200	17944100	19034800	23735900	27360700	27637700
14384400	16388400	17080100	17945100	19035000	23768500	27362800	27656300
14804300	16391900	17080600	17945800	19041900	23811300	27363900	27656400
14816400	16396200	17084900	17945900	19042100	23833900	27369600	27658700
15056300	16396800	17085500	17947600	19045100	23918100	27371100	27659000
15067900	16399900	17089800	17956700	19045800	23947700	27372700	27691600
15068200	16400700	17094100	17958000	19046600	23950600	27373700	27693400
15077900	16401600	17099100	17958400	19048800	24744100	27375500	27697600
15166800	16401700	17099300	17961700	19052000	24825100	27375800	27718300
15227100	16407000	17116900	17965900	19052600	24974800	27376700	27744600
15228900	16407900	17117000	17971500	19063900	25255800	27377900	27760700
15261500	16423400	17121500	17978700	19070600	25258400	27381200	27763400
15261700	16423900	17123000	17979900	19071100	25301000	27382900	27763500
15262000	16425600	17127100	18023400	19077100	25304000	27383300	27765300
15297900	16426600	17142200	18029900	19098900	25370100	27384900	27765800
15300600	16428100	17145100	18040100	19100300	25580300	27387100	27766600
15309200	16429800	17147400	18042800	19101100	25871200	27388300	27766800
15357200	16433200	17153200	18049200	19102500	26100000	27389600	27769700
15375900	16434800	17154000	18078000	19104300	26219400	27397000	27770900
15380100	16434900	17156500	18078200	19104400	26335300	27397400	27773000

15381100	16435500	17157700	18085600	19108200	26656500	27399800	27775500
15383400	16435600	17166300	18141500	19108800	26833400	27407900	27776200
15383800	16438600	17172100	18144200	19116400	26929000	27410800	27776400
15384000	16444100	17174000	18147500	19116800	26930500	27411200	27776700
15384700	16444300	17176800	18215200	19117200	26932600	27411900	27777100
15386000	16451600	17178500	18443200	19117800	26934200	27414400	27778500
15386300	16467200	17180200	18699900	19119800	26935800	27417100	27779300
15404000	16469800	17182400	18762800	19128600	26940700	27417600	27780400
15407300	16478900	17182500	18763400	19131400	26942300	27424500	27783600
15412600	16479500	17187400	18766800	19136100	26945900	27428100	27783800
15431700	16491000	17188500	18772200	19150100	26948800	27428400	27784100
15434600	16494700	17193500	18782400	19151900	26961400	27430700	27796700
15435600	16504800	17193700	18782600	19162200	26971700	27431100	27799400
15436100	16505800	17197300	18788400	19166300	26973100	27431200	27812100
15436700	16506400	17206900	18793000	19167200	26978700	27434300	27817200
15436900	16506500	17207100	18793300	19167300	26980800	27440500	27818000
15442600	16507400	17210000	18807500	19173600	26986400	27440700	27818500
15442700	16510800	17211500	18808900	19174700	26986600	27443300	27822300
15443000	16511000	17212800	18809700	19175600	26997800	27443400	27823900
15443100	16521700	17213100	18809900	19177800	26998000	27445200	27825700
15444800	16522600	17218600	18810300	19188900	26998200	27446900	27827800
15447000	16536900	17221000	18812500	19196300	27003800	27448400	27831100
15448400	16547800	17222100	18813900	19196900	27020000	27449100	27835300
15451300	16551900	17226200	18816600	19202000	27038000	27449300	27838000
15452900	16560600	17232500	18817500	19213400	27050200	27450800	27840200
15453000	16569600	17236600	18817600	19228600	27054700	27452300	27840900
15455900	16572400	17247200	18818700	19278100	27055500	27459000	27843400
15456600	16574500	17247400	18820500	19280100	27072600	27463900	27846500
15457200	16577000	17261000	18821800	19294600	27072900	27465900	27855900
15458000	16581900	17268600	18822500	19311000	27090600	27467700	27857900
15464500	16585300	17277600	18822900	19318500	27094500	27468400	27867400
15464700	16591800	17279700	18823100	19345900	27098000	27468500	27868200
15465300	16592400	17280700	18824500	19514500	27098200	27469200	27874100
15468700	16592500	17300600	18826000	19764200	27098400	27470200	27874900

15471100	16600400	17305200	18827900	20037300	27102000	27471200	27875500
15473800	16611500	17305400	18828300	20173200	27109900	27476700	27877200
15474300	16615800	17333200	18829500	20216000	27122500	27477300	27887800
15474400	16615900	17341500	18829800	20250500	27127200	27479800	27889100
15477900	16620100	17350300	18831300	20270100	27127300	27481500	27903600
15491600	16625100	17352300	18834100	20508400	27135600	27485300	27923600
15491800	16627700	17353900	18834500	20649200	27140300	27489700	27942700
15552200	16633100	17354100	18834600	20966100	27157500	27490800	27945000
15647300	16647900	17356000	18835600	21390900	27161300	27491000	27958500
15650300	16663300	17357600	18842600	21540500	27173500	27493200	27960200
15705500	16664500	17362400	18843000	21546100	27184800	27495100	27960300
15731300	16670800	17363500	18848200	21594000	27185000	27497800	27963700
15734600	16672300	17371300	18849100	22347600	27185100	27498300	28021600
15743100	16673600	17376500	18853800	22367200	27190500	27500200	28026000
15748000	16677500	17377500	18854600	22369700	27192700	27502400	28027800
15748600	16688000	17422500	18858800	22370000	27194600	27503000	28031600
15758400	16710100	17433700	18861900	22370200	27200700	27503200	28041800
15765100	16717600	17442900	18862400	22381400	27207100	27504200	28047900
15807300	16729800	17443400	18864000	22386400	27207500	27505400	28049900
15811600	16732800	17457400	18865600	22396900	27208700	27508300	28051800
15851300	16769900	17485500	18866400	22397500	27213300	27509100	28056300
15854600	16799800	17485700	18867100	22399400	27214200	27509200	28074300
15869800	16815100	17489400	18867400	22413800	27217000	27510800	28075700
15983000	16816700	17496000	18868000	22421500	27218200	27511400	28080900
16007100	16818200	17505000	18868600	22429800	27232100	27511500	28081500
16016200	16828600	17541600	18870800	22440800	27243600	27518500	28081900
16105700	16842900	17542100	18872900	22452600	27247400	27518800	28093200
16197300	16854200	17544000	18873100	22461200	27252100	27519700	28094900
16202200	16855700	17552100	18876400	22493100	27256300	27522300	28095900
16213600	16859000	17552200	18878800	22514900	27258500	27522600	28100300
16213800	16866200	17565400	18879100	22537800	27260300	27524100	28104200
16213900	16867200	17568100	18880800	22537900	27261700	27524400	28105700
16214600	16872200	17568500	18883100	22555600	27275300	27527500	28105800
16215100	16872400	17612000	18891400	22564300	27276400	27528200	28106000

16222100	16893900	17636600	18894500	22572100	27277200	27529400	28106900
16240400	16894500	17651900	18894600	22573400	27278600	27529900	28107200
16241200	16914400	17653200	18894900	22591200	27281000	27534800	28107900
16248200	16915700	17659500	18895500	22619600	27281400	27537800	28108900
16248900	16916300	17675200	18901000	22620800	27281900	27537900	28109400
16249300	16932100	17675400	18902800	22631200	27282500	27538800	28109800
16251500	16936900	17690400	18904100	22640300	27298500	27544700	28110400
16253600	16940600	17728700	18908700	22651800	27298600	27551800	28112300
16255000	16948100	17741300	18912400	22728200	27300300	27552500	28114800
16260700	16952900	17763100	18913800	22737400	27303000	27553700	28114900
The selected T21-specific hm-DLRs							
27300500	35948700	39631800	43336700	45754400	48054800	40036100	45715400
27447600	36053400	39790900	43722500	46170300	15496700	40305700	45747100
30341400	36175700	39841200	43763200	46261400	15841200	40411000	45884900
30692000	36185500	40204700	43896900	46387900	16481500	42682100	46235600
32936900	36215200	40303500	44427300	46551600	20885400	43256500	46463000
32942700	36381000	40340900	44511200	46984700	34790500	43319100	46851000
33019400	37847300	40704800	44615300	47183600	35616700	43418800	46932200
33801400	38262700	40717600	44906600	47707300	35894400	43932600	47983300
34419100	38327400	40973900	44916000	47844900	35913900	44775800	
35203200	38434500	42694700	45546000	47897800	35936600	45244300	
35937700	39484900	43127700	45753000	47947900	35948600	45331400	

[0123] [Table 6. Selected u-CG-DLRs and hm-CG-DLRs for fetal T21 and fetal gender determination]

DLR type		Position
Detection of fetal T21 aneuploidy	uCG	chr21 29732020
Detection of fetal T21 aneuploidy	uCG	chr21 33462648
Detection of fetal T21 aneuploidy	uCG	chr21 34672959
Detection of fetal T21 aneuploidy	uCG	chr21 36193512
Detection of fetal T21 aneuploidy	uCG	chr21 40801830
Detection of fetal T21 aneuploidy	uCG	chr21 44303692
Detection of fetal T21 aneuploidy	uCG	chr21 44741616
Detection of fetal T21 aneuploidy	uCG	chr21 45798427

Detection of fetal T21 aneuploidy	hmCG	chr21 30341466
Detection of fetal T21 aneuploidy	hmCG	chr21 35898716
Detection of fetal T21 aneuploidy	hmCG	chr21 38327475
Detection of fetal T21 aneuploidy	hmCG	chr21 40074274
Detection of fetal T21 aneuploidy	hmCG	chr21 40135661
Detection of fetal T21 aneuploidy	hmCG	chr21 44084933
Detection of fetal T21 aneuploidy	hmCG	chr21 45546038
Detection of fetal T21 aneuploidy	hmCG	chr21 46964859
Fetal gender determination	uCG	chrX 22425661
Fetal gender determination	uCG	chrX 50774868
Fetal gender determination	uCG	chrX 23776534
Fetal gender determination	uCG	chrX 9624546
Fetal gender determination	uCG	chrX 9389347
Fetal gender determination	uCG	chrX 62584036
Fetal gender determination	uCG	chrX 138802442
Fetal gender determination	uCG	chrY 14774154

[0124] [Table 7. The list of selected DLRs in chromosome 13 and 18. The coordinate is shown for the first base pair of 100 bp u-DLRs and hm-DLRs]

Pregnancy-specific chr13 u-DLRs							
100008100	101482600	104426200	108936500	110709500	112672700	113632800	113742100
100038800	101710500	104949900	109038400	110846700	112681700	113649800	113761500
100066600	101742200	105608400	109386000	111057200	112690800	113653700	114185600
100315300	101779900	106272200	109429500	111090000	113103000	113673300	114187400
100392100	101961000	106323700	109819300	111773200	113138200	113684400	114203600
100479400	102346200	106590100	109944500	111852400	113279700	113694800	114215200
100529300	102578800	106662300	109949500	111997000	113416500	113697000	114441300
100570600	102811900	107601600	110174500	112101500	113420400	113698300	114458800
100575700	102906700	108033300	110178400	112226000	113532000	113707900	114471100
100596500	103155900	108233300	110193200	112288900	113544500	113709900	
101100600	103702300	108310100	110254600	112293800	113551300	113715800	
101185900	103951500	108413600	110481200	112623000	113551800	113731600	
101313000	104351000	108869700	110653400	112664300	113556700	113739100	
Pregnancy-specific chr18 u-DLRs							
10164100	11127100	1225900	13326200	14966900	21431200	23230100	28368600
10230000	11280000	12431600	13421100	14970000	21579300	23449800	29048800
10248300	11283300	12561500	13431900	18700600	21587400	24037600	29144400

10263100	11378600	12565400	13432000	19028000	21668700	24125900	29926800
10272700	11378800	12723100	13497800	1911400	21709600	24318400	30488500
10433300	11532400	12741900	13511300	19222900	21972200	24360100	30722200
10563500	11750800	13135100	13517000	19273800	22278700	24421300	31581500
10706400	11759500	13226200	13527500	19294100	22307200	24459600	31941500
10723700	11802400	13246300	13625400	19898200	22733400	24709600	32154300
10842000	11817700	13247600	13627100	19991500	22783900	24873100	
1091900	11847900	13254200	13645500	20008200	22800300	25465700	
10936900	12035600	13270000	13647500	20815500	23006400	25734400	
11101200	12234800	13278200	14162800	20895400	23092300	28207100	
Tissue-specific chr13 u-DLRs							
111000000	100286200	100395800	100591400	101203000	101763500	102608900	103229800
100057600	100291500	100406500	100596700	101212600	101820800	102732300	103236500
100066900	100315300	100442900	100656600	101288800	101825400	102775200	103354900
100078400	100318100	100446000	100689500	101314300	101885900	102852000	103365800
100080400	100328100	100456000	100704300	101334100	101931900	102901900	103400700
100097800	100341200	100463200	100932000	101391500	101996400	102906700	103427900
100110300	100344400	100479400	100989300	101404700	102271000	102979800	103430200
100122700	100358700	100541600	101034400	101425600	102293100	103044900	103539000
100140900	100375400	100557000	101045700	101593600	102397600	103045200	103547600
100142900	100375800	100559900	101097200	101593900	102498800	103094700	
100152100	100377300	100563200	101160600	101596900	102548800	103174600	
100172600	100387200	100565000	101194500	101605400	102558900	103202900	
100271900	100395500	100570600	101199900	101742200	102573800	103207500	
Tissue-specific chr18 u-DLRs							
10004000	10218000	10366100	10472500	10723700	10825100	10890600	11037100
10007600	10218900	10369400	10472800	10724200	10828600	10902200	11049800
10010500	10220300	10372500	1047300	10730800	10834900	10925700	11054500
10013200	10230100	10373000	10500900	10731400	10838000	10936900	11058000
10029700	10231800	10381300	10571200	10734700	10838800	10971200	11063500
10030300	10263000	10398500	10582400	10737400	10844200	10986100	11068000
10035100	10272700	10403400	10592900	10745300	10844600	10990400	11071000
10052400	10287000	10404600	10682200	10755600	10845500	10993600	11074000
10068500	10300900	10408400	10682500	10774400	10847900	10994000	11099500
10100200	10301900	10410400	10703600	10775500	10864900	11009700	
10120900	10332200	10423100	10708300	10776700	10873300	11012000	
10153400	10343100	10433300	10717300	10785400	10878300	11021400	
10164600	10346600	10450400	10721900	10806500	10888800	11027200	
Pregnancy-specific chr13 hm-DLRs							
100305000	107282100	114215200	28102000	43394700	46000500	50682600	92422900

100776700	110322500	20563600	28571600	44470900	47112300	50238200	99310800
107214300	111140600	21527500	28936500	45023500			
Pregnancy-specific chr18 hm-DLRs							
24079700	3473100	56528700	72186200	9478700	3172300	35234800	61869500
73934900							
Tissue-specific chr13 hm-DLRs							
111000000	100756100	101237300	101687300	101833600	102068100	102116200	103304300
100015300	100765100	101242700	101701700	101837400	102076800	102168800	103304500
100033700	100828300	101255600	101702000	101898100	102078200	102183900	103344400
100078000	100931800	101263700	101710300	101956100	102082400	102204700	103349700
100084900	100980400	101281000	101734400	101960500	102102200	102206000	103358800
100085400	100982800	101286200	101751100	101961200	102105900	102228800	103362900
100126100	101075300	101305600	101751500	101990200	102106400	102238000	103408800
100136900	101094300	101320900	101764100	101991600	102106800	102344000	103481700
100138400	101098400	101365300	101777000	101992300	102108000	102407700	105737500
100211300	101122000	101399900	101794700	102007400	102108700	102553800	
100231000	101182400	101451600	101796000	102052700	102109100	102580000	
100243900	101199800	101525100	101799300	102060500	102109800	103259500	
100589400	101202400	101533600	101831100	102060600	102112500	103265400	
Tissue-specific chr18 hm-DLRs							
10018900	10207900	10935800	11956100	12326400	12659400	12855600	13622800
10020300	10373100	11208700	11971200	12367700	12660600	12871700	1379600
10030100	10377900	11274300	12027100	12375000	12734300	12908700	1399600
10034200	10547100	11571800	12027200	12389700	12738100	12908900	14090000
10045400	10560700	11690300	12231400	12443300	12738600	1296400	14975600
10046100	10710600	11807300	12251400	12463100	12738700	12969400	15021300
10052400	107600	11829700	12254300	12467300	12748100	12972900	18573300
10055600	10796000	11857200	12254900	12476900	12775300	12995300	18637700
10073000	10798100	11900	12255500	12521400	12782800	12996400	18710400
10093500	10799200	11912400	12282900	12547600	12788800	13137700	
10121200	10923400	11921600	12289600	12565700	12839200	1331300	
10169200	10927300	11947700	12301800	12641500	12849500	13608200	
10190600	10929600	11952800	12324700	12646700	12850200	13611300	

Non Patent Literature

[0125] NPL1: Akolekar R, Beta J, Picciarelli G, Ogilvie C, D'Antonio F. Procedure-related risk of miscarriage following amniocentesis and chorionic villus sampling: a systematic review and meta-analysis. Ultrasound Obstet Gynecol. 2015 Jan;45(1):16-26. doi: 10.1002/uog.14636.

[0126] NPL2: Chan KC, Zhang J, Hui AB, Wong N, Lau TK, Leung TN, Lo KW, Huang DW, Lo YM. Size distributions of maternal and fetal DNA in maternal plasma. Clin Chem. 2004 Jan;50(1):88-92.

[0127] NPL3: Chim SS, Jin S, Lee TY, Lun FM, Lee WS, Chan LY, Jin Y, Yang N, Tong YK, Leung TY, Lau TK, Ding C, Chiu RW, Lo YM. Systematic search for placental DNA-methylation markers on chromosome 21: toward a maternal plasma-based epigenetic test for fetal trisomy 21. Clin Chem. 2008 Mar;54(3):500-11.

[0128] NPL3: Chim SS, Tong YK, Chiu RW, Lau TK, Leung TN, Chan LY, Oudejans CB, Ding C, Lo YM. Detection of the placental epigenetic signature of the maspin gene in maternal plasma. Proc Natl Acad Sci U S A. 2005 Oct 11;102(41):14753-8.

[0129] NPL4: Chiu RW, Chan KC, Gao Y, Lau VY, Zheng W, Leung TY, Foo CH, Xie B, Tsui NB, Lun FM, Zee BC, Lau TK, Cantor CR, Lo YM. Noninvasive prenatal diagnosis of fetal chromosomal aneuploidy by massively parallel genomic sequencing of DNA in maternal plasma. Version 2. Proc Natl Acad Sci U S A. 2008 Dec 23;105(51):20458-63.

[0130] NPL5: Daniels G, Finning K, Martin P, Summers J. Fetal blood group genotyping: present and future. Ann N Y Acad Sci. 2006 Sep;1075:88-95.

[0131] NPL6: Fan HC, Blumenfeld YJ, Chitkara U, Hudgins L, Quake SR. Analysis of the size distributions of fetal and maternal cell-free DNA by paired-end sequencing. Clin Chem. 2010 Aug;56(8):1279-86.

[0132] NPL7: Gibas P, Narmontė M, Staševskij Z, Gordevičius J, Klimašauskas S, Kriukienė E. Precise genomic mapping of 5-hydroxymethylcytosine via covalent tether-directed sequencing. PLoS Biol. 2020 accepted

[0133] NPL8: Jensen TJ, Kim SK, Zhu Z, Chin C, Gebhard C, Lu T, Deciu C, van den Boom D, Ehrich M. Whole genome bisulfite sequencing of cell-free DNA and its cellular contributors uncovers placenta hypomethylated domains. Genome Biol. 2015 Apr 15;16(1):78.

[0134] NPL9: Keravnou A, Ioannides M, Tsangaras K, Loizides C, Hadjidaniel MD, Papageorgiou EA, Kyriakou S, Antoniou P, Mina P, Achilleos A, Neofytou M, Kypri E, Sismani C, Koumbaris G, Patsalis PC. Whole-genome fetal and maternal DNA

methylation analysis using MeDIP-NGS for the identification of differentially methylated regions. Genet Res (Camb). 2016 Nov 11;98:e15.

[0135] NPL10: Kriukienė E, Labrie V, Khare T, Urbanavičiūtė G, Lapinaitė A, Koncevičius K, Li D, Wang T, Pai S, Ptak C, Gordevičius J, Wang SC, Petronis A, Klimašauskas S. DNA unmethylome profiling by covalent capture of CpG sites. Nat Commun. 2013;4:2190.

[0136] NPL11: Li Y, Zimmermann B, Rusterholz C, Kang A, Holzgreve W, Hahn S. Size separation of circulatory DNA in maternal plasma permits ready detection of fetal DNA polymorphisms. Clin Chem 2004;50: 1002–11.

[0137] NPL12: Lo YM, Chan KC, Sun H, Chen EZ, Jiang P, Lun FM, Zheng YW, Leung TY, Lau TK, Cantor CR, Chiu RW. Maternal plasma DNA sequencing reveals the genome-wide genetic and mutational profile of the fetus. Sci Transl Med. 2010 Dec 8;2(61):61ra91.

[0138] NPL13: Lo YM, Chiu RW. Prenatal diagnosis: progress through plasma nucleic acids. Nat Rev Genet. 2007 Jan;8(1):71-7.

[0139] NPL14: Lo YM, Corbetta N, Chamberlain PF, Rai V, Sargent IL, Redman CW, Wainscoat JS. Presence of fetal DNA in maternal plasma and serum. Lancet 1997;350:485–487.

[0140] NPL15: Lo YM, Hjelm NM, Fidler C, Sargent IL, Murphy MF, Chamberlain PF, Poon PM, Redman CW, Wainscoat JS. Prenatal diagnosis of fetal RhD status by molecular analysis of maternal plasma. N Engl J Med. 1998 Dec 10;339(24):1734-8.

[0141] NPL16: Lun FM, Chiu RW, Sun K, Leung TY, Jiang P, Chan KC, Sun H, Lo YM. Noninvasive prenatal methylomic analysis by genomewide bisulfite sequencing of maternal plasma DNA. Clin Chem. 2013 Nov;59(11):1583-94.

[0142] NPL17: Masevičius V, Nainytė M, Klimašauskas S. Synthesis of S-Adenosyl-L-Methionine Analogs with Extended Transferable Groups for Methyltransferase-Directed Labeling of DNA and RNA. Curr Protoc Nucleic Acid Chem. 2016 Mar 1;64:1.36.1-1.36.13.

[0143] NPL18: Old RW, Crea F, Puszyk W, Hultén MA. Candidate epigenetic biomarkers for non-invasive prenatal diagnosis of Down syndrome. Reprod Biomed Online. 2007 Aug;15(2):227-35.

[0144] NPL19: Papageorgiou EA, Fiegler H, Rakyan V, Beck S, Hulten M, Lamnissou K, Carter NP, Patsalis PC. Sites of differential DNA methylation between placenta and peripheral blood: molecular markers for noninvasive prenatal diagnosis of aneuploidies. Am J Pathol. 2009 May;174(5):1609-18.

[0145] NPL20: Parker SE, Mai CT, Canfield MA, Rickard R, Wang Y, Meyer RE, Anderson P, Mason CA, Collins JS, Kirby RS, Correa A; National Birth Defects Prevention Network. Updated National Birth Prevalence estimates for selected birth defects in the United States, 2004-2006. Birth Defects Res A Clin Mol Teratol. 2010 Dec;88(12):1008-16.

[0146] NPL21: Song CX, Szulwach KE, Fu Y, Dai Q, Yi C, Li X, Li Y, Chen CH, Zhang W, Jian X, Wang J, Zhang L, Looney TJ, Zhang B, Godley LA, Hicks LM, Lahn BT, Jin P, He C. Selective chemical labeling reveals the genome-wide distribution of 5-hydroxymethylcytosine. Nat Biotechnol. 2011 Jan;29(1):68-72.

[0147] NPL22: Staševskij Z, Gibas P, Gordevičius J, Kriukienė E, Klimašauskas S. Tethered Oligonucleotide-Primed Sequencing, TOP-Seq: A High-Resolution Economical Approach for DNA Epigenome Profiling. Mol Cell. 2017 Feb 2;65(3):554-564.e6.

[0148] NPL23: Tong YK, Jin S, Chiu RW, Ding C, Chan KC, Leung TY, Yu L, Lau TK, Lo YM. Noninvasive prenatal detection of trisomy 21 by an epigenetic-genetic chromosome-dosage approach. Clin Chem. 2010 Jan;56(1):90-8.

[0149] NPL24: Tsaliki E, Papageorgiou EA, Spyrou C, Koumbaris G, Kypri E, Kyriakou S, Sotiriou C, Touvana E, Keravnou A, Karagrigoriou A, Lamnissou K, Velissariou V, Patsalis PC. MeDIP real-time qPCR of maternal peripheral blood reliably identifies trisomy 21. Prenat Diagn. 2012 Oct;32(10):996-1001.

[0150] NPL25: Weber M, Davies JJ, Wittig D, Oakeley EJ, Haase M, Lam WL, Schübeler D. Chromosome-wide and promoter-specific analyses identify sites of differential DNA methylation in normal and transformed human cells. Nat Genet. 2005 Aug;37(8):853-62.

[0151] NPL26: Zimmermann B, Holzgreve W, Wenzel F, Hahn S. Novel real-time quantitative PCR test for trisomy 21. Clin Chem. 2002 Feb;48(2):362-3.

Claims

[Claim 1] A method for prenatal diagnosis of a trisomy 21 using a sample of maternal blood, the method comprising:

(a) enzymatic covalent labeling of nucleic acid molecules at unmodified CG and hydroxymethylated CG sites and their derivatization with DNA oligonucleotide (ODN) in a sample of maternal blood;

(b) producing nucleic acid molecules from a template nucleic acid sequence using a nucleic acid polymerase which contacts a template nucleic acid sequence at or around the site of the labeled uCG/hmCG and starts polymerization from the 3'-end of a primer non-covalently attached to the ODN; for further amplification of template DNA regions with labeled CG sites, a primer non-covalently attached to the ODN and yet another DNA primer that binds to one strand of an adaptor sequence attached to the DNA fragment through ligation-mediated PCR are used in order to obtain a sample enriched in unmodified or hydroxymethylated fetal DNA;

(c) determining the presence or availability of the labeled CG sites and hence the level of the unmodified or hydroxymethylated template genomic nucleic acid molecules across the regions of chromosomal DNA shown in Tables 4, 5 or 6;

(d) comparing the acquired value of the regions of step (c) to a standard reference value for the combination of at least one region from the list shown in Tables 4-6, wherein the standard reference value is (i) a value for a DNA sample from a woman bearing a fetus without trisomy 21; or (ii) a value for a DNA sample from a woman bearing a fetus with trisomy 21;

(e) diagnosing a trisomy based on said comparison, wherein trisomy 21 is diagnosed if the acquired value of the regions of step (d) is (i) higher than the standard reference value from a woman bearing a fetus without trisomy 21; or (ii) lower than the standard reference value from a woman bearing a fetus without trisomy 21; or (iii) comparable to the standard reference value from a woman bearing a fetus with trisomy 21;

(f) detecting fetal gender based on said comparison, wherein female gender of a fetus is detected if the acquired value of the regions of step (d) is comparable to the standard reference value from a woman bearing a female fetus, and male gender of a fetus is detected if the acquired value of the regions of step (d) is comparable to the standard reference value from a woman bearing a male fetus.

[Claim 2] The method according to claim 1, wherein the maternal blood sample is a fractionated portion of maternal peripheral blood or a maternal peripheral blood sample.

[Claim 3] The method according to claim 1 or 2, wherein the labeled CG sites are enriched by PCR amplification as described in claim 1, prior to performing the DNA modification ratio analysis.

[Claim 4] The method according to claim 3, wherein the level of at least one labeled CG is determined in a pre-amplified or a non-amplified maternal peripheral blood DNA sample.

[Claim 5] The method according to any one of the preceding claims, wherein the levels of the labeled CG-containing regions in the sample are determined by real time quantitative polymerase chain reaction (qPCR) or sequencing.

[Claim 6] The method according to any one of the preceding claims, wherein the method further comprises determining a labeling value of at least one of the regions of chromosomal DNA chosen from the lists shown in Tables 4-6.

[Claim 7] The method according to any one of the preceding claims, wherein one or more pairs/sets of oligonucleotide primers selected from SEQ ID 1-18 are used.

[Claim 8] A kit comprising the primers of claim 7 and an enzyme for covalent labeling of uCG and hmC sites.

[Claim 9] The kit according to claim 8 further comprising DNA oligonucleotide (ODN) for derivatization and enrichment of the labeled uCG and hmC sites.

[Claim 10] The kit according to any one claim 8 to 9, which further comprises oligonucleotide primers for the ODN-directed amplification and enrichment of the labeled regions.

[Claim 11] The kit according to any one claim 8 to 10, which further comprises oligonucleotide primers for the evaluation of a labeling value in a preamplified or non-amplified female blood DNA sample by qPCR.

[Fig. 1]

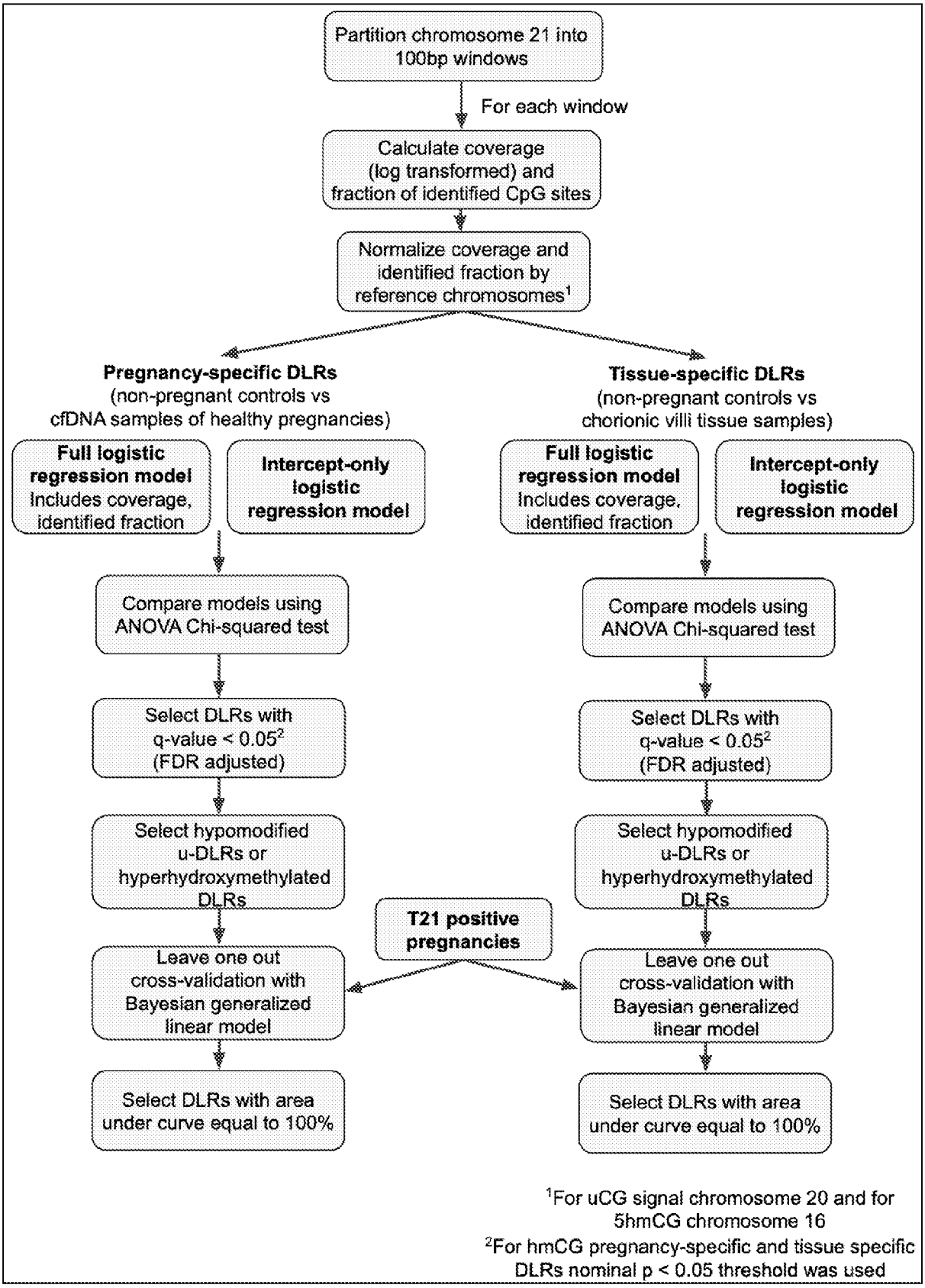
Partition chromosome 21 into 100bp windows
For each window
Calculate coverage (log transformed) and fraction of identified CpG sites
Normalize coverage and identified fraction by reference chromosomes[1]
Pregnancy-specific DLRs
(non-pregnant controls vs cfDNA samples of healthy pregnancies)
Tissue-specific DLRs
(non-pregnant controls vs chorionic villi tissue samples)
Full logistic regression model Includes coverage, identified fraction
Intercept-only logistic regression model
Full logistic regression model Includes coverage, identified fraction
Intercept-only logistic regression model
Compare models using ANOVA Chi-squared test
Compare models using ANOVA Chi-squared test
Select DLRs with q-value < 0.05[2] (FDR adjusted)
Select DLRs with q-value < 0.05[2] (FDR adjusted)
Select hypomodified u-DLRs or hyperhydroxymethylated DLRs
Select hypomodified u-DLRs or hyperhydroxymethylated DLRs
T21 positive pregnancies
Leave one out cross-validation with Bayesian generalized linear model
Leave one out cross-validation with Bayesian generalized linear model
Select DLRs with area under curve equal to 100%
Select DLRs with area under curve equal to 100%
[1]For uCG signal chromosome 20 and for 5hmCG chromosome 16
[2]For hmCG pregnancy-specific and tissue specific DLRs nominal p < 0.05 threshold was used

[Fig. 2]

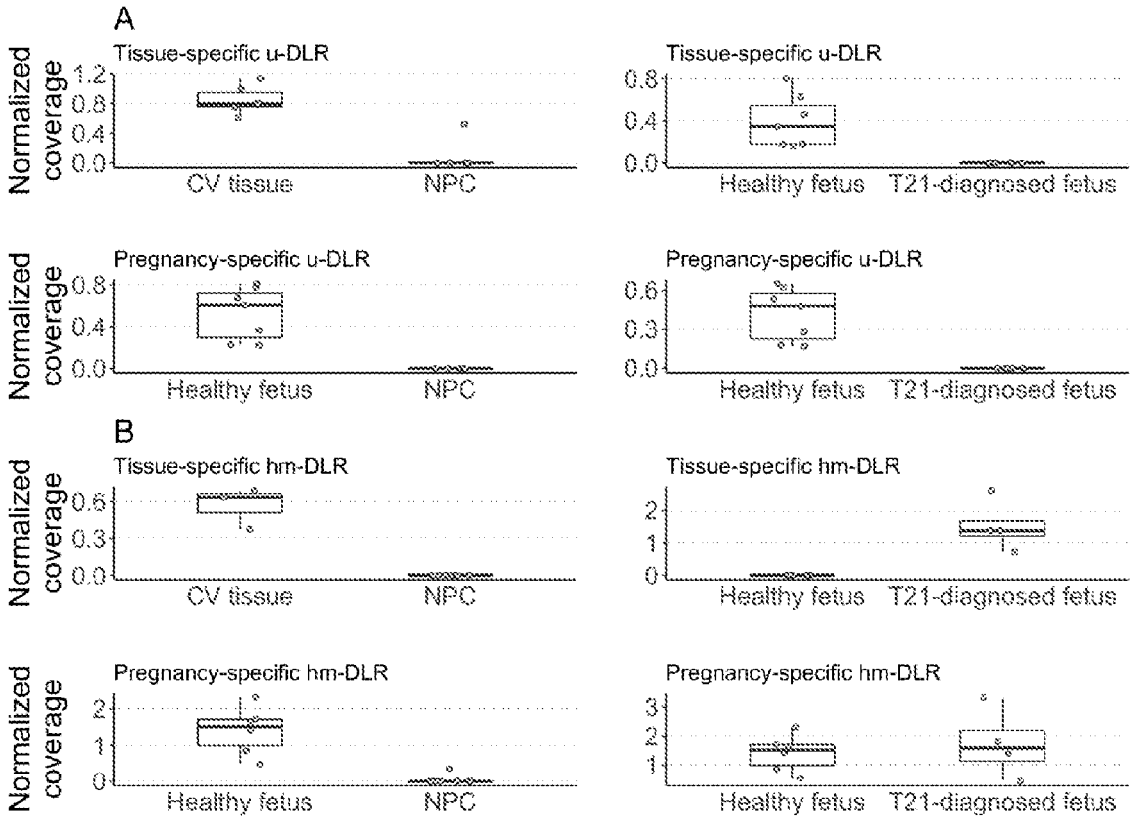
A
Tissue-specific u-DLR
Normalized coverage
1.2
0.8
0.4
0.0
CV tissue
NPC
Tissue-specific u-DLR
0.8
0.4
0.0
Healthy fetus
T21-diagnosed fetus
Pregnancy-specific u-DLR
0.8
0.4
0.0
Healthy fetus
NPC
Pregnancy-specific u-DLR
0.6
0.3
0.0
Healthy fetus
T21-diagnosed fetus
B
Tissue-specific hm-DLR
0.6
0.3
0.0
CV tissue
NPC
Tissue-specific hm-DLR
2
1
0
Healthy fetus
T21-diagnosed fetus
Pregnancy-specific hm-DLR
2
1
0
Healthy fetus
NPC
Pregnancy-specific hm-DLR
3
2
1
Healthy fetus
T21-diagnosed fetus

[Fig. 3]

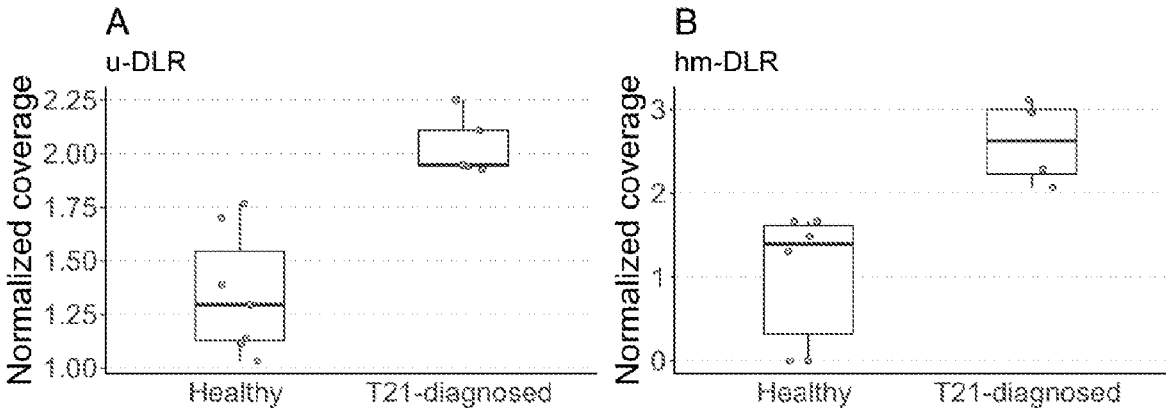
A
u-DLR
Normalized coverage
2.25
2.00
1.75
1.50
1.25
1.00
Healthy
T21-diagnosed
B
hm-DLR
Normalized coverage
3
2
1
0
Healthy
T21-diagnosed

[Fig. 4]

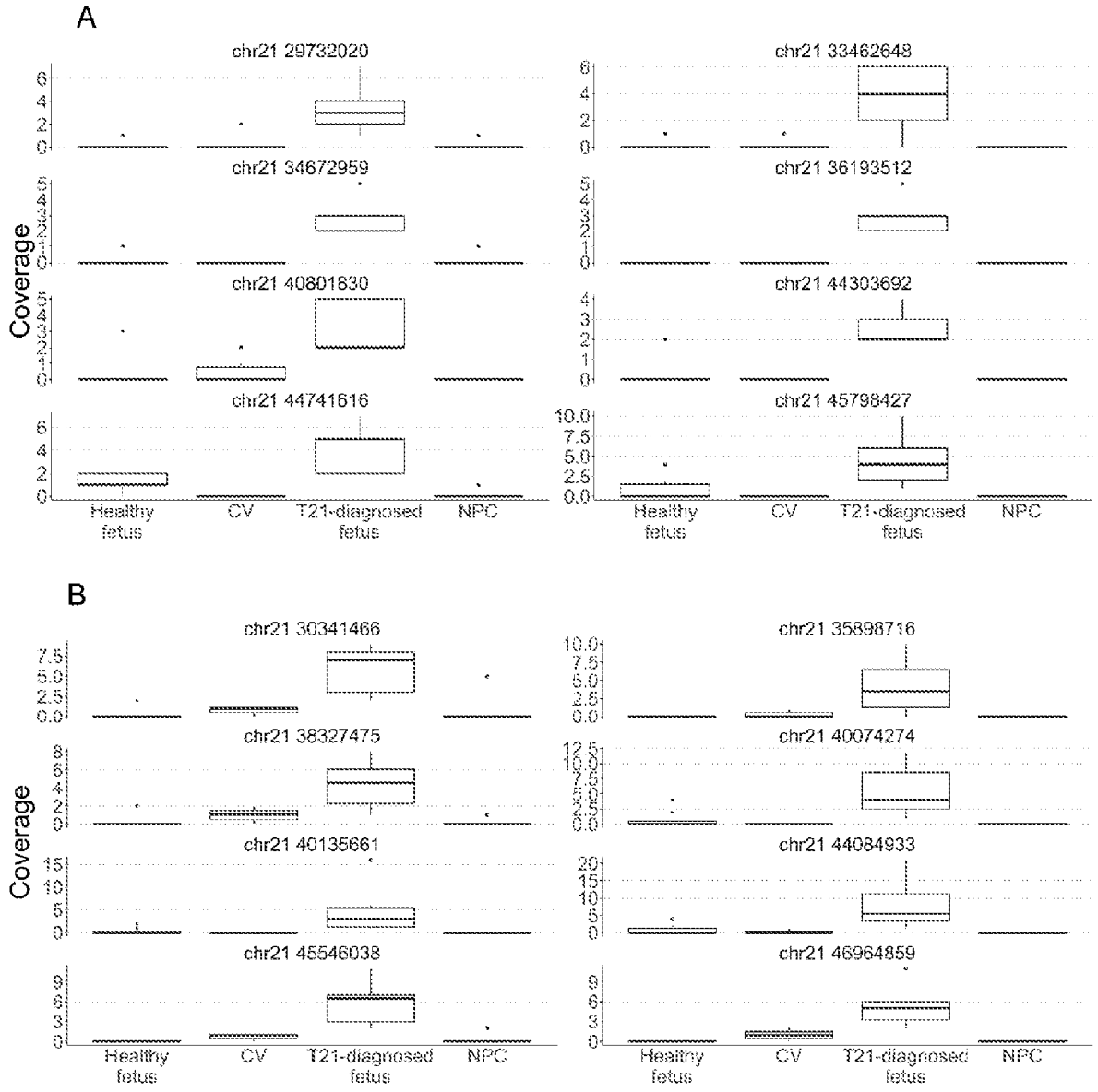
A
chr21 29732020
chr21 33462648
chr21 34672959
chr21 36193512
chr21 40801830
chr21 44303692
chr21 44741616
chr21 45798427
Coverage
Healthy fetus
CV
T21-diagnosed fetus
NPC
B
chr21 30341466
chr21 35898716
chr21 38327475
chr21 40074274
chr21 40135661
chr21 44084933
chr21 45546038
chr21 46964859
Coverage
Healthy fetus
CV
T21-diagnosed fetus
NPC

[Fig. 5]

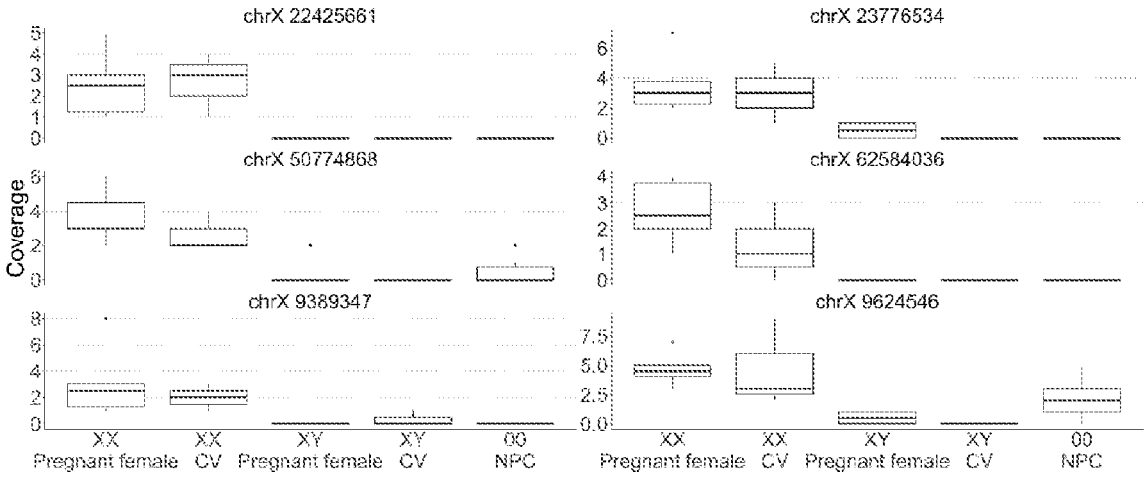
chrX 22425661
chrX 23776534
chrX 50774868
chrX 62584036
chrX 9389347
chrX 9624546
Coverage
XX Pregnant female
XX CV
XY Pregnant female
XY CV
00 NPC

[Fig. 6]

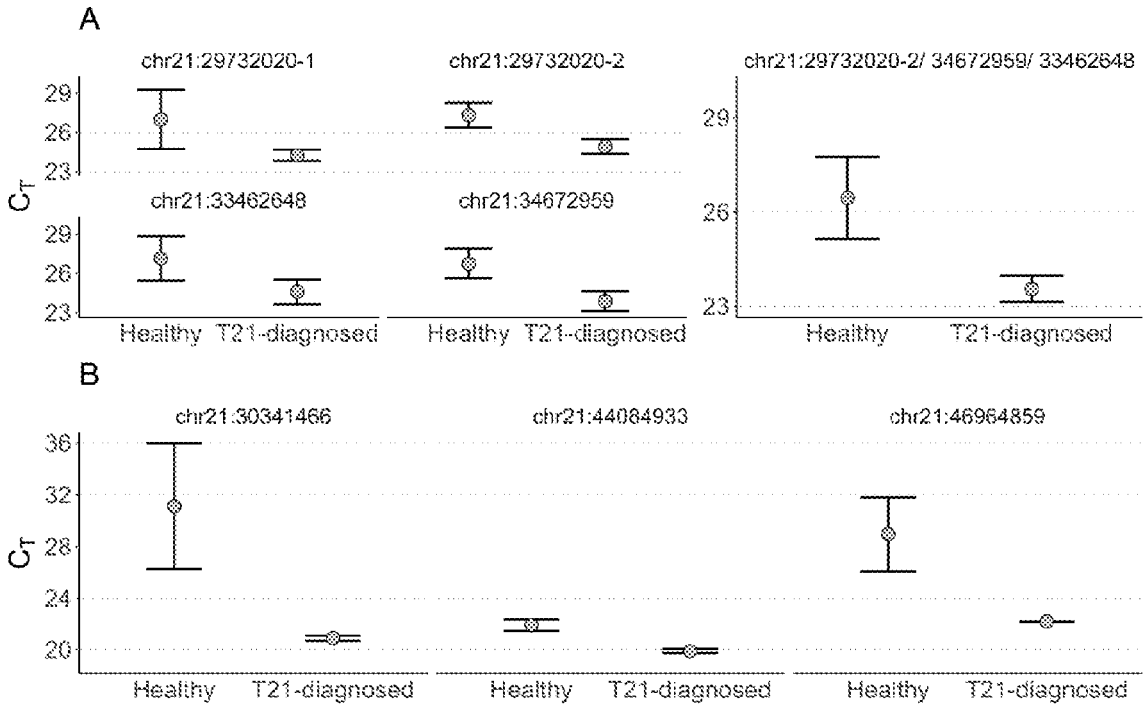
A
chr21:29732020-1
chr21:29732020-2
chr21:29732020-2/ 34672959/ 33462648
chr21:33462648
chr21:34672959
C_T
Healthy
T21-diagnosed
B
chr21:30341466
chr21:44084933
chr21:46964859

[Fig. 7]

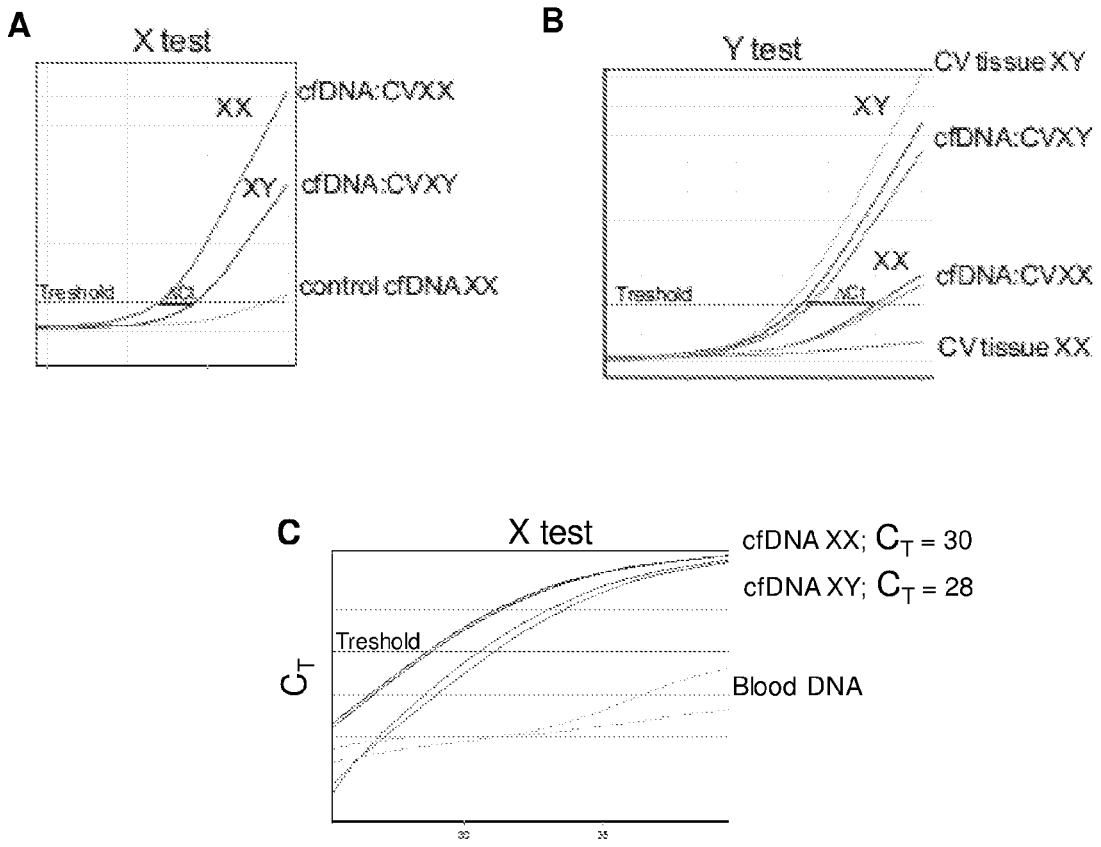
A
X test
XX
cfDNA:CVXX
XY
cfDNA:CVXY
Treshold
control cfDNA XX
B
Y test
CV tissue XY
XY
cfDNA:CVXY
XX
cfDNA:CVXX
Treshold
CV tissue XX
C
X test
cfDNA XX; C_T = 30
cfDNA XY; C_T = 28
Treshold
C_T
Blood DNA

[Fig. 8]

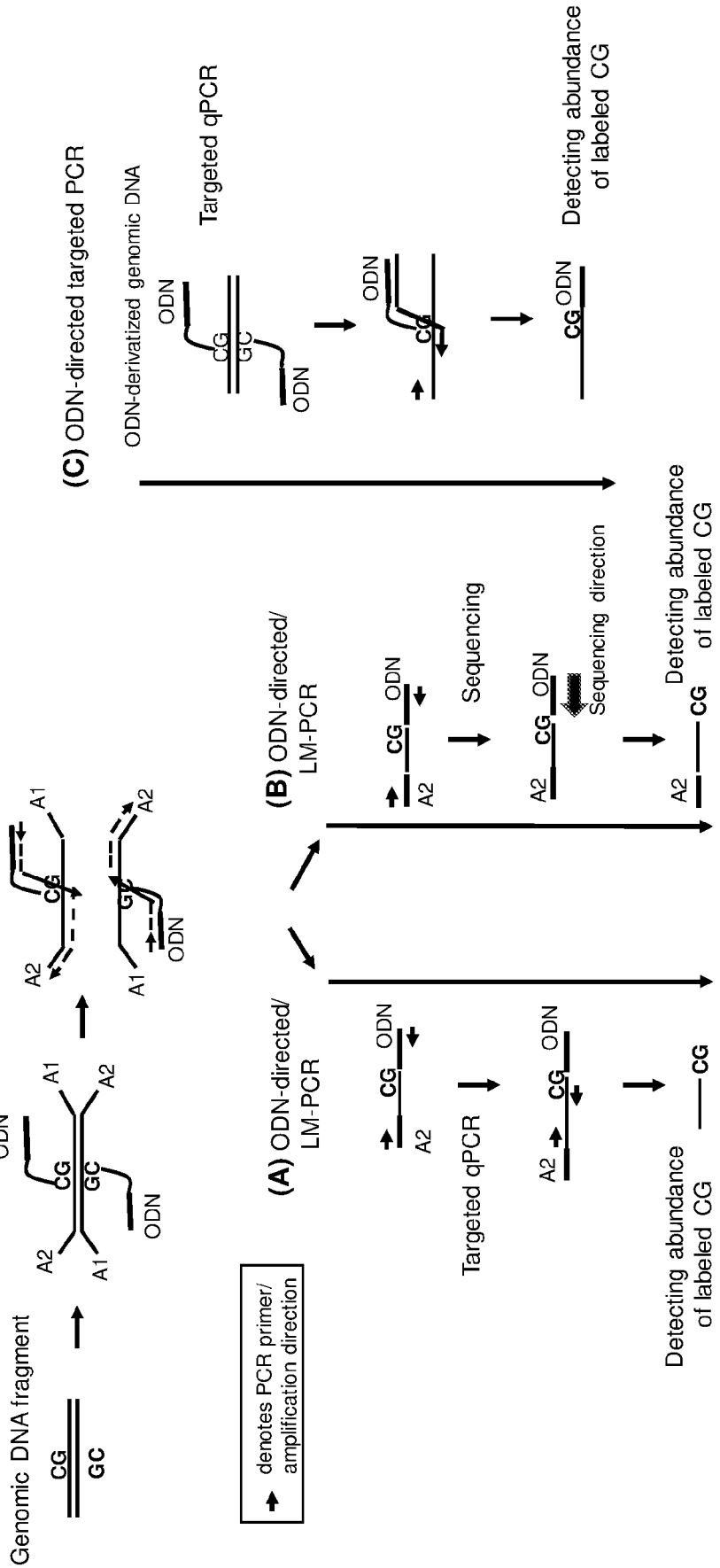
Genomic DNA fragment
CG
GC
ODN
A1
A2
(A) ODN-directed/ LM-PCR
(B) ODN-directed/ LM-PCR
(C) ODN-directed targeted PCR
ODN-derivatized genomic DNA
Targeted qPCR
Sequencing
Sequencing direction
Detecting abundance of labeled CG
denotes PCR primer/ amplification direction

[Fig. 9]

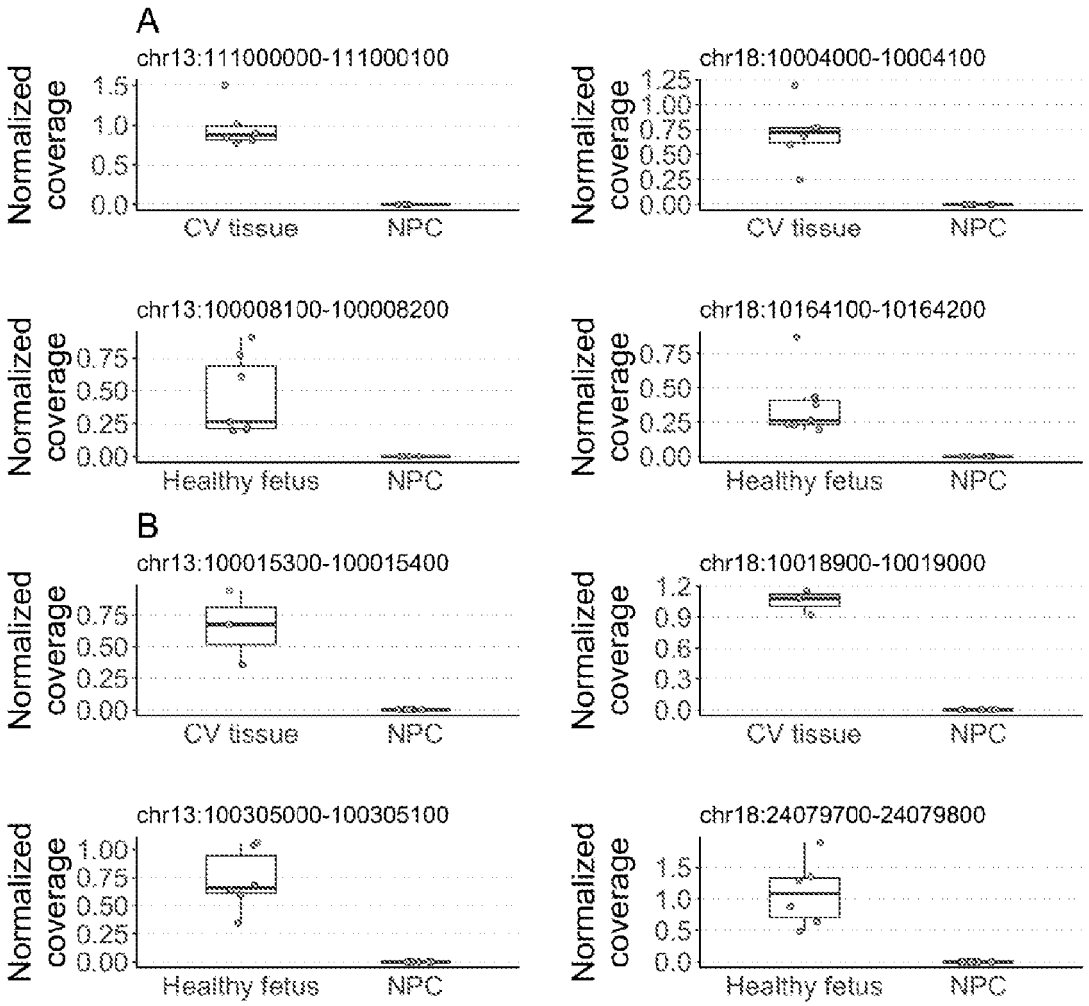
A
chr13:111000000-111000100
chr18:10004000-10004100
chr13:100008100-100008200
chr18:10164100-10164200
B
chr13:100015300-100015400
chr18:10018900-10019000
chr13:100305000-100305100
chr18:24079700-24079800
Normalized coverage
CV tissue
Healthy fetus
NPC

[Fig. 10]

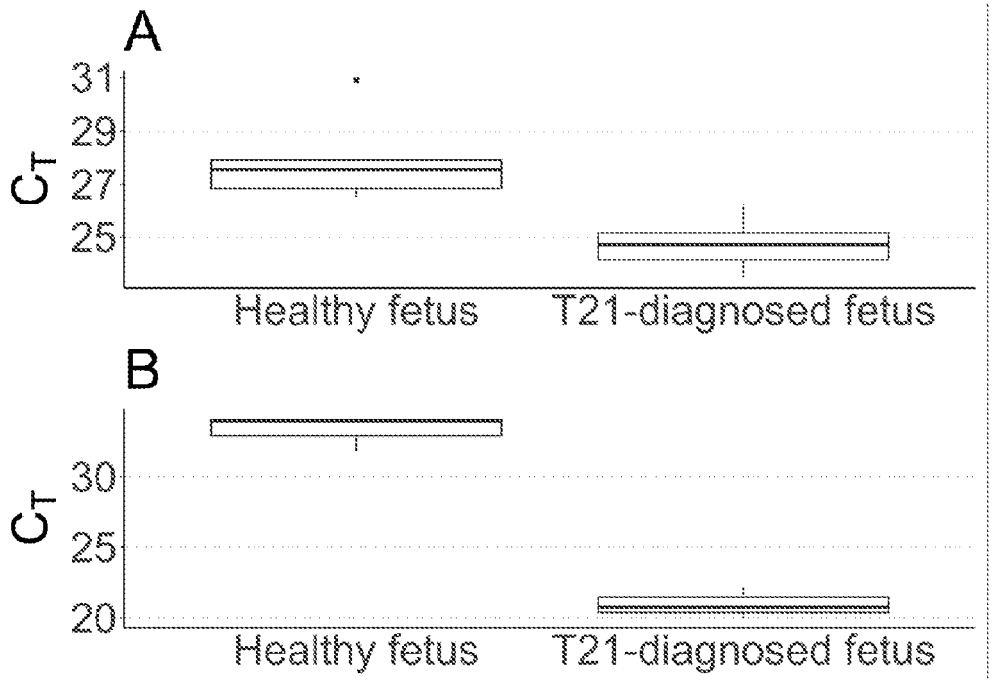
A
B
C_T
Healthy fetus
T21-diagnosed fetus

INTERNATIONAL SEARCH REPORT

International application No
PCT/IB2020/053011

A. CLASSIFICATION OF SUBJECT MATTER
INV. C12Q1/6827 C12Q1/6853 C12Q1/6883
ADD.

According to International Patent Classification (IPC) or to both national classification and IPC

B. FIELDS SEARCHED

Minimum documentation searched (classification system followed by classification symbols)
C12Q

Documentation searched other than minimum documentation to the extent that such documents are included in the fields searched

Electronic data base consulted during the international search (name of data base and, where practicable, search terms used)
EPO-Internal, BIOSIS, EMBASE, FSTA, WPI Data

C. DOCUMENTS CONSIDERED TO BE RELEVANT

Category*	Citation of document, with indication, where appropriate, of the relevant passages	Relevant to claim No.
Y	US 2012/282613 A1 (PATSALIS PHILIPPOS C [CY] ET AL) 8 November 2012 (2012-11-08) para. 9-19	1-11
Y	STASEVSKIJ ZDISLAV ET AL: "Tethered Oligonucleotide-Primed Sequencing, TOP-Seq: A High-Resolution Economical Approach for DNA Epigenome Profiling", MOLECULAR CELL, ELSEVIER, AMSTERDAM, NL, vol. 65, no. 3, 19 January 2017 (2017-01-19), page 554, XP029906273, ISSN: 1097-2765, DOI: 10.1016/J.MOLCEL.2016.12.012 abstract; p. 55, right-hand col., last para.; fig. 1	1-11

-/--

[X] Further documents are listed in the continuation of Box C.

[X] See patent family annex.

* Special categories of cited documents :

"A" document defining the general state of the art which is not considered to be of particular relevance

"E" earlier application or patent but published on or after the international filing date

"L" document which may throw doubts on priority claim(s) or which is cited to establish the publication date of another citation or other special reason (as specified)

"O" document referring to an oral disclosure, use, exhibition or other means

"P" document published prior to the international filing date but later than the priority date claimed

"T" later document published after the international filing date or priority date and not in conflict with the application but cited to understand the principle or theory underlying the invention

"X" document of particular relevance; the claimed invention cannot be considered novel or cannot be considered to involve an inventive step when the document is taken alone

"Y" document of particular relevance; the claimed invention cannot be considered to involve an inventive step when the document is combined with one or more other such documents, such combination being obvious to a person skilled in the art

"&" document member of the same patent family

Date of the actual completion of the international search	Date of mailing of the international search report
17 November 2020	27/11/2020

Name and mailing address of the ISA/	Authorized officer
European Patent Office, P.B. 5818 Patentlaan 2 NL - 2280 HV Rijswijk Tel. (+31-70) 340-2040, Fax: (+31-70) 340-3016	Ripaud, Leslie

INTERNATIONAL SEARCH REPORT

International application No
PCT/IB2020/053011

C(Continuation). DOCUMENTS CONSIDERED TO BE RELEVANT

Category*	Citation of document, with indication, where appropriate, of the relevant passages	Relevant to claim No.
Y	US 2013/130249 A1 (KLIMASAUSKAS SAULIUS [LT] ET AL) 23 May 2013 (2013-05-23) claims 15-32; fig. 1-2	1-11
Y	WO 2018/129120 A1 (UNIV CHICAGO [US]) 12 July 2018 (2018-07-12) para. 5, 14, 187; fig. 1, 7	1-11
A	US 2019/017109 A1 (SONG CHUNXIAO [GB] ET AL) 17 January 2019 (2019-01-17) the whole document	1-11
A	ELISAVET A. PAPAGEORGIOU ET AL: "Sites of Differential DNA Methylation between Placenta and Peripheral Blood", AMERICAN JOURNAL OF PATHOLOGY., vol. 174, no. 5, 1 May 2009 (2009-05-01), pages 1609-1618, XP055751192, US ISSN: 0002-9440, DOI: 10.2353/ajpath.2009.081038 the whole document	1-11
A	S. S.C. CHIM ET AL: "Systematic Search for Placental DNA-Methylation Markers on Chromosome 21: Toward a Maternal Plasma-Based Epigenetic Test for Fetal Trisomy 21", CLINICAL CHEMISTRY, vol. 54, no. 3, 1 March 2008 (2008-03-01), pages 500-511, XP055003626, ISSN: 0009-9147, DOI: 10.1373/clinchem.2007.098731 cited in the application the whole document	1-11
A	TAYLOR J JENSEN ET AL: "Whole genome bisulfite sequencing of cell-free DNA and its cellular contributors uncovers placenta hypomethylated domains", GENOME BIOLOGY, BIOMED CENTRAL LTD, vol. 16, no. 1, 15 April 2015 (2015-04-15) , page 78, XP021221764, ISSN: 1465-6906, DOI: 10.1186/S13059-015-0645-X cited in the application the whole document	1-11

INTERNATIONAL SEARCH REPORT

Information on patent family members

International application No
PCT/IB2020/053011

Patent document cited in search report	Publication date	Patent family member(s)	Publication date
US 2012282613 A1	08-11-2012	AU 2011210255 A1	26-07-2012
		BR 112012018458 A2	10-07-2018
		CA 2786174 A1	04-08-2011
		CN 102892899 A	23-01-2013
		CY 1118864 T1	10-01-2018
		DK 2529032 T3	01-05-2017
		EA 201290716 A1	28-06-2013
		EP 2529032 A2	05-12-2012
		ES 2623156 T3	10-07-2017
		JP 2013517789 A	20-05-2013
		KR 20120107512 A	02-10-2012
		NZ 601079 A	29-08-2014
		PL 2529032 T3	31-07-2017
		PT 2529032 T	04-05-2017
		SG 182322 A1	30-08-2012
		US 2012282613 A1	08-11-2012
		WO 2011092592 A2	04-08-2011
US 2013130249 A1	23-05-2013	EP 2776575 A1	17-09-2014
		US 2013130249 A1	23-05-2013
		US 2017016055 A1	19-01-2017
		WO 2013072515 A1	23-05-2013
WO 2018129120 A1	12-07-2018	US 2020190581 A1	18-06-2020
		WO 2018129120 A1	12-07-2018
US 2019017109 A1	17-01-2019	AU 2017246318 A1	08-11-2018
		CA 3019836 A1	12-10-2017
		CN 109312399 A	05-02-2019
		EP 3440205 A1	13-02-2019
		JP 2019520791 A	25-07-2019
		RU 2018138848 A	12-05-2020
		SG 11201808775P A	29-11-2018
		US 2019017109 A1	17-01-2019
		US 2020248248 A1	06-08-2020
		US 2020248249 A1	06-08-2020
		US 2020277666 A1	03-09-2020
		US 2020277667 A1	03-09-2020
		US 2020283838 A1	10-09-2020
		US 2020299760 A1	24-09-2020
		WO 2017176630 A1	12-10-2017

(12) INTERNATIONAL APPLICATION PUBLISHED UNDER THE PATENT COOPERATION TREATY (PCT)

(19) World Intellectual Property Organization
International Bureau

(43) International Publication Date
01 April 2021 (01.04.2021)

WIPO | PCT

(10) International Publication Number
WO 2021/059066 A1

(51) International Patent Classification:
G16B 20/50 (2019.01) *G16B 40/30* (2019.01)
G16B 40/20 (2019.01)

(21) International Application Number:
PCT/IB2020/058401

(22) International Filing Date:
10 September 2020 (10.09.2020)

(25) Filing Language: English

(26) Publication Language: English

(30) Priority Data:
LT2019 524 27 September 2019 (27.09.2019) LT

(71) Applicants: **UAB "BIOMATTER DESIGNS"** [LT/LT]; Zirmunu st. 139A, LT-09120 Vilnius (LT). **VILNIUS UNIVERSITY** [LT/LT]; Universiteto st. 3, 01513 Vilnius (LT).

(72) Inventors: **KARPUS, Laurynas**; Baltupio st. 121-8, Vilnius (LT). **JAUNISKIS, Vykintas**; Rukainiu st. 143, Vilnius (LT). **REPECKA, Donatas**; Grigalaukio st. 22-33, Vilnius (LT). **MESKYS, Rolandas**; Rinktines st. 19-72, Vilnius (LT).

(74) Agent: **PETNIUNAITE, Jurga**; A. Gostauto 40B, LT-03163 Vilnius (LT).

(81) Designated States *(unless otherwise indicated, for every kind of national protection available)*: AE, AG, AL, AM, AO, AT, AU, AZ, BA, BB, BG, BH, BN, BR, BW, BY, BZ, CA, CH, CL, CN, CO, CR, CU, CZ, DE, DJ, DK, DM, DO, DZ, EC, EE, EG, ES, FI, GB, GD, GE, GH, GM, GT, HN, HR, HU, ID, IL, IN, IR, IS, IT, JO, JP, KE, KG, KH, KN, KP, KR, KW, KZ, LA, LC, LK, LR, LS, LU, LY, MA, MD, ME, MG, MK, MN, MW, MX, MY, MZ, NA, NG, NI, NO, NZ, OM, PA, PE, PG, PH, PL, PT, QA, RO, RS, RU, RW, SA, SC, SD, SE, SG, SK, SL, ST, SV, SY, TH, TJ, TM, TN, TR, TT, TZ, UA, UG, US, UZ, VC, VN, WS, ZA, ZM, ZW.

(84) Designated States *(unless otherwise indicated, for every kind of regional protection available)*: ARIPO (BW, GH, GM, KE, LR, LS, MW, MZ, NA, RW, SD, SL, ST, SZ, TZ, UG, ZM, ZW), Eurasian (AM, AZ, BY, KG, KZ, RU, TJ, TM), European (AL, AT, BE, BG, CH, CY, CZ, DE, DK, EE, ES, FI, FR, GB, GR, HR, HU, IE, IS, IT, LT, LU, LV, MC, MK, MT, NL, NO, PL, PT, RO, RS, SE, SI, SK, SM,

(54) Title: METHOD FOR GENERATING FUNCTIONAL PROTEIN SEQUENCES WITH GENERATIVE ADVERSARIAL NETWORKS

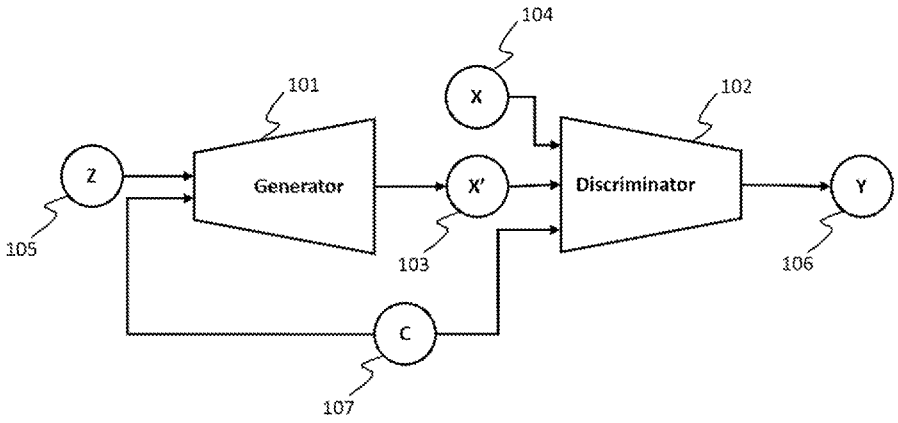

Fig. 1

(57) Abstract: The invention generally relates to the field of protein sequences and of generation of functional protein sequences. More particularly, the invention concerns a method for generating functional protein sequences with generative adversarial networks. The described method for functional sequence generation comprises plurality of steps, each of which is crucial to ensure the high percentage of functional sequences in the final sequence set: selecting a plurality of existing protein sequences to define the approximate sequence space for the later generated synthetic sequences, processing the selected protein sequences, approximating the unknown true distribution of amino acids of the pre-processed sequences using a variation of generative adversarial networks, obtaining protein sequences from the approximated distribution, processing of the obtained protein sequences. The described method provides a resource (e.g. time, cost) efficient way of producing synthetic protein sequences which have a high probability of being functional experimentally.

WO 2021/059066 A1

[Continued on next page]

TR), OAPI (BF, BJ, CF, CG, CI, CM, GA, GN, GQ, GW, KM, ML, MR, NE, SN, TD, TG).

Declarations under Rule 4.17:

— *of inventorship (Rule 4.17(iv))*

Published:

— *with international search report (Art. 21(3))*
— *with sequence listing part of description (Rule 5.2(a))*
— *in black and white; the international application as filed contained color or greyscale and is available for download from PATENTSCOPE*

Method for generating functional protein sequences with generative adversarial networks

Field of the invention

The invention generally relates to the field of protein sequences and of generation of functional protein sequences. More particularly, the invention concerns a method for generating functional protein sequences with generative adversarial networks.

Background of the invention

Proteins are molecules consisting of chains of amino acids which can fold in 3-dimensional space to form molecular machines for catalysis of various chemical reactions. Recombinant proteins were found to be extremely useful and are frequently used in medical applications such as antibodies, vaccines and growth factors. Additionally, proteins which have catalytic properties (enzymes) are actively used in various industries, e.g. biofuel, food and chemical synthesis. With the 20 commonly occurring proteinogenic amino acids, a protein comprising 100 amino acids, for instance, can be made from up to 20^{100} unique sequence variants, making the systematic exploration of protein variants extremely challenging. In such an astronomical sequence space, as little as 1 in 10^{77} of the possible protein sequences fold into the requisite three-dimensional structures to carry out their biological functions (Keefe and Szostak 2001; Taverna and Goldstein 2002; Axe 2004). The use of standard random mutagenesis to navigate this protein fitness landscape (Romero and Arnold 2009a) is often inefficient, as protein fitness declines exponentially with each random mutation (Bloom et al. 2005; Guo, Choe, and Loeb 2004a). Hence, it is immensely difficult to find a desired, functional protein variant due to the large part of sequence space being non-functional or not folding correctly - a tiny fraction of sequence space that needs to be tested. Experimental screening techniques are also limited to testing only 10^{6-9} protein variants. Additionally, up to 70% of single amino acid substitutions result in a decline of protein activity and 50% are deleterious to protein function (Romero and Arnold 2009b; Bloom et al. 2006; Guo, Choe, and Loeb 2004b; Rennell et al. 1991; Axe, Foster, and Fersht 1998; Shafikhani et al. 1997; Rockah-Shmuel, Tóth-Petróczy, and Tawfik 2015; Sarkisyan et al. 2016). In contrast, recombination of naturally occurring homologous proteins generates functional proteins with many mutations in a single step (Voigt et al. 2002; Hansson et al. 1999; Crameri et al. 1998). For instance, β-lactamase containing 75 mutations derived from a recombination library is 10^{16} times more likely to fold than one containing 75 random mutations (Drummond et al. 2005). However, these strategies are strongly limited by the number of available parent molecules.

Recent deep learning approaches have demonstrated great potential in capturing the structural, evolutionary, and biophysical information found in natural protein sequences,

enabling inference of protein properties and prediction of protein function (Alley et al., n.d.). Machine learning models of complex epistatic sequence relationships can predict protein variant activity-based merely on existing sequences (Riesselman, Ingraham, and Marks 2018). Yet, despite the promise that these computational methods hold for navigating the fitness landscapes (Romero, Krause, and Arnold 2013; Yang, Wu, and Arnold 2019), they have until now been used primarily for sequence inference-based function prediction using readily available data. Deep generative algorithms capable of producing protein sequences have been tested recently using autoregressive neural networks (WO2019097014). However, these methods do not ensure the correct folding or chemical activity of the generated proteins, making the whole procedure effectively as inefficient as currently used random experimental approaches.

Therefore, there is a need for a novel method that can efficiently produce experimentally active protein sequences.

Summary of the invention

The invention generally relates to the field of protein sequences and of generation of functional protein sequences. More particularly, the invention concerns a method for generating functional protein sequences with generative adversarial networks.

The described method for functional sequence generation comprises plurality of steps, each of which is crucial to ensure the high percentage of functional sequences in the final produced sequence set: selecting a plurality of existing protein sequences to define the approximate sequence space for the later generated synthetic sequences **601**, processing the selected protein sequences **602**, approximating the unknown true distribution of amino acids of the pre-processed sequences using a variation of generative adversarial networks **603**, obtaining protein sequences from the approximated distribution **604**, processing of the obtained protein sequences **605**.

The described method provides a cost (as well as other resources such as time and similar) effective way of producing synthetic protein sequences which have a high probability of being functional experimentally.

Brief description of drawings

Non-limiting embodiments of the present invention will be described by way of example with reference to the accompanying figures, which are schematic and are not intended to be drawn to scale. In the figures, each identical or nearly identical component illustrated is typically represented by a single numerical. For purposes of clarity, not every component is labelled in every figure, nor is every component of each embodiment of the invention shown where illustration is not necessary to allow those of ordinary skill in the art to understand the invention. In the figures:

Fig. 1 illustrates a flowchart describing high level architecture of the generative adversarial network;

Fig. 2 illustrates a flowchart describing the architecture of the generator network;

Fig. 3 illustrates a flowchart describing the architecture of Resnet block in the generator network;

Fig. 4 illustrates a flowchart describing the architecture of the discriminator network;

Fig. 5 illustrates a flowchart describing the architecture of the Resnet block in the discriminator network;

Fig. 6 illustrates a flowchart describing the main steps involved in the invented method;

Fig. 7 illustrates a flowchart of the overall network architecture used in example 1;

Fig. 8 illustrates generated sequence identity to the nearest natural sequence throughout training in different timestamps;

Fig. 9 illustrates the losses of generator and discriminator during training period. Generator and Discriminator losses become relatively stable after initial phase and eventually reach plateau;

Fig. 10 illustrates the sequence variability expressed as Shannon entropies for generated and training sequences estimated from multiple-sequence alignment (MSA). Low Shannon entropy values represent highly conserved and thus functionally relevant positions, whereas high entropy indicates high amino acid diversity at a given position;

Fig. 11 illustrates the fact that the generative adversarial network learns evolutionary conserved and functionally relevant positions;

Fig. 12 illustrates the GAN's ability to recreate positional amino acid distribution shown as Pearson's correlation coefficient for generated and natural sequences estimated from multiple-sequence alignment. Positions with lower correlation coefficients matches positions with higher sequence variability. Only positions with number of gaps lower than 75% are represented, moving average;

Fig. 13 illustrates the amino acid pair association (Zm) matrices for Natural and Generated protein sequences. Positive values indicate larger distance in comparison to random sequences with the same amino acid frequency, i.e., an integer number indicates how many positions on average the amino acids are further apart than in a random sequence;

Fig. 14 illustrates the amino acid pair correlations of produced synthetic and selected training sequences. Every point on the map represents the correlation of frequencies amino acid pairs between two different data sets. High correlation denotes that the same pairwise long-distance amino acid interactions were found in both datasets;

Fig. 15 illustrates the protein sequence space, visualized by transforming a distance matrix derived from k-tuple measures of protein sequence alignment into a t-SNE embedding. Dot sizes represent the 70% identity cluster size for each representative;

Fig. 16 illustrates the CATH domain diversity generated throughout evolution of ProteinGAN. At every 1200 training steps, 64 sequences were sampled and searched for representative CATH domains (E-value <1e-6). Inset: ProteinGAN generated novel domains not found in natural sequences, as comparison of natural and generated sequences to mutated random control sequences demonstrated that sequence generation was not a random process (Fisher's exact test p-value < 8.2e-16);

Fig. 17 illustrates the comparison of sequence diversity between the produced synthetic sequences and the natural (training) MDH dataset. Generated sequences are grouped into more diverse clusters. Inset shows the ratio of number of clusters (Y-axis) at different sequence identity cut-offs (X-axis);

Fig. 18 illustrates the activity levels of synthetic MDH proteins, as well as natural MDH protein controls;

Fig. 19 illustrates the malate production levels of synthetic MDH proteins in comparison to natural MDH proteins.

Detailed description of the invention

Reference will now be made in detail to exemplary embodiments of the invention. While the invention will be described in conjunction with the exemplary embodiments, it should be understood that they are not intended to limit the invention to these embodiments. On the contrary, the invention is intended to cover alternatives, modifications and equivalents, which may be included within the scope of the invention.

Throughout this disclosure, various aspects of this invention can be presented in a range format. It should be understood that the description in range format is merely for convenience and brevity and should not be construed as an inflexible limitation on the scope of the invention.

The described method for functional sequence generation comprises plurality of steps, each of which are crucial to ensure the high percentage of functional sequences in the final produced sequence set: selecting a plurality of existing protein sequences to define the approximate sequence space for the later generated synthetic sequences **601**, processing the selected protein sequences **602**, approximating the unknown true distribution of amino acids of the pre-processed sequences using a variation of generative adversarial networks **603**, obtaining protein sequences from the approximated distribution **604**, processing of the obtained protein sequences **605**.

The described method provides a cost (as well as other resources such as time and similar) effective way of producing synthetic protein sequences which have a high chance of being functional experimentally.

Definitions

To aid in understanding the invention, several terms are defined below.

Unless defined otherwise, all technical and scientific terms used herein have the same meaning as commonly understood by a person skilled in the art. Although any methods similar or equivalent to those described herein can be used in the practice or testing of the claims, the exemplary methods are described herein.

The terms “comprising”, “having”, “including”, and “containing” are to be construed as open-ended terms (i.e., meaning “including, but not limited to”) unless otherwise noted.

The term “bio-molecule” or “biomolecule” refers to a molecule that is generally found in a biological organism. Preferred biological molecules include biological macromolecules that are typically polymeric in nature being composed of multiple subunits (i.e., “biopolymers”). Typical bio-molecules include, but are not limited to molecules that share some structural features with naturally occurring polymers such as an RNAS (formed from nucleotide subunits), DNAs (formed from nucleotide Subunits), and polypeptides (formed from amino acid Subunits), including, e.g., RNAs, RNA analogues, DNAs, DNA analogues, polypeptides, polypeptide analogues, peptide nucleic acids (PNAS), combinations of RNA and DNA (e.g., chimeraplasty), or the like. Bio-molecules also include, e.g., lipids, carbohydrates, or other organic molecules that are made by one or more genetically encodable molecules (e.g., one or more enzymes or enzyme pathways) or the like.

The term “natural sequence” refers to amino acid sequences which are known from nature (e.g. a sequence derived from a gene such as a germline gene, or a sequence of a naturally occurring antibody). Accordingly, the term “artificial sequence” refers to amino acid sequences which are not known from nature.

The term “synthetic sequence” or “generated sequence” as used herein, refers to a protein sequences created by the described invention.

The term “sequence space” as used herein, refers to a space where all possible protein neighbours can be obtained by a series of single point mutations.

The term “neural network” or “network” as used herein, refers to a machine learning model that can be tuned (e.g. trained) based on inputs to approximate unknown functions. In particular, the term neural network can include a model of interconnected neurons that communicate and learn to approximate complex functions and generate outputs based on a plurality of inputs provided to the model. For instance, the term neural network includes one or

more machine learning algorithms. In particular, the term neural network can include deep convolutional neural networks, such as a spatial transformer network. In addition, a neural network is an algorithm (or set of algorithms) that implements deep learning techniques that utilize the algorithm to model high - level abstractions in data.

The term "adversarial learning" refers to a machine learning algorithm (e.g. generative adversarial network) where opposing learning models are learned together. In particular, the term "adversarial learning" includes solving a plurality of learning tasks in the same model (e.g. in sequence or in parallel) while utilizing the roles and constraints across the tasks. In some embodiments, adversarial learning includes employing a minimax function (e.g. a minimax objective function) that both minimizes a first type of loss and maximizes a second type of loss. For example, the image composite system employs adversarial learning to minimize loss for generating warp parameters by a geometric prediction neural network and maximize discrimination of an adversarial discrimination neural network against non-realistic images generated by the geometric prediction neural network.

The term "motif" refers to a pattern of subunits in/or among biological molecules. For example, the motif can refer to a Subunit pattern of the unencoded biological molecule or to a Subunit pattern of an encoded representation of a biological molecule.

The terms "polypeptide" and "protein" are used interchangeably herein to refer to a polymer (or sequence) of amino acid residues. Typically, the polymer has at least about 30 amino acid residues, and usually at least about 50 amino acid residues. More typically, they contain at least about 100 amino acid residues. The terms apply to amino acid polymers in which one or more amino acid residues are analogues, derivatives or mimetics of corresponding naturally occurring amino acids, as well as to naturally occurring amino acid polymers. For example, polypeptides can be modified or derivatized, e.g., by the addition of carbohydrate residues to form glycoproteins. The terms "polypeptide" and "protein" include glycoproteins, as well as non-glycoproteins.

A "amino acid sequence" refers to the order and identity of the amino acids comprising a polypeptide or protein.

The term "screening" refers to the process in which one or more properties of one or more bio-molecule is determined. For example, typical screening processes include those in which one or more properties of one or more members of one or more libraries is/are determined.

The term "selection" refers to the process in which one or more bio-molecules are identified as having one or more properties of interest. Thus, for example, one can screen a library to determine one or more properties of one or more library members. If one or more of the library members is/are identified as possessing a property of interest, it is selected.

Selection can include the isolation of a library member, but this is not necessary. Further, selection and screening can be, and often are, simultaneous.

The terms “subsequence” or “fragment” refers to any portion of an entire sequence of nucleic acids or amino acids.

The terms “library” or “population” refers to a collection of at least two different molecules and/or character Strings, such as nucleic acid sequences (e.g., genes, oligonucleotides, etc.) or expression products (e.g., enzymes) therefrom. A library or population generally includes a number of different molecules. For example, a library or population typically includes at least about 10 different molecules. Large libraries typically include at least about 100 different molecules, more typically at least about 1000 different molecules. For some applications, the library includes at least about 10000 or more different molecules.

The term “identity” (of proteins and polypeptides) with respect to amino acid sequences is used for a comparison of proteins chains. Calculations of "sequence identity" between two sequences are performed as follows. The sequences are aligned for optimal comparison purposes (e.g., gaps can be introduced in one or both of a first and a second amino acid sequence for optimal alignment and non-homologous sequences can be disregarded for comparison purposes). The optimal alignment is determined as the best score using the “ssearch36” program in the FASTA36 software package (http://faculty.virginia.edu/wrpearson/fasta/) with a Blosum50 scoring matrix with a gap-open penalty of -10, and a gap-extension penalty of -2. The amino acid residues at corresponding amino acid positions are then compared. When a position in the first sequence is occupied by the same amino acid residue at the corresponding position in the second sequence, then the molecules are identical at that position. The percent identity between the two sequences is a function of the number of identical positions shared by the sequences.

The term “functional protein” or “functional sequence” refers to a protein that is in a form in which it exhibits a property and/or activity by which it is characterized.

The term “tag”, “tag sequence” or “protein tag” refers to a chemical moiety, either a nucleotide, oligonucleotide, polynucleotide or an amino acid, peptide or protein or other chemical, that when added to another sequence, provides additional utility or confers useful properties, particularly in the detection or isolation, to that sequence. Thus, for example, a homopolymer nucleic acid sequence or a nucleic acid sequence complementary to a capture oligonucleotide may be added to a primer or probe sequence to facilitate the subsequent isolation of an extension product or hybridized product. In the case of protein tags, histidine residues (e.g., 4 to 8 consecutive histidine residues) may be added to either the amino- or carboxy-terminus of a protein to facilitate protein isolation by chelating metal chromatography. Alternatively, amino acid sequences, peptides, proteins or fusion partners representing epitopes or binding determinants reactive with specific antibody molecules or other molecules

(e.g., flag epitope, c-myc epitope, transmembrane epitope of the influenza A virus hemagglutinin protein, protein A, cellulose binding domain, calmodulin binding protein, maltose binding protein, chitin binding domain, glutathione S-transferase, and the like) may be added to proteins to facilitate protein isolation by procedures such as affinity or immunoaffinity chromatography. Chemical tag moieties include such molecules as biotin, which may be added to either nucleic acids or proteins and facilitates isolation or detection by interaction with avidin reagents, and the like. Numerous other tag moieties are known to, and can be envisioned by, the trained artisan, and are contemplated to be within the scope of this definition.

The term "data augmentation" as used herein, refers to a strategy that enables to artificially increase the diversity of data available for training, without physically collecting data samples. Examples of data augmentation techniques for images are cropping, padding, and horizontal flipping.

The term "dataset" as used herein, refers to a collection of items that are used for training or evaluating neural networks.

The term "true distribution" as used herein, refers to a distribution which contains all real elements including the elements from a dataset.

The term "blocks" as used herein, in the context of neural networks refers to a group of architectural neural network components that are combined together and reused.

The term "differentiable discrete approximation" as used herein, refers to a function that converts continuous values to a discrete space and this function is differentiable.

The term "vocabulary size" as used herein, refers to a number of unique tokens used to construct items in the dataset. These tokens are discrete (e.g. amino acids).

The term "training step" as used herein, refers to neural network optimization cycle that process a set of elements where the size of set is equal to batch size.

Selection and pre-processing of existing sequences

In one set of embodiments, existing sequences may be specifically selected for the training of generative adversarial network. Initial selection of sequence set(s) is an important procedure for several reasons: the selected sequences will define the sequence space in which the produced functional synthetic sequences will appear (i), the characteristics of selected sequences will define the unknown distribution that may be approximated in the generative adversarial network learning step (ii) and in turn may define some of the characteristics of produced synthetic sequences. An experimental, data driven example is shown in Fig. 15. In this figure, natural and synthetic (output from the described method) are displayed, wherein the distances between different clusters are comparable to cluster sequence-wise similarities and other similar characteristics. As described previously, the synthetic sequences appear in

the approximate boundaries set by the natural clusters, making the first step of the method - selection of the sequences - extremely important.

For example, in order to explore the sequence space containing functional variants of Glycerol-3-phosphate dehydrogenase, one may choose the training sequences that fall into that area of sequence space. Such sequences may be homologs of Glycerol-3-phosphate dehydrogenase. These functional sequences may be acquired from public databases, metagenomics screening, random mutagenesis screening, rational variant screening or other sources. The collected sequenced dataset may then be further modified.

The selected sequences may then be processed by bioinformatic algorithms. This step is of high importance as unprocessed sequences used in the training of generative adversarial network have a high chance of yielding non-functional and/or insoluble final produced synthetic protein sequences.

In one set of embodiments, the pre-processing of the selected protein sequences may include the filtering of sequences using defined criteria, such as sequence origin, similarity, diversity, sequence cluster sizes, structural similarity, presence of domains, function or functional characteristics, statistical properties (e.g. amino acid frequencies or presence of non-canonical amino acids, working conditions), physicochemical properties, or other similar techniques.

In another set of embodiments, the pre-processing of the selected protein sequences may include modifying the selected sequences. Modification of the selected sequences may be sequence up sampling using techniques such as domain and/or motif shuffling, performing circular permutation, introducing mutations to sequences, including additional sequence fragments (e.g. linkers, tags, motifs), using only defined parts of the sequences (e.g. domains, motifs), combining different sequences into one sequence entity or similar techniques.

Data augmentation techniques may be used to increase the number and/or diversity of selected sequences (e.g. in events when the selected sequence number is too low to be used with described method), such as introduction of invariant transformations, interpolation, introduction of noise or other techniques.

In yet another set of embodiments, the selected sequences may be converted into different representations such as one-hot encoding, sequence embeddings (conversion of sequences into numerical values) or other. These different representations may also be modified by adding or removing quantitative or qualitative information, by techniques such as concatenation, input multiplication or other.

Generative adversarial network architecture for protein sequence generation

The selected and pre-processed sequences may then be used as training (example) sequences for generative adversarial networks. The architecture of generative adversarial networks required for functional protein sequence generation is described further.

The reference numbers in the following paragraphs should be understood as an example, and other similar variants of architecture may also be viable.

Generative adversarial network architecture is comprised of two neural networks: the generator network **101** and discriminator network **102**. The function of generator network **101** is to produce outputs **103** that appear to be drawn from the true distribution of the dataset **104** without having access to items of the distribution during the training. Discriminator network **102** receives inputs **104** from the dataset and generator **101** and is tasked with distinguishing generated items from the real ones. In general case, the training of generative adversarial network consists of: randomly choosing points from selected distribution **105** and generating samples **103** using the generator **101** (i), randomly choosing elements from dataset **104** (ii), using the discriminator **102** to get scores **106** for the generated **103** and dataset samples **104** (iii), using discriminator scores **106** to optimize the discriminator network **102** and the generator network **101** independently (iv), repeating described i-iv steps until generated samples are of desired quality or discriminator network **102** is unable to distinguish generated samples **103** from the real ones **104**. The discriminator and generator networks may also be provided with additional information **107** making the overall generative adversarial network conditioned on the provided additional information.

In one set of embodiments, the generative adversarial network architecture consists of two networks - generator **101** and discriminator **102** - each of which may contain a number of building blocks such as Resnet blocks **201, 401** (He et al. 2015). As an alternative to Resnet blocks, convolutional layers, fully connected layers, multi-head attention mechanism (Vaswani et al. 2017) or other architectural building blocks may be used.

In another set of embodiments, the generator input **105** may be a vector that is drawn from any known distribution such as uniform or normal. Generator network may contain one or more fully connected **201**, convolutional layers before ResNet blocks **202** (e.g. 6 Resnet Blocks **202-[1-6]**) to transform an input **105** to required dimensions. The generator network may have one or more self-attention (Zhang et al. 2018) layers **203**. The generator network may contain one or more fully connected or convolutional layers **204** with non-linear activation function such as leaky ReLu **205**, ReLu and others to produce an output **103** of desired dimensions. The output may be passed through an non-linear activation function (for example, Tahn, Softmax and others) as well as a differentiable discrete approximation of the output such as Gumbel-Softmax **206** or REINFORCE (Williams 1992). Additionally, during the training, the generator network may also be provided with additional information **107**, such as a class label, which

may be encoded using embeddings, one-hot encoding or transformed in other ways and then concatenated with one or more of the layers in the generator network.

In another set of embodiments, each Resnet block in generator **201** may consist of 1 to 10 transposed convolution layers **301** (e.g. 2 transposed convolution layers **301-[1-2]**) and 1 to 10 convolution layers **302** with the filter size (1 to 100) x (1 to100). Convolution layers may contain dilation rates ranging from 1 to 10000. The blocks may contain a plurality of regularization layers such as batch normalization (Ioffe and Szegedy 2015), instance normalization (Ulyanov, Vedaldi, and Lempitsky 2016) and others. Moreover, blocks may also contain various activation functions such as leaky ReLu **303** (Maas 2013) (e.g. 2 leaky ReLu activations **303-[1-2]**), ReLu (Nair and Hinton 2010) and others. Blocks also may contain 1-10 skip connections **304** which may be concatenated **305** with other parts of the block. To increase the dimensions of the layer output instead of transposed convolution layer **301**, nearest-neighbour interpolation, sub-pixel shuffle (Shi et al. 2016) or other techniques may be used.

In another set of embodiments, the input **104** to discriminator network may be one-hot encoded with vocabulary size ranging from 10 to 10 000 or similar. Alternatively, the input may be encoded using amino acid embeddings or physicochemical attributes. Discriminator network may contain one or more embedding **401**, convolution or fully connected layers before Resnet blocks **402** (e.g. 6 Resnet blocks **402-[1-6]**) to transform the input **104**. Moreover, it may contain one or more self-attention layers **403**. Discriminator network may contain a layer to maintain high variety between generated sequences such as minibatch standard deviation layer **404** as described in (Karras et al. 2017). Discriminator network may contain one or more convolution **405,** fully connected **406** layers, or global average poolings with non-linear activation functions such as leaky ReLu **407**, ReLu and others to produce an output of desired dimensions. Some of layers may be flattened using Flatten layers **408**. The final outcome of the discriminator may be passed through a non-linear activation function such as Softmax, Tanh or other.

In another set of embodiments, each Resnet block in the discriminator may contain 1, 2, 3, 4, 5, 6, 7, 8, 9 or 10 convolution **501** (e.g. 3 convolution layers **501-[1-3]**) and/or fully connected layers with filter the size of (1 to 100) x (1 to 100). Convolution layers may contain dilation rates (1 to 10000). Blocks may contain a plurality of regularization layers such as batch normalization **502** (e.g. 2 batch normalization layers **502-[1-2]**), instance normalization and others. Blocks may also contain various non-linear activation functions such as leaky ReLu **503**, ReLu and others. Blocks also may contain 1-10 skip connections **504** which may be concatenated **505** with other part of block. During the training, the discriminator network may also be provided with additional information **107** along with the pre-processed training sequences, such as a class label, which may be encoded using embeddings, one-hot encoding

or transformed in other ways and then concatenated with one or more of the layers in the discriminator network.

In another set of embodiments, for the network loss, non-saturating (Goodfellow et al. 2014), non-saturating with R1 regularization (Mescheder, Geiger, and Nowozin 2018), hinge (Tran, Ranganath, and Blei 2017; Lim and Ye 2017; Miyato et al. 2018), hinge with relativistic average (Jolicoeur-Martineau 2018), Wasserstein (Arjovsky, Chintala, and Bottou 2017) and Wasserstein with gradient penalty (Gulrajani et al. 2017) or other functions may be used. To ensure Lipschitz constraint spectral normalization (Miyato et al. 2018), gradient penalty (Gulrajani et al. 2017) or other techniques may be used.

In another set of embodiments, the dimensions of generated outputs depend on the maximum length of the sequence required to be generated and the type of discriminator network encoding used. For example, for maximum sequence length of 400 amino acids and one-hot encoding with vocabulary size of 21, the dimensions of generated output would be 400x21.

Depending on the chosen generated output dimensions sequences selected for training may be further filtered to remove sequences containing more amino acids than the output dimensions allow. For example, if the dimensions of generated outputs are 400x21, sequence dataset may be filtered to remove sequences that are over 400 amino acids. The dataset may also be clustered into clusters with specific identities. For example, this may be achieved by using clustering tools such as mmseq2 or other. The clustering allows to balance the generative adversarial network training process, which is important in order to achieve synthetic functional sequence variation. Sequences based on their cluster size may be grouped into buckets of various sizes (1,2,3,5,10,20,30, etc.). Then the upsampling factor is determined by dividing maximum bucket size by cluster bucket size for all buckets. This factor is used to upsample under represented clusters during the training. A part of the dataset may be selected randomly or rationally and taken out of the training dataset. Such sequences may then act as validation sequences that the network will not see during the training but can later be used for network performance analysis purposes.

In another set of embodiments, to optimize neural network weights, ADAM optimizer (Kingma and Ba 2014), Stochastic Gradient Descent (Kiefer and Wolfowitz 1952), RMSProp (Graves 2013) and other optimizers may be used for the generator and discriminator networks. The learning rate may be gradually decreased for both generator and discriminator to increase training stability and aid the convergence. For example, the gradual decrease for the learning rate may be from 1e-3 to 5e-5. Ratio between generator and discriminator training steps may be 1:1 1:2, 1:5 or other.

In yet another set of embodiments, to normalize the data cluster sizes during the generative adversarial network training, under-represented sequence clusters may be

dynamically up-sampled. This may be achieved by up-sampling under-represented clusters (duplicating sequences inside of the cluster) by up-sampling factor that was calculated at the earlier stages. This process may be repeated throughout the generative adversarial network training in order to preserve the sequence variation. Sequences may be padded with special character dynamically to denote absence of amino acid. This may be used to pad shorter sequences if constructed network contains layers which require fixed size input such as fully connected. Sequences may be padded from the left, right or both sides. Padding is removed from generated sequences when final output is produced (for example, when one-hot encoded sequences are converted to sequences of single letter amino acids).

In yet another set of embodiments, in order to track the network's performance, the generated data should be evaluated throughout the training process. For example, every 1200 steps the generated sequences may be automatically aligned with the training and validation dataset sequences using BLAST or similar algorithms. To further exemplify, the periodically generated sequence during training procedure may also be subjected to calculation of blosum45, e-value and identity scores.

In yet another set of embodiments, after the training of generative adversarial network is done, in order to obtain protein sequences from learned distribution, random points are selected from the distribution that was used during training. To increase the quality of the generated examples, the standard deviation of used distribution may be reduced at the expense of sample variety. These points then are feed-forwarded through the trained generator to obtain generated representation of the sequence drawn from the determined true distribution that was learned during the training procedure. Obtained representation (e.g. one-hot encoded or embeddings) is then converted to sequences of amino acids and any gaps at the beginning or end of the sequences are removed.

Processing of the obtained synthetic protein sequences

The synthetic protein sequences obtained by the generative adversarial network determined distribution may be subjected to further processing (post-processing) using bioinformatic techniques. This step is of great importance as it dramatically increases the probability of finding sequences that will yield experimentally functional proteins.

In one set of embodiments, the post-processing may incorporate computational filtering of obtained synthetic sequences. Such filtering procedure may be used to rank the obtained synthetic sequences by a defined criterion, such as discriminator score, generated qualitative or quantitative descriptors, scores or labels predicted by other models (e.g. machine learning models, quantitative structure-property relationship models, structural or molecular dynamics models) or other.

In another set of embodiments, the post-processing of synthetic sequences may be the modification of those sequences, such as providing stabilizing mutations, linker sequences, protein tags, combining the sequences with other protein sequences or other.

Usage of the produced functional protein library

The output of the described method - a highly functional protein sequence library - may be then used in multiple applications such as experimental protein screening, data augmentation or other. The functional sequence library may be physically built by gene or protein synthesis methods. Then, the physical library may be screened experimentally using standard methods such as in-vitro/in-vivo protein expression and characteristic measurement, droplet microfluidics, or other. The screening may target a wide range of characteristics, such as the type of chemical reaction produced by protein variants, the activity level, thermostability, solubility or other. An example of the functional protein library generation and experimental screening is described in Example 1. The functional sequence library produced by the described invention may also be used for data augmentation purposes. In such cases, the method is used to enrich sequence set used by other machine learning algorithms with additional sequences produced by the described invention. Examples of such algorithms may be predicting optimal enzyme catalytic temperature, predicting secondary structure of protein or other.

Examples

Hereafter, the present invention is described in greater detail with reference to the examples, although the technical scope of the present invention is not limited to the following examples.

Example 1. Production of functional synthetic malate dehydrogenase sequences

This is an example of the production of functional malate dehydrogenase (E.C. 1.1.1.37) synthetic protein sequences using the described invention. The goal of this example is to show how every step of the method may be executed.

In this example, the generative adversarial network architecture consisted of two networks - discriminator and generator - each of which used ResNet blocks. The flowchart of the overall generative adversarial network architecture used in this example can be seen in Fig. 7. Each block in the discriminator contained 3 convolution layers with filter size of 3x3, 2 batch normalization layers and leaky ReLU activations. The generator residual blocks consisted of two transposed convolution layers, one convolution layer with the same filter size of 3x3 and leaky ReLU activations. Each network had one self-attention layer. Transposed convolution technique was chosen for up-sampling as it yielded the best results experimentally.

For loss, non-saturating loss with R1 regularization was used. To ensure training stability spectral normalization was implemented in all layers.

The input to the discriminator was one-hot encoded with vocabulary size 21 (20 canonical amino acids and a sign that denoted space at the beginning or end of the sequence). The generator input was a vector of 128 values that were drawn from a random distribution with mean 0 and standard deviation of 0.5, except that values whose magnitude was more than 2 standard deviations away from the mean were re-sampled. The dimensions of generated outputs were 512x21 wherein some of the positions denoted spaces.

In this example, bacterial malate dehydrogenase (MDH) sequences were collected from public protein sequence database Uniprot. Sequences longer than 512 amino acids or containing non-canonical amino acids were filtered out. The final dataset consisted of 16898 sequences which were clustered into 70% identity clusters using MMseq2 tool (Steinegger and Söding 2017) for balancing the dataset during the training process. 20% of the clusters with less than 3 sequences were randomly selected for validation (192 sequences) and the rest of the dataset was used for training (16706 sequences). Eight representative, natural MDH sequences from the training dataset is provided (SEQ ID NO:1 - SEQ ID NO:8).

The ratio between generator and discriminator training steps was selected 1:1. ADAM algorithm was used to optimize both networks. Throughout the training, the learning rate was gradually decreased from 1e-3 to 5e-5 for both generator and discriminator. To avoid bias towards sequences with large number of homologues, smaller clusters were dynamically up-sampled during the training. In order to track the performance, along with GAN losses, generated data was constantly evaluated. Without halting the training process, every 1200 training steps generated sequences were automatically aligned with the training and validation datasets using BLAST (Fig. 8). The training took 210 hours (~9 days) on NVIDIA Tesla P100 (16 GB).

After 2.5M training steps, at which training was terminated, the mean sequence identities between the generated and natural sequence sets had reached a plateau (median seq. identity to the closest natural sequences was 61.3%, (Fig. 9). Following the initial quality assessment, 20 000 sequences were generated for further analysis of the trained network.

Neural network's ability to capture which positions in the sequence are conserved and which are variable by computing Shannon entropies for each position in the network-generated and natural sequences (Fig. 10).

The positional variability in generated sequences was highly similar to that in natural sequences, with peaks (high entropy) and valleys (low entropy) appearing at similar positions in the sequence alignment. Indeed, there is an almost perfect correlation between the entropy values of generated and natural sequences (Pearson's r = 0.89, P-value < 1e-16). The

generated sequences preserved substrate-binding and catalytic residues by learning the conserved amino acid positions that are critical for catalysis (Fig. 11).

Further comparative analysis of generated and natural sequences showed that even in highly variable sequence regions, the frequencies of individual amino acids were perfectly correlated (Pearson's $r = 0.96$, P-value < 1e-16, Fig. 12).

As a result, our specific generative network architecture inferred the specific physicochemical signatures in the variable sequence regions, which are unique for every homologue, yet complementarity add up to the same physicochemical signature of the individual sequence. For instance, despite the high sequence diversity, the fractions of hydrophobic, aromatic, charged and cysteine-containing residues were the same in generated sequences (Wilcoxon rank sum test P-value > 0.05) as in natural ones. Apart from the differences (P-value = 7e-5; 1e-28, respectively) in hydrophilic and polar uncharged residues, the network has learned the overall amino acid patterns of similar evolutionary and physicochemical context (Table 1).

Table 1. Physicochemical properties of amino acids.

Amino acids	Statistic	p-value	Properties
W	-44.5535	0	-
T	-32.6757	3.45E-234	-
N	-31.0134	3.55E-211	-
P	5.414836	6.13E-08	-
F	36.10193	2.12E-285	-
A	-7.00421	2.48E-12	-
G	2.373175	0.017636	-
I	10.88373	1.38E-27	-
L	24.0913	3.08E-128	-

H	0.883687	0.376865	-
R	16.52561	2.40E-61	-
M	2.927137	0.003421	-
V	-37.0289	3.93E-300	-
E	-17.0094	7.00E-65	-
Y	-2.82555	0.00472	-
V, I, L, F, W, Y, M	-0.64435	0.519345	Hydrophobic
S, T, H, N, Q, E, D, K, R	-3.965	7.34E-05	Hydrophilic
F, W, Y, H	-1.00434	0.315217	Aromatic
P, G, A, S	7.263205	3.78E-13	Small
K, R, H	5.612656	1.99E-08	Positive
D, E	-22.965	1.04E-116	Negative
V, I, L, M	-2.04672	0.040685	Aliphatic
S, C, T, M	-0.12037	0.904194	Hydroxyl
S, T, C, M, N, Q	-11.1188	1.02E-28	Polar uncharged
H, K, R, E, D	1.296764	0.194713	Charged

In proteins many amino acids pairs which are remote on the primary sequence are spatially close and interact in the 3D structure, ensuring the appropriate protein stability and function. We assessed whether the network was able to learn such local and global amino acid

relationships by looking for long-distance pairwise amino acid relationships across the full length of the MDH sequences. For all the generated MDH sequences we calculated the amino acid association measures using the minimal proximity function Z_m (Santoni et al. 2016). The function $Z_m(A,B)$ counts the closest average distance from each amino acid A to any amino acid B in the sequence and can be expressed as a matrix for all possible pairs (Fig. 13).

The matrices for the natural (training) and generated (synthetic) sequences were 88% similar with a slight difference for tryptophan as 22% of the natural sequences used did not have tryptophan. To further investigate the pairwise amino acid relationships, we calculated the correlation for all possible amino acid pairs for each combination of positions in multiple sequence alignments from natural and generated sequences. Overall, we found strong correlations between the natural and generated sequences (averaged Pearson's $r = 0.95$, Fig. 14) demonstrating that the pairwise relationships are highly similar in both sets of sequences.

To expand on this, we inspected whether generated MDH sequences had the two main Pfam (Finn et al. 2014) domains identified (E-value < 1e-10) in the natural MDH sequences (Ldh_1_N and Ldh_1_C). Indeed, we found that 98% of the generated sequences contained both signatures, with the rest containing only one of the domains. These results show that sequences generated by our invented method are of high quality and closely mimic natural MDH proteins, both in terms of amino acid distributions at individual sites, as well as in terms of long-distance relationships between pairs of amino acids present throughout the primary sequence of MDH family.

Next, we aimed to explore whether our trained network was also able to generalize the protein family and generate novel sequence diversity. First, we visualized generated and natural sequences sequence diversity using t-distributed stochastic neighbour embedding (t-SNE) dimension reduction (Maaten and Hinton 2008). As a majority of natural MDH sequences were highly similar (median pairwise identity 92%), they grouped into clusters and the generated sequences interpolated between the natural sequence clusters resembling a learned manifold of the MDH sequence space (Fig. 15).

To assess whether generated diverse sequences would contain novel and functionally relevant biological properties, we performed a search of all CATH (Dawson et al. 2017) sequence models corresponding to all known 3D structural protein domains. First, we evaluated whether the network would evolve during the training by generating structural domain diversity over the training period (Fig. 16).

While the number of identified structural domains plateaued at the early stage of training (after 0.2M training steps) totalling in 79% of all identified domain space, structural CATH domains were discovered throughout the entire training process. In total, 119 novel structural sequence motifs (E-value < 1e-6) were identified (inset of Fig. 16) in generated sequences that do not exist in natural bacterial malate dehydrogenase enzyme family. Afterwards, we have

evaluated whether the generated structural domain diversity was not due to chance. To test this, as a control, we randomly introduced amino acid substitutions into the natural sequences, while preserving natural amino acid frequency distribution and the rate of mutations mimicking the natural sequence variability (inset of Fig. 16). The structural domain diversity was reduced by 38.9% in mutated natural sequences, 97.4% of mutated motifs were present in natural sequences demonstrating that random mutations do not produce biologically relevant sequence diversity (inset of Fig. 16), Fisher's exact test p-value < 8.2e-16). Overall, over 95% of generated sequences were not more than 10% similar to each other (Fig. 17), in contrast to only 17% of the natural sequences with the same identity level, expanding up to 4 times (inset of Fig. 17) the currently known malate dehydrogenase family's sequence space.

As typical for up to 70% of all random amino mutations can be deleterious of variety of protein functions (Romero and Arnold 2009a; Bloom et al. 2006; Guo, Choe, and Loeb 2004a; Rennell et al. 1991; Axe, Foster, and Fersht 1998; Shafikhani et al. 1997; Rockah-Shmuel, Tóth-Petróczy, and Tawfik 2015; Sarkisyan et al. 2016), we wanted experimentally verify the generated natural-like diversity of novel homologous proteins were showing the malate dehydrogenase catalytic activity.

Before experimental testing, the obtained synthetic protein sequences were further subjected to post-processing in order to maximise the percentage of functional protein sequences in the generated set. The generated sequences were filtered via defined criteria: after assigning discriminator score to each of the sequence only the sequences from the first quartile of discriminator score were selected (i), synthetic sequences were aligned with the selected protein sequences used to train generative adversarial network and synthetic sequences with identity lower than 60% in comparison to the closest natural sequence are discarded (ii), the obtained synthetic sequences were scored and filtered by comparing them to the sequences selected for network's training in terms of their structural information (iii).

The structural comparison and evaluation of synthetic and natural sequences is a multi-step process. The most similar natural sequences which have solved protein structures were selected and assigned to every synthetic sequence. For every residue in a given structure, the number of other residues in close proximity to that residue were assigned. Then, every synthetic sequence was aligned with the initially assigned natural sequence. If an amino acid did not match in the natural and synthetic sequence pair alignment, the number of contacts associated to that residue position was added to a score. Finally, the synthetic sequences with the lowest scores were selected (variants which have their amino acid residue contacts changed the least)

Out of the produced synthetic sequences we have randomly selected 40 sequences with their pairwise sequence identity ranging from 64% to 98% and having from 6 to 45 amino acid substitutions compared to their closest neighbour in the natural MDH sequence space. The

synthesized generated sequences were then recombinantly expressed in *Escherichia coli,* purified and *in vitro* tested for MDH catalytic activity.

In the following paragraph, detailed experimental conditions are provided. The sequences generated by invented method were synthesized, cloned into the pET21a expression vector and sequence-verified by Twist Bioscience. In addition to the enzyme sequence a C-terminal linker and four histidines (AAALEHHHH) were added, resulting in a deca-His-tag in the final construct which includes six histidines derived from the expression vector, to enable downstream affinity purification. The constructs were transformed into the BL21(DE3) *E. coli* expression strain. From the resulting transformation mixture 15 µl was used to inoculate 500 µl LB broth supplemented with 100 µg/ml carbenicillin. Cells were grown overnight at 32°C in a 96 deep well plate with 700 rpm orbital shaking. Protein expression was achieved by diluting the overnight cultures 1:30 into 1 ml autoinduction TB including trace elements (Formedium, UK) supplemented with 100 µg/ml carbenicillin and grown for 4 h in 37°C, followed by overnight growth at 18°C and 700 rpm shaking. Cells were collected by centrifugation and the cell pellets frozen in -80°C overnight. To purify the recombinant proteins, cells were thawed, resuspended in 200 µl lysis buffer (50 mM HEPES pH 7.4, 5% glycerol, 300 mM NaCl, 0.5 mM TCEP, 0.5 mg/ml lysozyme, 10 U/ml DNaseI, 2 mM $MgCl_2$), and incubated for 30 min at room temperature. To improve lysis triton-X-100 was added to a final concentration of 0.125% (v/v), and the cells were frozen in -80°C for 30 min. After thawing in room temperature water bath, the lysates were spun down for 10 min in 3000 x g to remove cell debris, and the supernatants were transferred to a new 96-well plate with 50 µl Talon resin in each well (Takara Bio, Japan). Unspecific binding of proteins to the resin was reduced by adding imidazole to a final concentration of 10 mM in each well. The plate was incubated at room temperature for 30 min with 400 rpm shaking, after which the lysates with the beads were transferred to a 96-well filter plate (Thermo Scientific, USA, Nunc 96-well filter plates) placed over a 96-well collection plate, and centrifuged for 1 min at 500 x g in a swing-out centrifuge. The resin was washed three times with 200 µl wash buffer (50 mM HEPES pH 7.4, 5% glycerol, 300 mM NaCl, 0.5 mM TCEP, 40 mM imidazole), and the proteins were eluted from the resin in two 50 µl fractions using elution buffer (50 mM HEPES pH 7.4, 5% glycerol, 300 mM NaCl, 0.5 mM TCEP, 250 mM imidazole). The two eluate fractions were combined and transferred to a 96-well desalting plate (Thermo Scientific, USA, Zeba Spin Desalting Plate, 7K MWCO) pre-equilibrated with sample buffer (50 mM HEPES pH 7.4, 5% glycerol, 300 mM NaCl, 0.5 mM TCEP). The plate was spun down 1000 x g for 1 min, and collected proteins were analysed by SDS-PAGE followed by Coomassie staining. The soluble proteins were carried on for further characterisation. To test for malate dehydrogenase activity, an aliquot of purified protein was added to a reaction mixture containing 0.15 mM NADH, 0.2 mM oxaloacetic acid, 20 mM HEPES buffer (pH 7.4). Final reaction volume was 100 µl, the reaction was carried out at room temperature in a UV-transparent 96-well half-area plate (UV-Star Microplate, Greiner, Austria).

Activity was measured in triplicates by following NADH oxidation to NAD+, with absorbance reading at 340 nm performed every 30 sec for 15 min in a BMG Labtech SPECTROstar Nano spectrophotometer. Un-specific oxidation of NADH was monitored in no-substrate controls, and these values were subtracted from the other samples. LC-MS/MS quantification was performed for selected active enzymes. The activity assay was performed as outlined above, in triplicates, with protein concentrations ranging between 10 and 250nM. Reactions were terminated after 45 min by diluting the assay mixtures in water to 1µg/ml starting concentration of oxaloacetate. For chromatographic separation a Zorbax Eclipse Plus C18 50 mm × 2.1 mm × 1.8 µm (Agilent) with a Nexera series HPLC (Shimadzu) were used. Mobile phase A was composed of H_2O (MiliQ HPLC grade) with 0.1% Formic acid (Sigma); mobile phase B was Methanol (Sigma) with 0.1% Formic acid (Sigma). The oven temperature was 40°C. The chromatographic gradient was set to consecutively increase from 0% to 100%, hold, decrease from 100% to 0% and hold, in 60 sec, 30 sec, 30 sec and 30 sec, respectively. The autosampler temperature was 15°C and the injection volume was 0.5 µl with full loop injection. For MS quantification a QTRAP® 6500 System (Sciex) was used, operating in negative mode with Multiple Reaction Monitoring (MRM) parameters optimized for Malic acid based on published parameters (McCloskey and Ubhi 2014). Electrospray ionization parameters were optimized for 0.8mL/min flow rate and were as follows: electrospray voltage of -4500 V, temperature of 500°C, curtain gas of 40, CAD gas set to Medium, and gas 1 and 2 of 50 and 50 psi, respectively. The instrument was mass calibrated with a mixture of polypropylene glycol (PPG) standards. The software Analyst 1.7 (Sciex) and MultiQuant 3 (Sciex) was used for analysis and quantitation of results, respectively.

Ten of these 40 protein variants (25%) were expressed at high levels and were present in the soluble fraction after cell lysis, indicating protein folded conformation. This is indeed a high success rate considering that even when expressing natural enzymes in *E. coli* in systematic studies the soluble enzyme fraction can be as little as 20% (Huang et al. 2015; Bastard et al. 2017). The 10 soluble proteins were purified using affinity chromatography and assessed for malate dehydrogenase activity by fluorescently monitoring NADH consumption. 8 of 10 (80%) soluble enzymes, including the variant with 45 amino acid substitutions, showed robust catalytic activity **(SEQ ID NO:9 - SEQ ID NO:16, Fig. 18**) with similar kinetics as wild-type sequences (**SEQ ID NO:17** and **SEQ ID NO: 18, Fig. 18**). To confirm the specificity of the reaction, we monitored the product formation using LC-MS/MS operating in selected reaction monitoring mode. We confirmed oxaloacetate to malate formation **(SEQ ID NO:9 - SEQ ID NO:16, Fig. 19)** with a comparable reaction yields as wild-type MDH analogues **(SEQ ID NO:17 - SEQ ID NO:18, Fig. 19)**.

To conclude, our provided experimental example demonstrates that our multi-step method for functional protein sequence generation confidently captures the numerous

properties of natural proteins, such as sequence motifs, position-specific amino acid composition and long-range amino acid interactions, while also allowing the generation of catalytically active, functional and diverse sequences. We have experimentally confirmed the robust enzymatic activity in 80% of soluble generated enzymes. The invented method thus enables large jumps to unexplored sections of sequence space allowing sampling of highly diverse novel functional proteins within the learned biological constraints of the enzyme family in a cost and resource effective manner.

References

1. Alley, Ethan C., Grigory Khimulya, Surojit Biswas, Mohammed AlQuraishi, and George M. Church. n.d. "Unified Rational Protein Engineering with Sequence-Only Deep Representation Learning." https://doi.org/10.1101/589333.
2. Arjovsky, Martin, Soumith Chintala, and Léon Bottou. 2017. "Wasserstein GAN." http://arxiv.org/abs/1701.07875.
3. Axe, Douglas D. 2004. "Estimating the Prevalence of Protein Sequences Adopting Functional Enzyme Folds." *Journal of Molecular Biology* 341 (5): 1295–1315.
4. Axe, Douglas D., Nicholas W. Foster, and Alan R. Fersht. 1998. "A Search for Single Substitutions That Eliminate Enzymatic Function in a Bacterial Ribonuclease†." *Biochemistry*. https://doi.org/10.1021/bi9804028.
5. Bastard, Karine, Alain Perret, Aline Mariage, Thomas Bessonnet, Agnès Pinet-Turpault, Jean-Louis Petit, Ekaterina Darii, et al. 2017. "Parallel Evolution of Non-Homologous Isofunctional Enzymes in Methionine Biosynthesis." *Nature Chemical Biology* 13 (8): 858–66.
6. Bloom, Jesse D., Sy T. Labthavikul, Christopher R. Otey, and Frances H. Arnold. 2006. "Protein Stability Promotes Evolvability." *Proceedings of the National Academy of Sciences of the United States of America* 103 (15): 5869–74.
7. Bloom, Jesse D., Jonathan J. Silberg, Claus O. Wilke, D. Allan Drummond, Christoph Adami, and Frances H. Arnold. 2005. "Thermodynamic Prediction of Protein Neutrality." *Proceedings of the National Academy of Sciences of the United States of America* 102 (3): 606–11.
8. Crameri, A., S. A. Raillard, E. Bermudez, and W. P. Stemmer. 1998. "DNA Shuffling of a Family of Genes from Diverse Species Accelerates Directed Evolution." *Nature* 391 (6664): 288–91.
9. Dawson, Natalie L., Tony E. Lewis, Sayoni Das, Jonathan G. Lees, David Lee, Paul Ashford, Christine A. Orengo, and Ian Sillitoe. 2017. "CATH: An Expanded Resource to Predict Protein Function through Structure and Sequence." *Nucleic Acids Research* 45 (D1): D289–95.
10. Drummond, D. Allan, Jonathan J. Silberg, Michelle M. Meyer, Claus O. Wilke, and Frances H. Arnold. 2005. "On the Conservative Nature of Intragenic Recombination." *Proceedings of the National Academy of Sciences of the United States of America* 102 (15): 5380–85.
11. Goodfellow, Ian J., Jean Pouget-Abadie, Mehdi Mirza, Bing Xu, David Warde-Farley, Sherjil Ozair, Aaron Courville, and Yoshua Bengio. 2014. "Generative Adversarial Networks." http://arxiv.org/abs/1406.2661.
12. Graves, Alex. 2013. "Generating Sequences With Recurrent Neural Networks." http://arxiv.org/abs/1308.0850.
13. Gulrajani, Ishaan, Faruk Ahmed, Martin Arjovsky, Vincent Dumoulin, and Aaron Courville. 2017. "Improved Training of Wasserstein GANs." http://arxiv.org/abs/1704.00028.
14. Guo, H. H., J. Choe, and L. A. Loeb. 2004a. "Protein Tolerance to Random Amino Acid Change." *Proceedings of the National Academy of Sciences*. https://doi.org/10.1073/pnas.0403255101.
15. ———. 2004b. "Protein Tolerance to Random Amino Acid Change." *Proceedings of the National Academy of Sciences*. https://doi.org/10.1073/pnas.0403255101.
16. Hansson, Lars O., Robyn Bolton-Grob, Tahereh Massoud, and Bengt Mannervik. 1999. "Evolution of Differential Substrate Specificities in Mu Class Glutathione Transferases Probed by DNA Shuffling 1 1Edited by R. Huber." *Journal of Molecular Biology*. https://doi.org/10.1006/jmbi.1999.2607.
17. He, Kaiming, Xiangyu Zhang, Shaoqing Ren, and Jian Sun. 2015. "Deep Residual Learning for Image Recognition." http://arxiv.org/abs/1512.03385.
18. Huang, Hua, Chetanya Pandya, Chunliang Liu, Nawar F. Al-Obaidi, Min Wang, Li Zheng, Sarah Toews Keating, et al. 2015. "Panoramic View of a Superfamily of Phosphatases through Substrate Profiling." *Proceedings of the National Academy of Sciences of the United States of America* 112 (16): E1974–83.
19. Ioffe, Sergey, and Christian Szegedy. 2015. "Batch Normalization: Accelerating Deep

Network Training by Reducing Internal Covariate Shift." http://arxiv.org/abs/1502.03167.
20. Jang, Eric, Shixiang Gu, and Ben Poole. 2016. "Categorical Reparameterization with Gumbel-Softmax." http://arxiv.org/abs/1611.01144.
21. Jolicoeur-Martineau, Alexia. 2018. "GANs beyond Divergence Minimization." http://arxiv.org/abs/1809.02145.
22. Karras, Tero, Timo Aila, Samuli Laine, and Jaakko Lehtinen. 2017. "Progressive Growing of GANs for Improved Quality, Stability, and Variation." http://arxiv.org/abs/1710.10196.
23. Keefe, A. D., and J. W. Szostak. 2001. "Functional Proteins from a Random-Sequence Library." *Nature* 410 (6829): 715–18.
24. Kiefer, J., and J. Wolfowitz. 1952. "Stochastic Estimation of the Maximum of a Regression Function." *Annals of Mathematical Statistics* 23 (3): 462–66.
25. Kingma, Diederik P., and Jimmy Ba. 2014. "Adam: A Method for Stochastic Optimization." http://arxiv.org/abs/1412.6980.
26. Lim, Jae Hyun, and Jong Chul Ye. 2017. "Geometric GAN." http://arxiv.org/abs/1705.02894.
27. Maas, Andrew L. 2013. "Rectifier Nonlinearities Improve Neural Network Acoustic Models."
https://pdfs.semanticscholar.org/367f/2c63a6f6a10b3b64b8729d601e69337ee3cc.pdf.
28. Maaten, Laurens van der, and Geoffrey Hinton. 2008. "Visualizing Data Using T-SNE." *Journal of Machine Learning Research: JMLR* 9 (Nov): 2579–2605.
29. McCloskey, Douglas, and Baljit K. Ubhi. 2014. "Quantitative and Qualitative Metabolomics for the Investigation of Intracellular Metabolism." *SCIEX Tech Note*, 1–11.
30. Mescheder, Lars, Andreas Geiger, and Sebastian Nowozin. 2018. "Which Training Methods for GANs Do Actually Converge?" http://arxiv.org/abs/1801.04406.
31. Miyato, Takeru, Toshiki Kataoka, Masanori Koyama, and Yuichi Yoshida. 2018. "Spectral Normalization for Generative Adversarial Networks." http://arxiv.org/abs/1802.05957.
32. Nair, Vinod, and Geoffrey E. Hinton. 2010. "Rectified Linear Units Improve Restricted Boltzmann Machines." In *Proceedings of the 27th International Conference on International Conference on Machine Learning*, 807–14. Omnipress.
33. Rennell, D., S. E. Bouvier, L. W. Hardy, and A. R. Poteete. 1991. "Systematic Mutation of Bacteriophage T4 Lysozyme." *Journal of Molecular Biology* 222 (1): 67–88.
34. Riesselman, Adam J., John B. Ingraham, and Debora S. Marks. 2018. "Deep Generative Models of Genetic Variation Capture the Effects of Mutations." *Nature Methods* 15 (10): 816–22.
35. Rockah-Shmuel, Liat, Ágnes Tóth-Petróczy, and Dan S. Tawfik. 2015. "Systematic Mapping of Protein Mutational Space by Prolonged Drift Reveals the Deleterious Effects of Seemingly Neutral Mutations." *PLoS Computational Biology* 11 (8): e1004421.
36. Romero, Philip A., and Frances H. Arnold. 2009a. "Exploring Protein Fitness Landscapes by Directed Evolution." *Nature Reviews. Molecular Cell Biology* 10 (12): 866–76.
37. ———. 2009b. "Exploring Protein Fitness Landscapes by Directed Evolution." *Nature Reviews. Molecular Cell Biology* 10 (12): 866–76.
38. Romero, Philip A., Andreas Krause, and Frances H. Arnold. 2013. "Navigating the Protein Fitness Landscape with Gaussian Processes." *Proceedings of the National Academy of Sciences of the United States of America* 110 (3): E193–201.
39. Sarkisyan, Karen S., Dmitry A. Bolotin, Margarita V. Meer, Dinara R. Usmanova, Alexander S. Mishin, George V. Sharonov, Dmitry N. Ivankov, et al. 2016. "Local Fitness Landscape of the Green Fluorescent Protein." *Nature* 533 (7603): 397–401.
40. Shafikhani, S., R. A. Siegel, E. Ferrari, and V. Schellenberger. 1997. "Generation of Large Libraries of Random Mutants in Bacillus Subtilis by PCR-Based Plasmid Multimerization." *BioTechniques* 23 (2): 304–10.
41. Shi, Wenzhe, Jose Caballero, Ferenc Huszár, Johannes Totz, Andrew P. Aitken, Rob Bishop, Daniel Rueckert, and Zehan Wang. 2016. "Real-Time Single Image and Video Super-Resolution Using an Efficient Sub-Pixel Convolutional Neural Network." http://arxiv.org/abs/1609.05158.
42. Steinegger, Martin, and Johannes Söding. 2017. "MMseqs2 Enables Sensitive Protein

Sequence Searching for the Analysis of Massive Data Sets." *Nature Biotechnology* 35 (11): 1026–28.
43. Taverna, Darin M., and Richard A. Goldstein. 2002. "Why Are Proteins Marginally Stable?" *Proteins* 46 (1): 105–9.
44. Tran, Dustin, Rajesh Ranganath, and David M. Blei. 2017. "Hierarchical Implicit Models and Likelihood-Free Variational Inference." http://arxiv.org/abs/1702.08896.
45. Ulyanov, Dmitry, Andrea Vedaldi, and Victor Lempitsky. 2016. "Instance Normalization: The Missing Ingredient for Fast Stylization." http://arxiv.org/abs/1607.08022.
46. Vaswani, Ashish, Noam Shazeer, Niki Parmar, Jakob Uszkoreit, Llion Jones, Aidan N. Gomez, Lukasz Kaiser, and Illia Polosukhin. 2017. "Attention Is All You Need." http://arxiv.org/abs/1706.03762.
47. Voigt, Christopher A., Carlos Martinez, Zhen-Gang Wang, Stephen L. Mayo, and Frances H. Arnold. 2002. "Protein Building Blocks Preserved by Recombination." *Nature Structural Biology* 9 (7): 553–58.
48. Williams, Ronald J. 1992. "Simple Statistical Gradient-Following Algorithms for Connectionist Reinforcement Learning." *Machine Learning* 8 (3-4): 229–56.
49. Yang, Kevin K., Zachary Wu, and Frances H. Arnold. 2019. "Machine-Learning-Guided Directed Evolution for Protein Engineering." *Nature Methods* 16 (8): 687–94.
50. Zhang, Han, Ian Goodfellow, Dimitris Metaxas, and Augustus Odena. 2018. "Self-Attention Generative Adversarial Networks." http://arxiv.org/abs/1805.08318.
51. WO2019097014

Claims

1. A method for production of functional synthetic protein sequences, comprising the steps of:

a) defining the approximate sequence space boundaries for the synthetic sequences to be produced by selecting a plurality of existing protein sequences,

b) processing the selected protein sequences,

c) approximating the unknown true distribution of amino acids of the pre-processed sequences using generative adversarial networks,

d) obtaining synthetic protein sequences from the approximated distribution,

e) processing of the obtained protein sequences.

2. A method according to claim 1, wherein the produced functional synthetic protein sequences are enzymes.

3. A method according to claim 1, wherein the pre-processing of the selected protein sequences includes filtering of sequences by their biological characteristics.

4. A method according to claim 1, wherein self-attention layers are included in the generative adversarial network architecture.

5. A method according to claim 1, wherein dilated convolutional layer are included in the generative adversarial network architecture.

6. A method according to claim 1, wherein generative adversarial network layers are normalized using spectral normalization.

7. A method according to claim 1, wherein during the generative adversarial network training the under-represented training sequence clusters are dynamically up-sampled.

8. A method according to claim 1, wherein additional information is provided to the discriminator and generator networks.

9. A method according to claim 1, wherein the amino acids are encoded using one-hot encoding.

10. A method according to claim 9, wherein the generator network produces one-hot encoded outputs using differentiable discrete approximation.

11. A method according to claim 1, wherein the amino acids are encoded using embeddings.

12. A method according to claim 1, wherein in the processing of the obtained synthetic protein sequences includes filtering the sequences by the score assigned by the discriminator network.

13. A method according to claim 1, wherein in the processing of the obtained synthetic protein

sequences includes filtering the sequences by subjecting them to machine learning models.

14. Use of the functional protein sequences produced by the method described in claim 1 for experimental protein screening.

15. Use of the functional protein sequences produced by the method described in claim 1 for data augmentation.

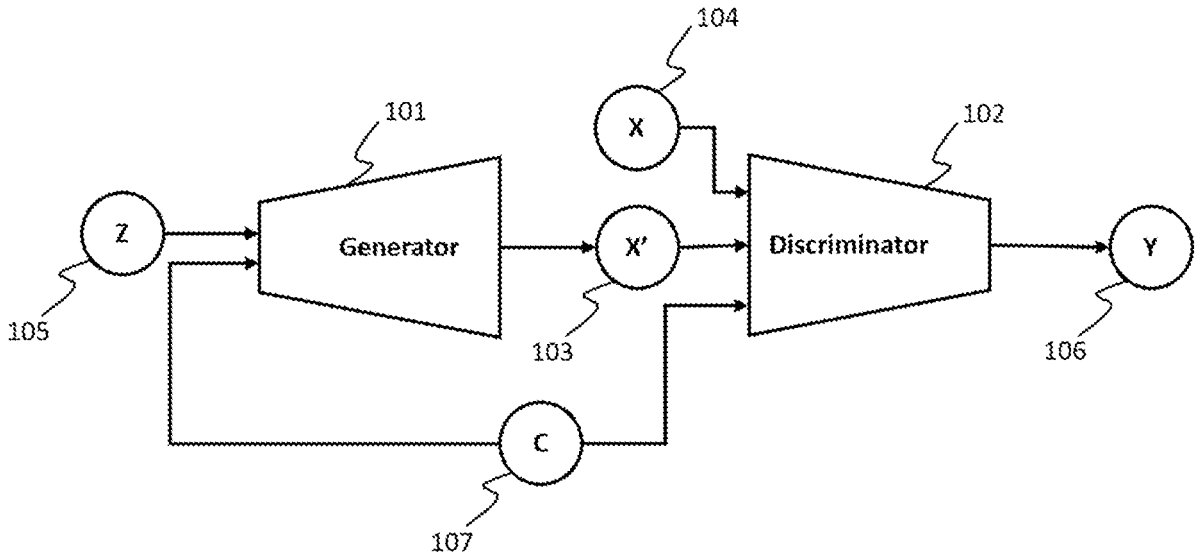

Fig. 1

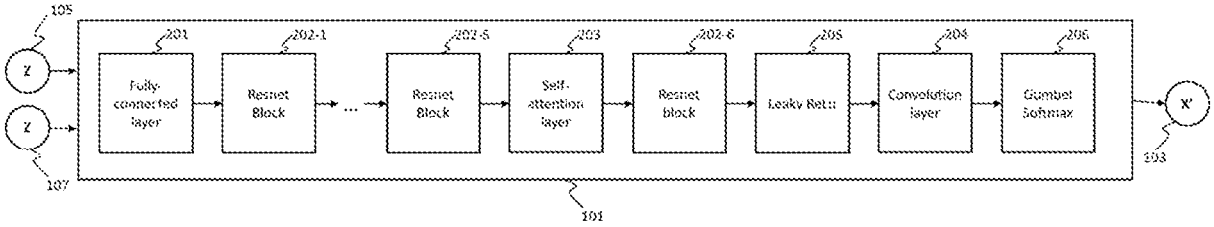

Fig. 2

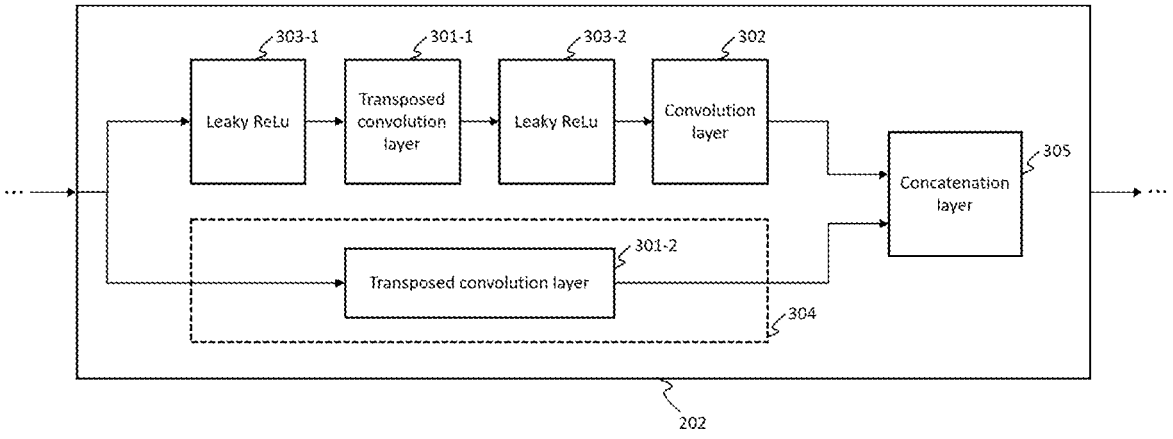

Fig. 3

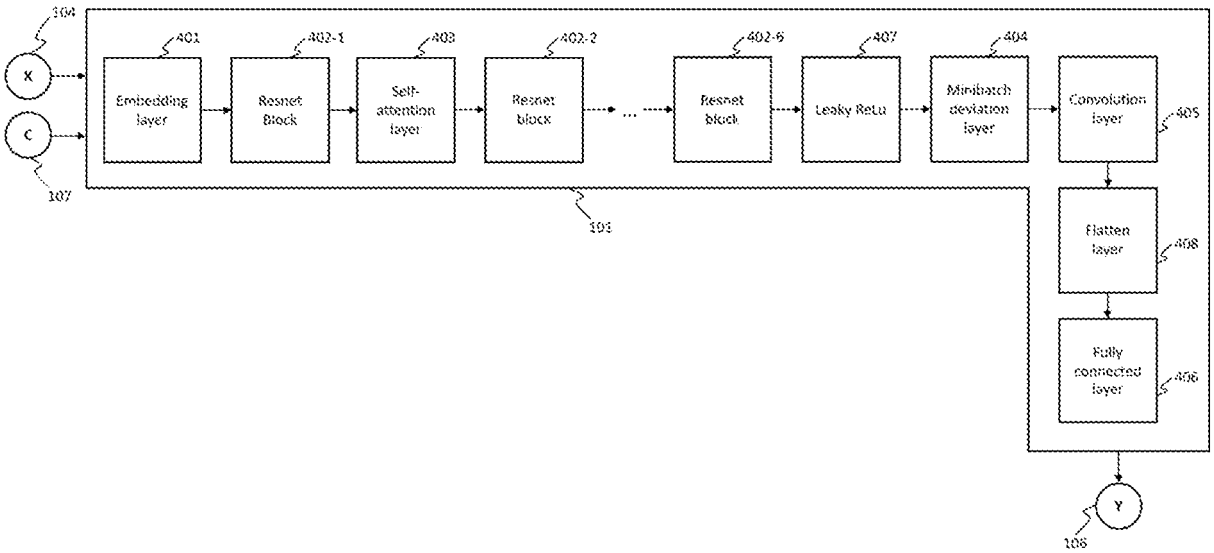
104
X
C
107
401
Embedding layer
402-1
Resnet Block
403
Self-attention layer
402-2
Resnet block
...
402-6
Resnet block
407
Leaky ReLu
404
Minibatch deviation layer
Convolution layer
405
Flatten layer
408
Fully connected layer
406
101
Y
108

Fig. 4

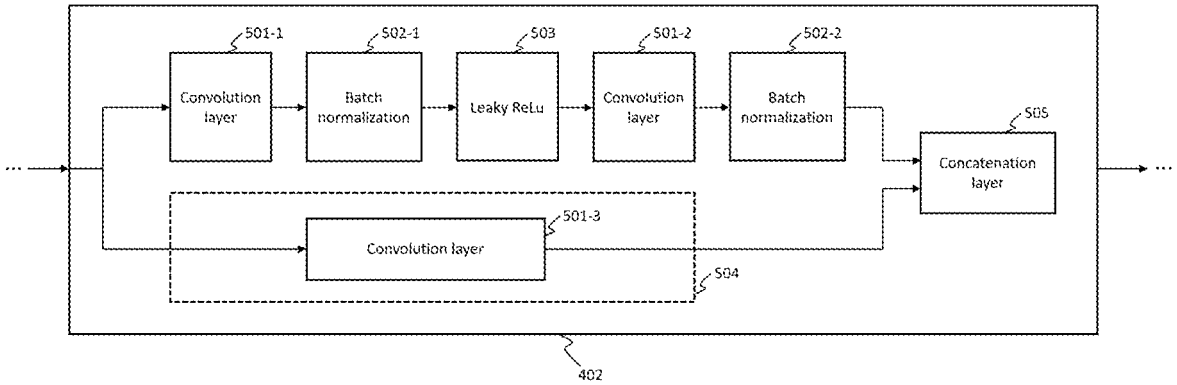
501-1
Convolution layer
502-1
Batch normalization
503
Leaky ReLu
501-2
Convolution layer
502-2
Batch normalization
505
Concatenation layer
501-3
Convolution layer
504
402

Fig. 5

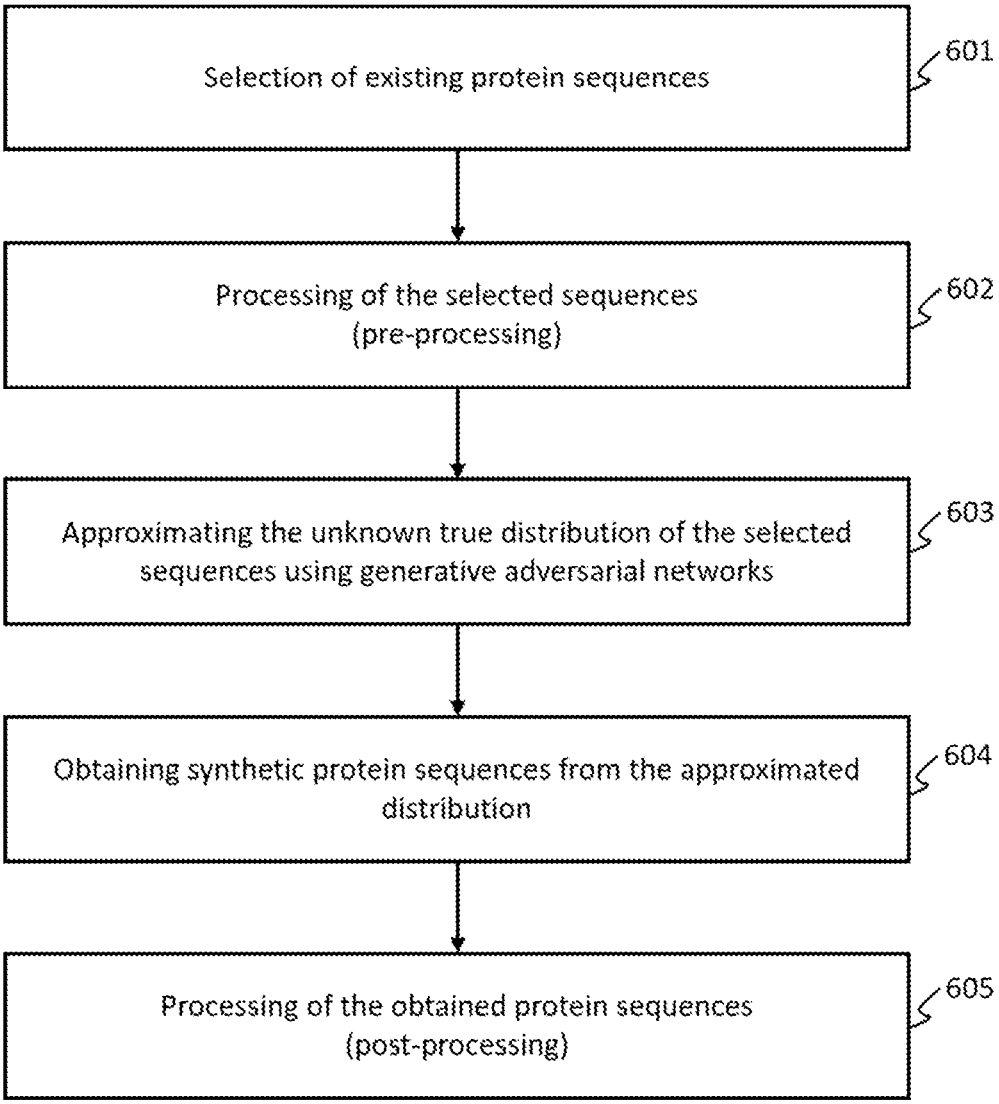
Selection of existing protein sequences
601
Processing of the selected sequences (pre-processing)
602
Approximating the unknown true distribution of the selected sequences using generative adversarial networks
603
Obtaining synthetic protein sequences from the approximated distribution
604
Processing of the obtained protein sequences (post-processing)
605

Fig. 6

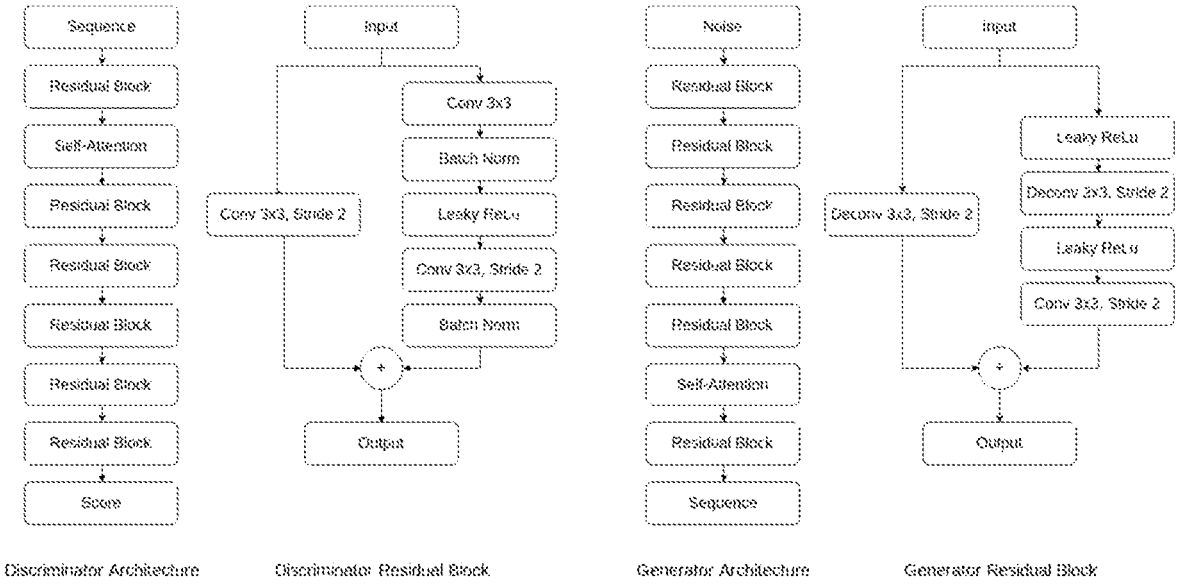
Sequence
Residual Block
Self-Attention
Residual Block
Residual Block
Residual Block
Residual Block
Residual Block
Score
Discriminator Architecture
Input
Conv 3x3
Batch Norm
Leaky ReLu
Conv 3x3, Stride 2
Batch Norm
Conv 3x3, Stride 2
Output
Discriminator Residual Block
Noise
Residual Block
Residual Block
Residual Block
Residual Block
Residual Block
Self-Attention
Residual Block
Sequence
Generator Architecture
Input
Leaky ReLu
Deconv 3x3, Stride 2
Deconv 3x3, Stride 2
Leaky ReLu
Conv 3x3, Stride 2
Output
Generator Residual Block

Fig. 7

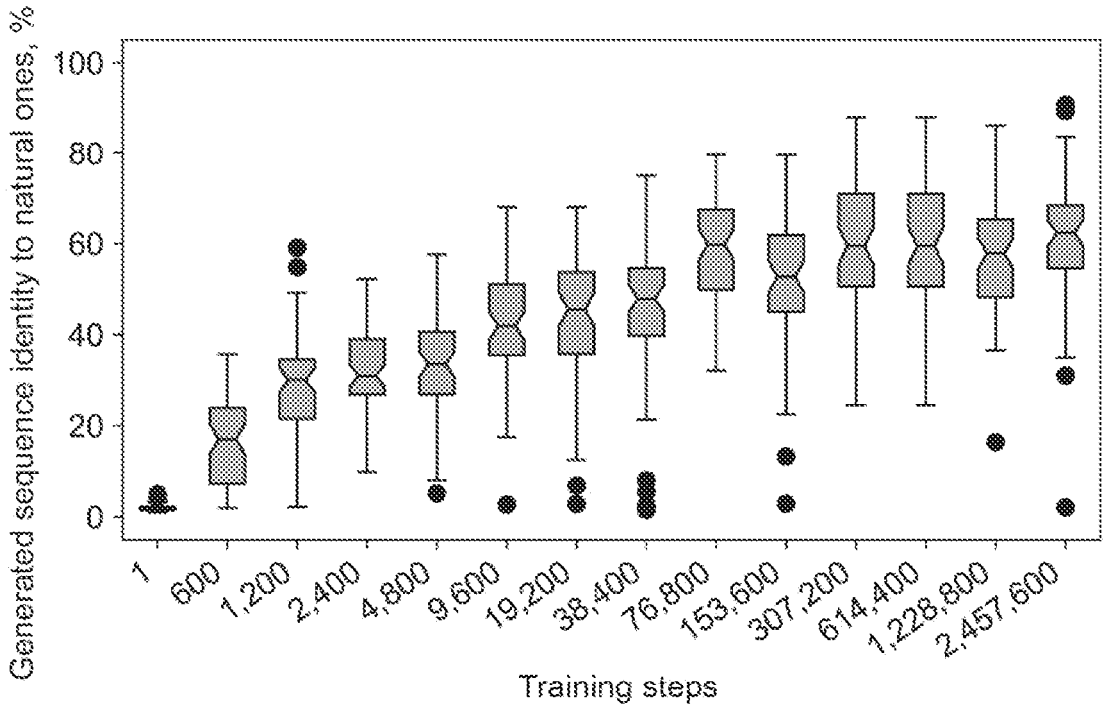
Generated sequence identity to natural ones, %
100
80
60
40
20
0
1
600
1,200
2,400
4,800
9,600
19,200
38,400
76,800
153,600
307,200
614,400
1,228,800
2,457,600
Training steps

Fig. 8

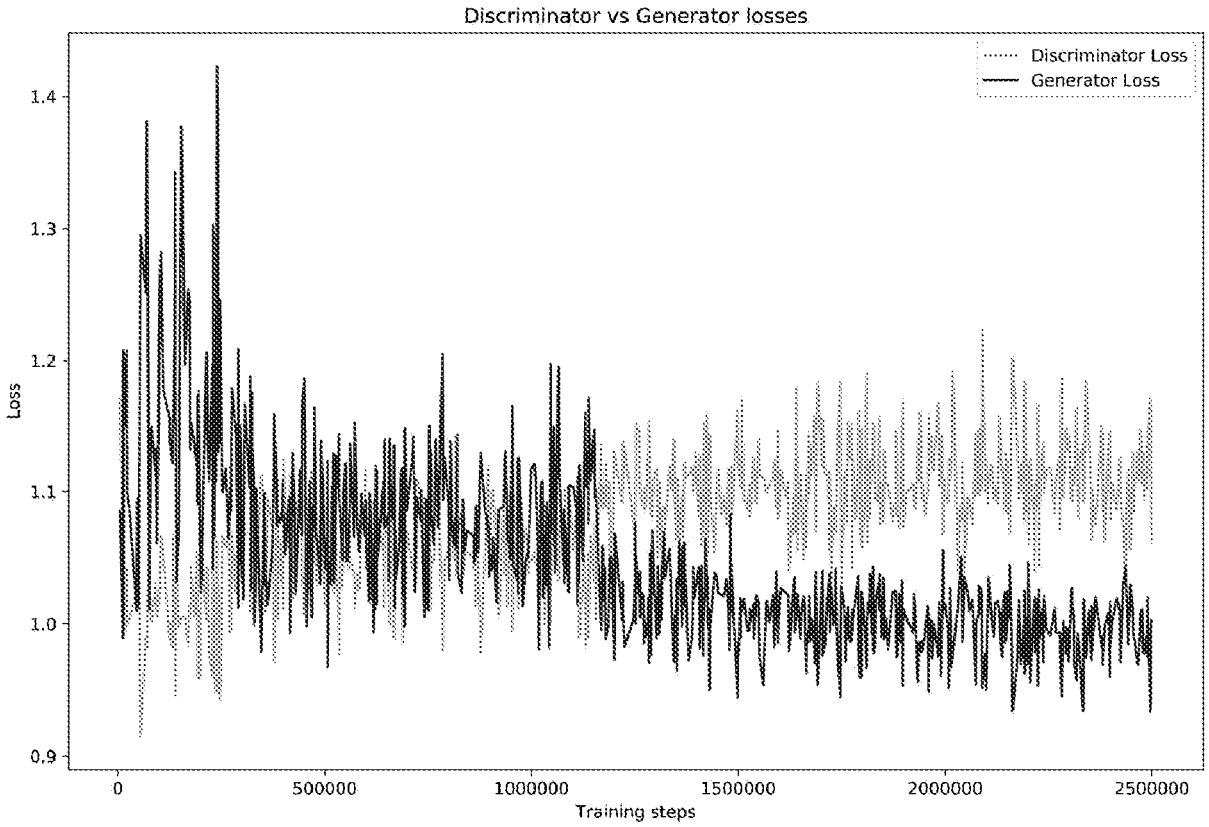
Discriminator vs Generator losses
Discriminator Loss
Generator Loss
Loss
1.4
1.3
1.2
1.1
1.0
0.9
0
500000
1000000
1500000
2000000
2500000
Training steps

Fig. 9

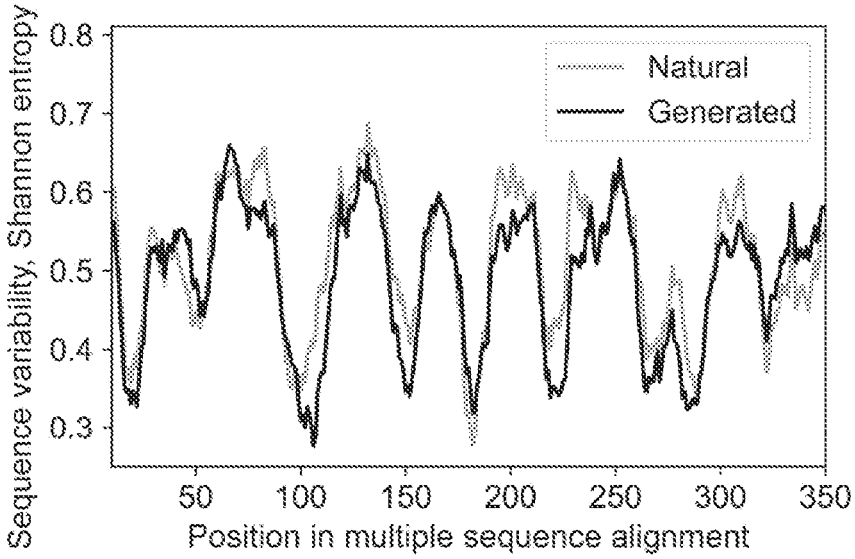
Natural
Generated
Sequence variability, Shannon entropy
0.8
0.7
0.6
0.5
0.4
0.3
50
100
150
200
250
300
350
Position in multiple sequence alignment

Fig. 10

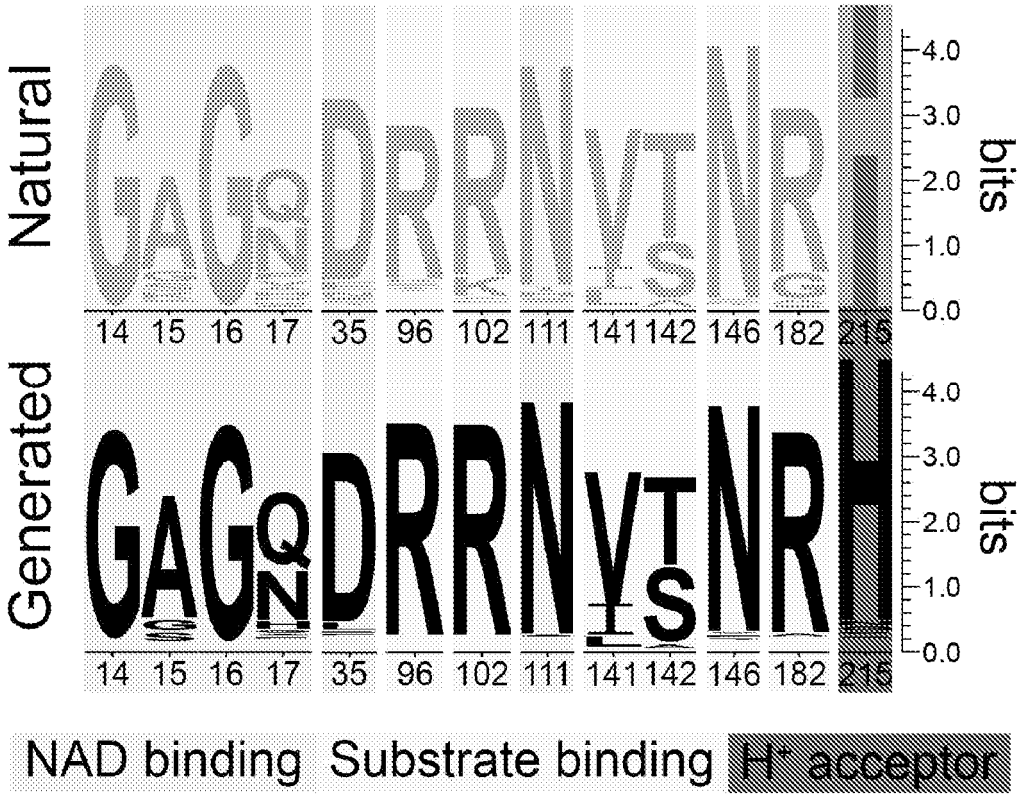
Natural
Generated
bits
4.0
3.0
2.0
1.0
0.0
14 15 16 17 35 96 102 111 141 142 146 182 215
NAD binding
Substrate binding
H+ acceptor

Fig. 11

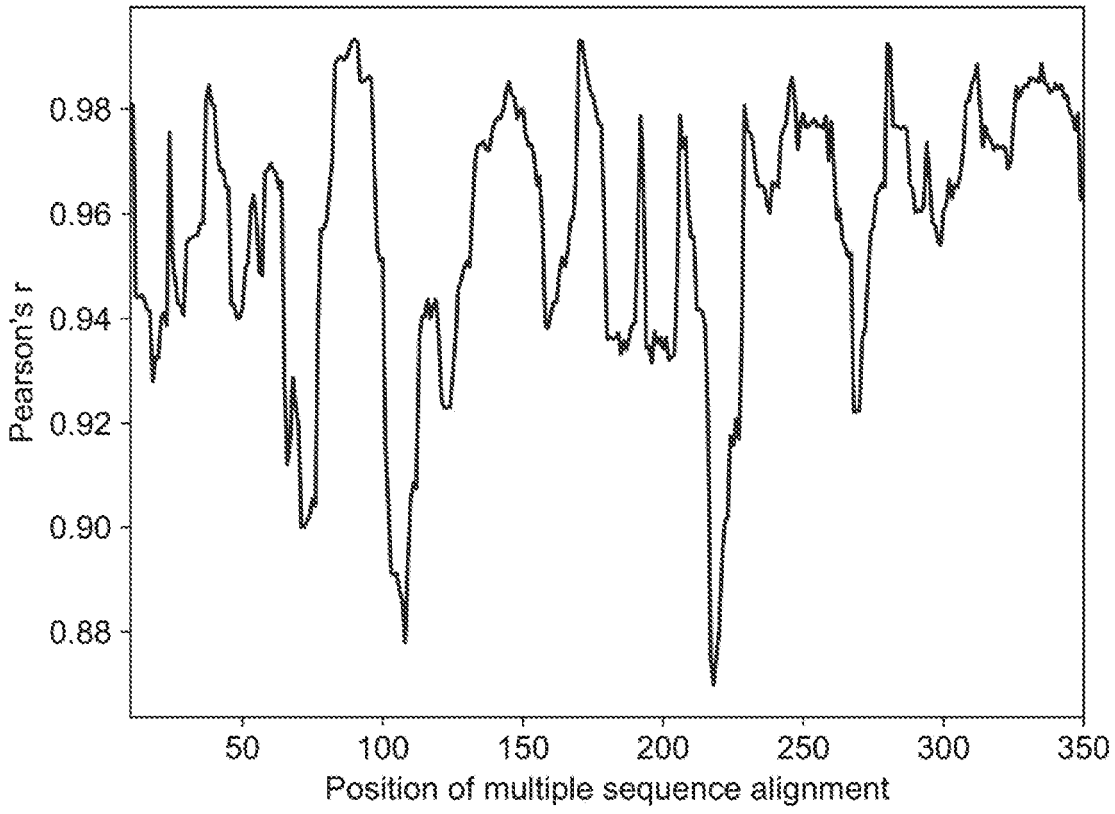
Pearson's r
0.98
0.96
0.94
0.92
0.90
0.88
50 100 150 200 250 300 350
Position of multiple sequence alignment

Fig. 12

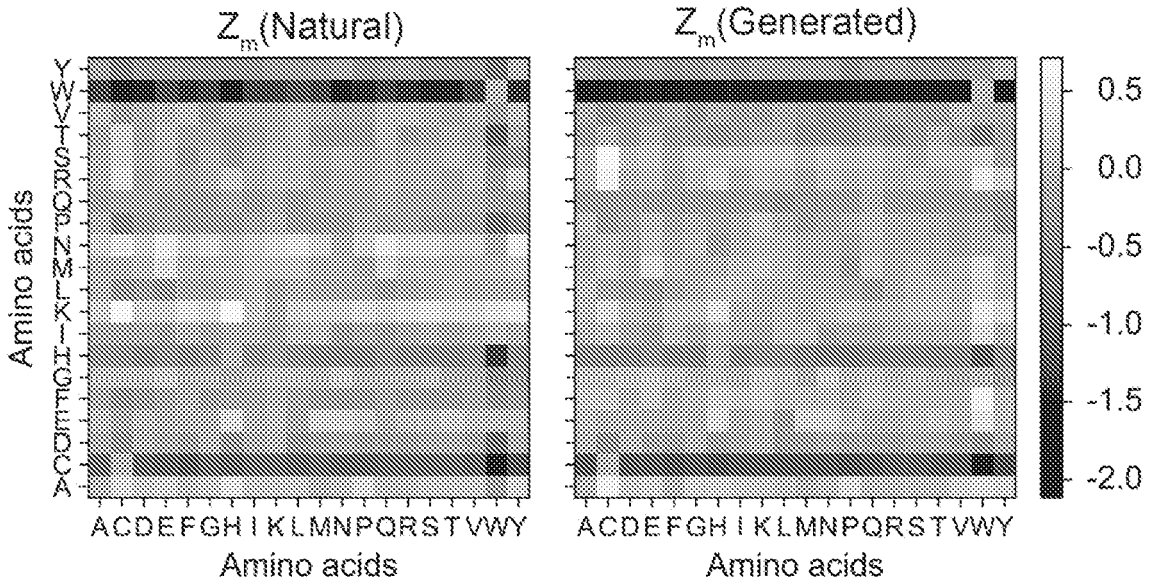
Z_m(Natural)
Z_m(Generated)
Amino acids
A C D E F G H I K L M N P Q R S T V W Y
Amino acids
0.5
0.0
-0.5
-1.0
-1.5
-2.0

Fig. 13

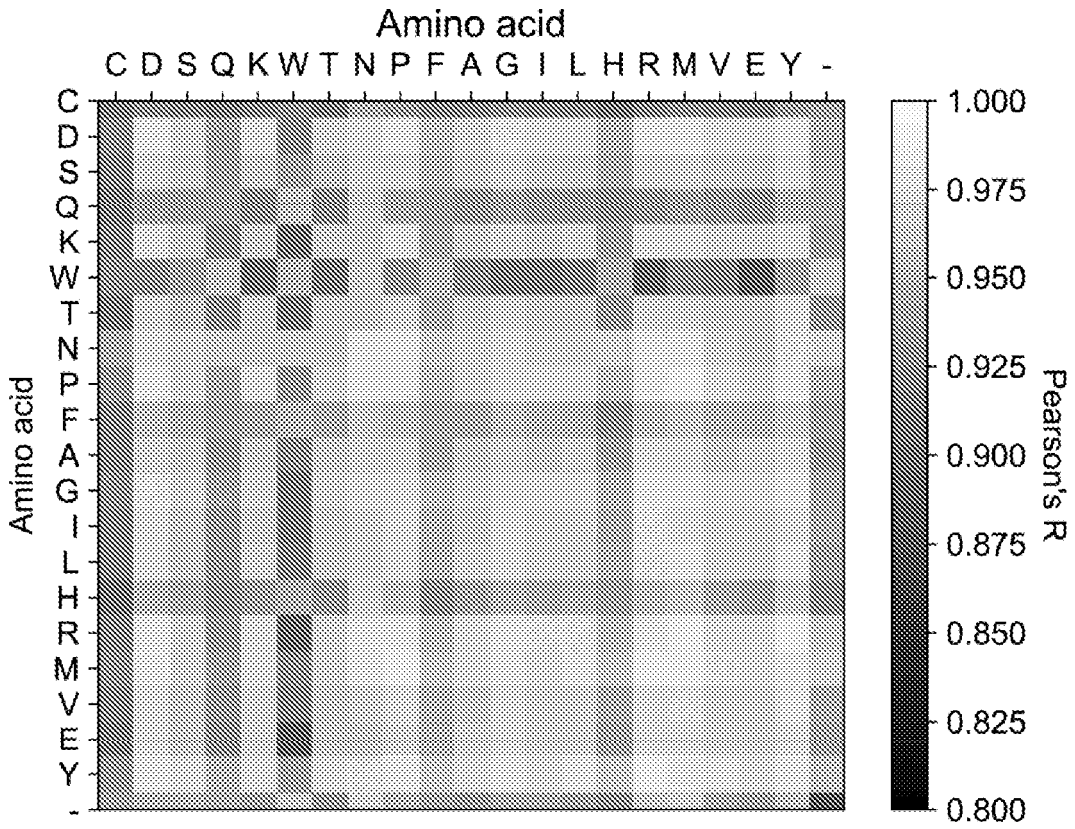
Amino acid
C D S Q K W T N P F A G I L H R M V E Y -
Amino acid
1.000
0.975
0.950
0.925
0.900
0.875
0.850
0.825
0.800
Pearson's R

Fig. 14

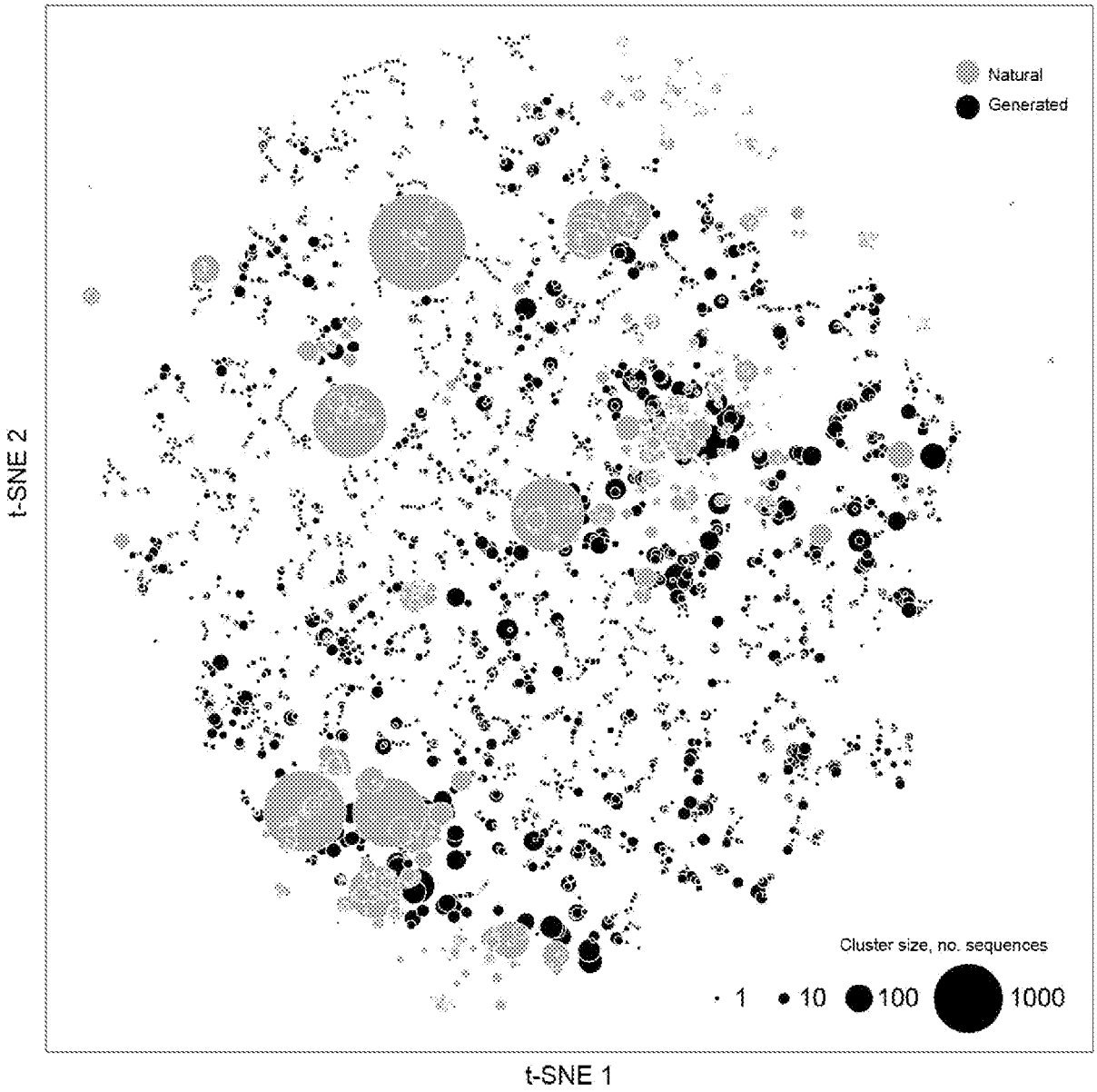
Natural
Generated
t-SNE 2
t-SNE 1
Cluster size, no. sequences
1
10
100
1000

Fig. 15

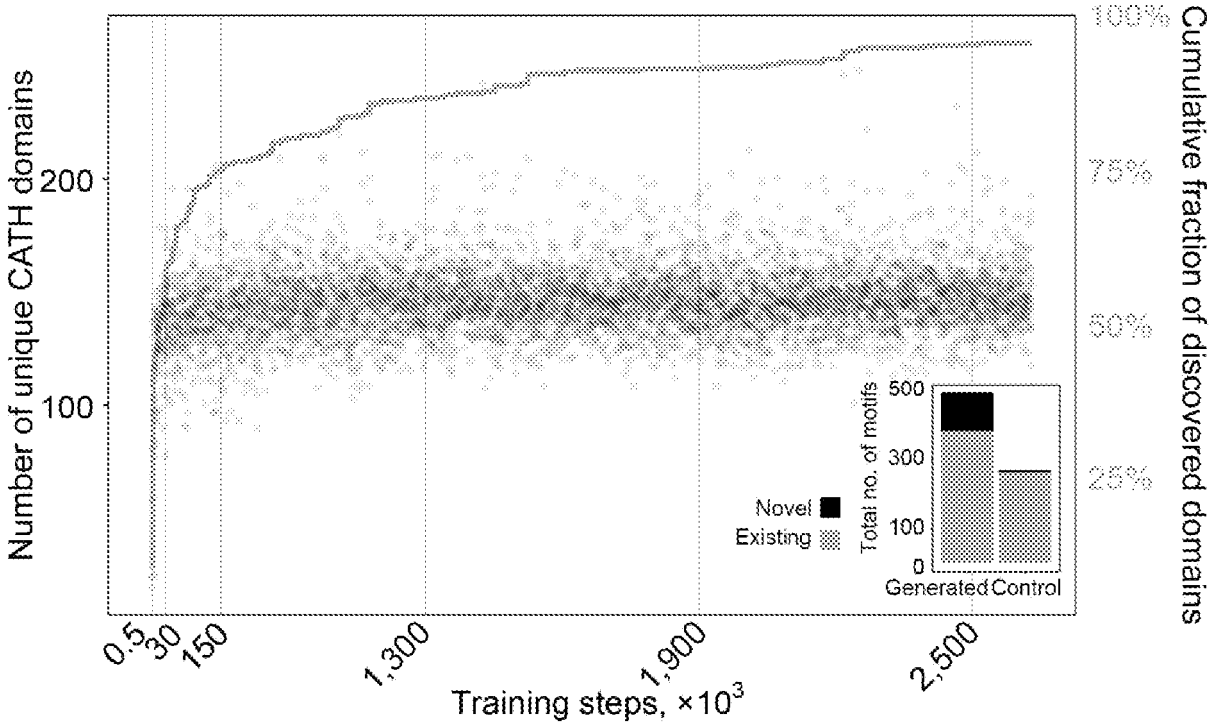
Number of unique CATH domains
200
100
100%
75%
50%
25%
Cumulative fraction of discovered domains
Novel
Existing
Total no. of motifs
500
300
100
0
Generated
Control
0.5
30
150
1,300
1,900
2,500
Training steps, ×10^3

Fig. 16

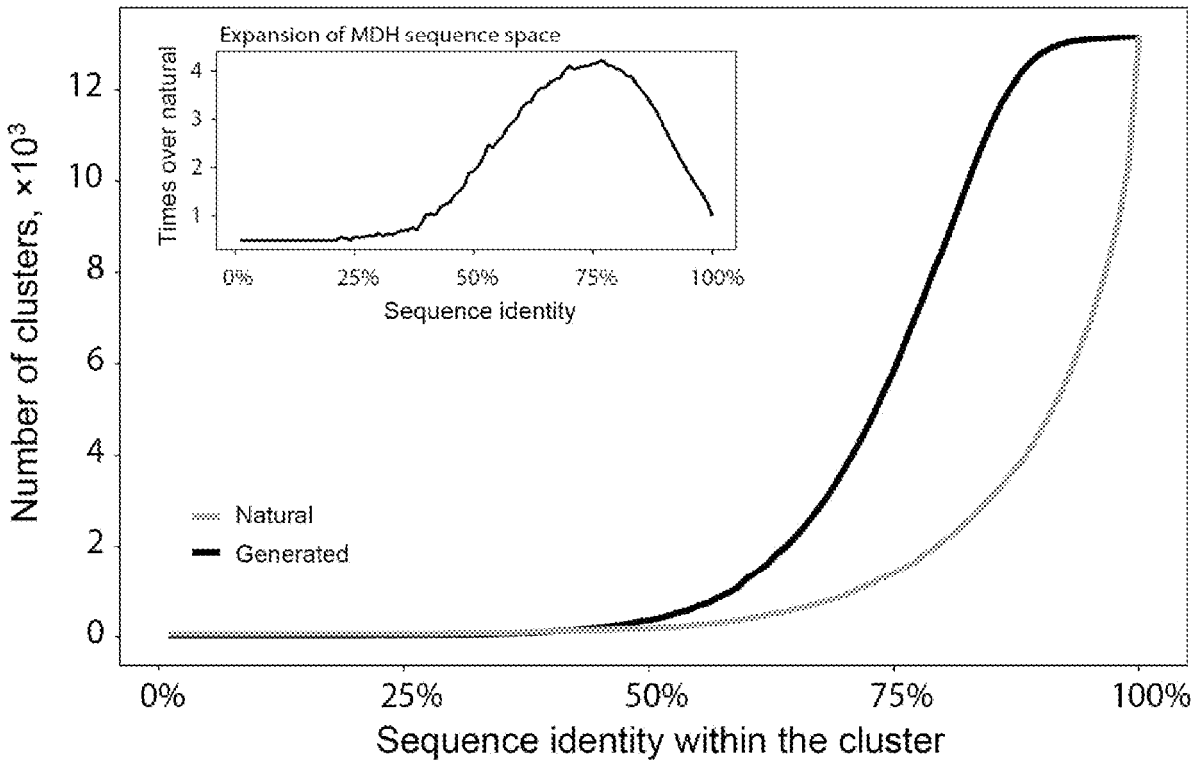
Number of clusters, ×10^3
12
10
8
6
4
2
0
Expansion of MDH sequence space
Times over natural
4
3
2
1
0%
25%
50%
75%
100%
Sequence identity
Natural
Generated
0%
25%
50%
75%
100%
Sequence identity within the cluster

Fig. 17

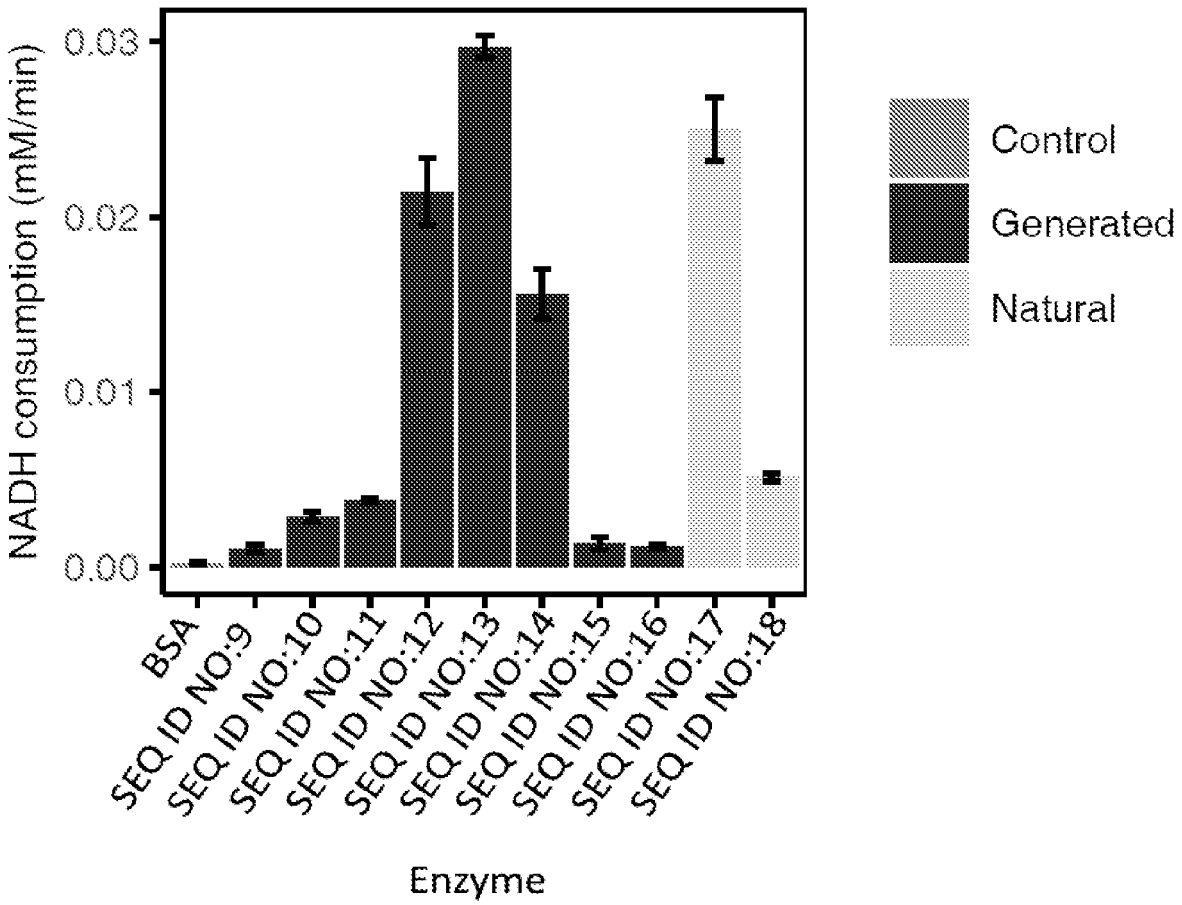
NADH consumption (mM/min)
0.03
0.02
0.01
0.00
BSA
SEQ ID NO:9
SEQ ID NO:10
SEQ ID NO:11
SEQ ID NO:12
SEQ ID NO:13
SEQ ID NO:14
SEQ ID NO:15
SEQ ID NO:16
SEQ ID NO:17
SEQ ID NO:18
Enzyme
Control
Generated
Natural

Fig. 18

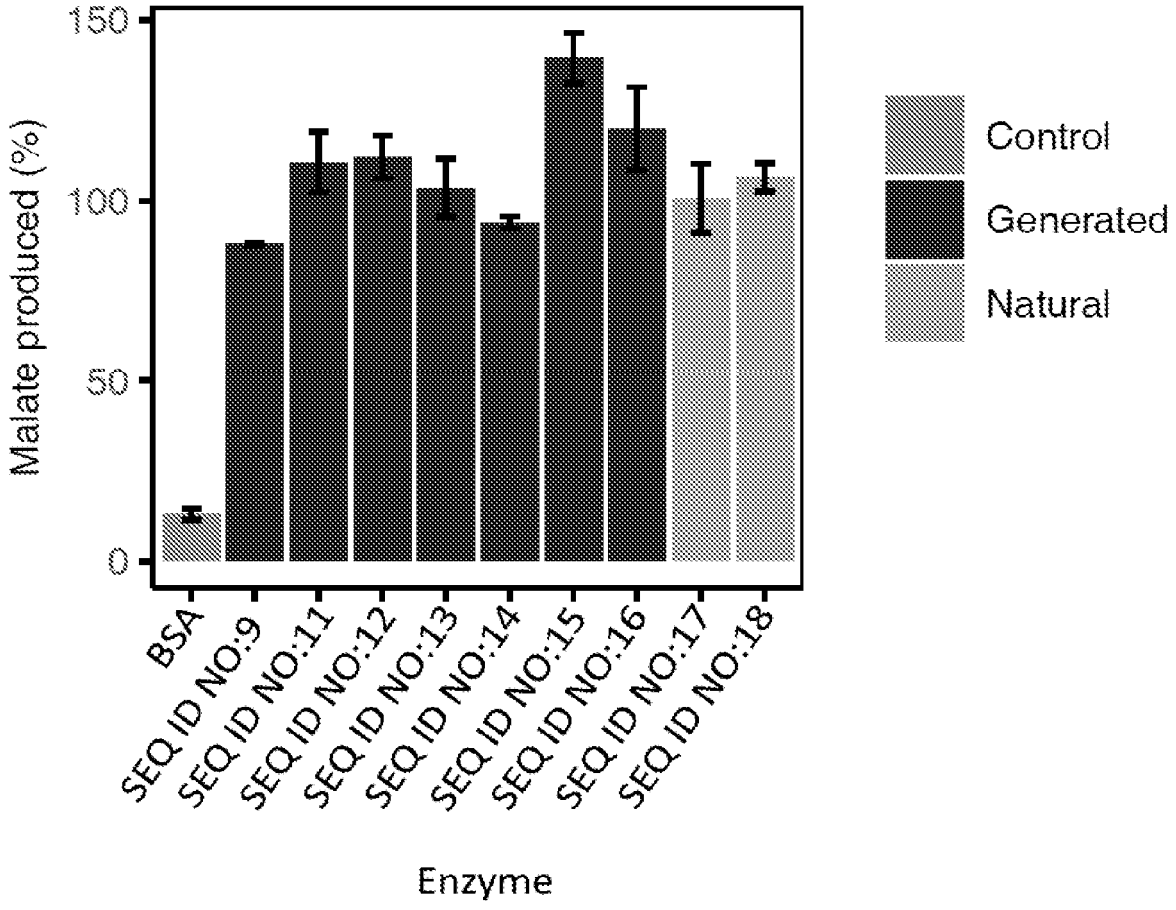
150
100
50
0
Malate produced (%)
BSA
SEQ ID NO:9
SEQ ID NO:11
SEQ ID NO:12
SEQ ID NO:13
SEQ ID NO:14
SEQ ID NO:15
SEQ ID NO:16
SEQ ID NO:17
SEQ ID NO:18
Enzyme
Control
Generated
Natural

Fig. 19

INTERNATIONAL SEARCH REPORT

International application No
PCT/IB2020/058401

A. CLASSIFICATION OF SUBJECT MATTER
INV. G16B20/50 G16B40/20 G16B40/30
ADD.

According to International Patent Classification (IPC) or to both national classification and IPC

B. FIELDS SEARCHED

Minimum documentation searched (classification system followed by classification symbols)
G16B

Documentation searched other than minimum documentation to the extent that such documents are included in the fields searched

Electronic data base consulted during the international search (name of data base and, where practicable, search terms used)
EPO-Internal, WPI Data

C. DOCUMENTS CONSIDERED TO BE RELEVANT

Category*	Citation of document, with indication, where appropriate, of the relevant passages	Relevant to claim No.
X	LI ZHAOYU ET AL: "Protein Loop Modeling Using Deep Generative Adversarial Network", 2017 IEEE 29TH INTERNATIONAL CONFERENCE ON TOOLS WITH ARTIFICIAL INTELLIGENCE (ICTAI), IEEE, 6 November 2017 (2017-11-06), pages 1085-1091, XP033353385, DOI: 10.1109/ICTAI.2017.00166 [retrieved on 2018-06-04]	1-3,5, 7-10,12, 13
Y	Title, abstract, p. 1087,1089	4,6,11

-/--

[X] Further documents are listed in the continuation of Box C.

[X] See patent family annex.

* Special categories of cited documents :

"A" document defining the general state of the art which is not considered to be of particular relevance

"E" earlier application or patent but published on or after the international filing date

"L" document which may throw doubts on priority claim(s) or which is cited to establish the publication date of another citation or other special reason (as specified)

"O" document referring to an oral disclosure, use, exhibition or other means

"P" document published prior to the international filing date but later than the priority date claimed

"T" later document published after the international filing date or priority date and not in conflict with the application but cited to understand the principle or theory underlying the invention

"X" document of particular relevance; the claimed invention cannot be considered novel or cannot be considered to involve an inventive step when the document is taken alone

"Y" document of particular relevance; the claimed invention cannot be considered to involve an inventive step when the document is combined with one or more other such documents, such combination being obvious to a person skilled in the art

"&" document member of the same patent family

Date of the actual completion of the international search	Date of mailing of the international search report
30 November 2020	09/12/2020

Name and mailing address of the ISA/	Authorized officer
European Patent Office, P.B. 5818 Patentlaan 2 NL - 2280 HV Rijswijk Tel. (+31-70) 340-2040, Fax: (+31-70) 340-3016	Lüdemann, Susanna

C(Continuation). DOCUMENTS CONSIDERED TO BE RELEVANT

Category*	Citation of document, with indication, where appropriate, of the relevant passages	Relevant to claim No.
Y	YU LI ET AL: "Deep learning in bioinformatics: introduction, application, and perspective in big data era", ARXIV.ORG, CORNELL UNIVERSITY LIBRARY, 201 OLIN LIBRARY CORNELL UNIVERSITY ITHACA, NY 14853, 28 February 2019 (2019-02-28), XP081036404, p. 10, last paragraph-p.11, fig. 5 and 6	11
Y	PAN ZHAOQING ET AL: "Recent Progress on Generative Adversarial Networks (GANs): A Survey", IEEE ACCESS, vol. 7, 2 April 2019 (2019-04-02), pages 36322-36333, XP011717226, DOI: 10.1109/ACCESS.2019.2905015 [retrieved on 2019-03-28] p.36327-36329	4,6
A	EP 3 486 816 A1 (PASTEUR INSTITUT [FR]) 22 May 2019 (2019-05-22) the whole document	1-13

INTERNATIONAL SEARCH REPORT

International application No.
PCT/IB2020/058401

Box No. II Observations where certain claims were found unsearchable (Continuation of item 2 of first sheet)

This international search report has not been established in respect of certain claims under Article 17(2)(a) for the following reasons:

1. ☐ Claims Nos.:
because they relate to subject matter not required to be searched by this Authority, namely:

2. ☒ Claims Nos.: 14, 15
because they relate to parts of the international application that do not comply with the prescribed requirements to such an extent that no meaningful international search can be carried out, specifically:
see FURTHER INFORMATION sheet PCT/ISA/210

3. ☐ Claims Nos.:
because they are dependent claims and are not drafted in accordance with the second and third sentences of Rule 6.4(a).

Box No. III Observations where unity of invention is lacking (Continuation of item 3 of first sheet)

This International Searching Authority found multiple inventions in this international application, as follows:

1. ☐ As all required additional search fees were timely paid by the applicant, this international search report covers all searchable claims.

2. ☐ As all searchable claims could be searched without effort justifying an additional fees, this Authority did not invite payment of additional fees.

3. ☐ As only some of the required additional search fees were timely paid by the applicant, this international search report covers only those claims for which fees were paid, specifically claims Nos.:

4. ☐ No required additional search fees were timely paid by the applicant. Consequently, this international search report is restricted to the invention first mentioned in the claims; it is covered by claims Nos.:

Remark on Protest

☐ The additional search fees were accompanied by the applicant's protest and, where applicable, the payment of a protest fee.

☐ The additional search fees were accompanied by the applicant's protest but the applicable protest fee was not paid within the time limit specified in the invitation.

☐ No protest accompanied the payment of additional search fees.

Continuation of Box II.2

Claims Nos.: 14, 15

Present claims 14 and 15 encompass use of functional protein sequences defined only by their desired function, contrary to the requirements of clarity of Article 6 PCT, because the result-to-be-achieved type of definition does not allow the scope of the claim to be ascertained. The fact that any compound could be produced by the method of claim 1 does not overcome this objection, as the skilled person would not have knowledge beforehand as to whether it would fall within the scope claimed.
The non-compliance with the substantive provisions is to such an extent that no meaningful search of said claims could be carried out at all (Article 17(2) PCT).

The applicant's attention is drawn to the fact that claims relating to inventions in respect of which no international search report has been established need not be the subject of an international preliminary examination (Rule 66.1(e) PCT). The applicant is advised that the EPO policy when acting as an International Preliminary Examining Authority is normally not to carry out a preliminary examination on matter which has not been searched. This is the case irrespective of whether or not the claims are amended following receipt of the search report or during any Chapter II procedure. If the application proceeds into the regional phase before the EPO, the applicant is reminded that a search may be carried out during examination before the EPO (see EPO Guidelines C-IV, 7.2), should the problems which led to the Article 17(2) PCT declaration be overcome.

INTERNATIONAL SEARCH REPORT

Information on patent family members

International application No
PCT/IB2020/058401

Patent document cited in search report	Publication date	Patent family member(s)	Publication date
EP 3486816 A1	22-05-2019	EP 3486816 A1	22-05-2019
		EP 3711057 A1	23-09-2020
		WO 2019097014 A1	23-05-2019